Integration and Dynamics of a Renewable Regenerative Hydrogen Fuel Cell System

by

Alvin Peter Bergen

B.A.Sc., University of Victoria, 1994
M.A.Sc., University of Victoria, 1999

A Dissertation Submitted in Partial Fulfillment
of the Requirements for the Degree of

DOCTOR OF PHILOSOPHY

in the Department of Mechanical Engineering

Supervisory Committee

Integration and Dynamics of a Renewable
Regenerative Hydrogen Fuel Cell System

by

Alvin Peter Bergen

B.A.Sc., University of Victoria, 1994
M.Sc., University of University, 1999

Supervisory Committee

Dr. Ned Djilali, Department of Mechanical Engineering
Supervisor

Dr. Peter Wild, Department of Mechanical Engineering
Supervisor

Dr. Andrew Rowe, Department of Mechanical Engineering
Departmental Member

Dr. Tom Fyles, Department of Chemistry
Outside Member

Dr. Brant Peppley, Department of Chemical Engineering, Queen's University
External Examiner

Abstract

Supervisory Committee

Dr. Ned Djilali, Department of Mechanical Engineering
Supervisor

Dr. Peter Wild, Department of Mechanical Engineering
Supervisor

Dr. Andrew Rowe, Department of Mechanical Engineering
Departmental Member

Dr. Tom Fyles, Department of Chemistry
Outside Member

Dr. Brant Peppley, Department of Chemical Engineering, Queen's University
External Examiner

This thesis explores the integration and dynamics of residential scale renewable-regenerative energy systems which employ hydrogen for energy buffering. The development of the Integrated Renewable Energy Experiment (IRENE) test-bed is presented. IRENE is a laboratory-scale distributed energy system with a modular structure which can be readily re-configured to test newly developed components for generic regenerative systems. Key aspects include renewable energy conversion, electrolysis, hydrogen and electricity storage, and fuel cells. A special design feature of this test bed is the ability to accept dynamic inputs from and provide dynamic loads to real devices as well as from simulated energy sources/sinks. The integration issues encountered while developing IRENE and innovative solutions devised to overcome these barriers are discussed.

Renewable energy systems that employ a regenerative approach to enable intermittent energy sources to service time varying loads rely on the efficient transfer of energy through the storage media. Experiments were conducted to evaluate the performance of the hydrogen energy buffer under a range of dynamic operating conditions. Results indicate that the operating characteristics of the electrolyser under transient conditions

limit the production of hydrogen from excess renewable input power. These characteristics must be considered when designing or modeling a renewable-regenerative system. Strategies to mitigate performance degradation due to interruptions in the renewable power supply are discussed.

Experiments were conducted to determine the response of the IRENE system to operating conditions that are representative of a residential scale, solar based, renewable-regenerative system. A control algorithm, employing bus voltage constraints and device current limitations, was developed to guide system operation. Results for a two week operating period that indicate that the system response is very dynamic but repeatable are presented. The overall system energy balance reveals that the energy input from the renewable source was sufficient to meet the demand load and generate a net surplus of hydrogen. The energy loss associated with the various system components as well as a breakdown of the unused renewable energy input is presented. In general, the research indicates that the technical challenges associated with hydrogen energy buffing can be overcome, but the round trip efficiency for the current technologies is low at only 22 percent.

Table of Contents

List of Tables

List of Figures

Acknowledgments

I would like to thank my supervisors, Dr. Peter Wild and Dr. Ned Djilali for their assistance, encouragement, and guidance in completing the IRENE project and this thesis.

I would thank my family and friends for their support and encouragement throughout this endeavour.

Dedication

This dissertation is dedicated to Peter E. Bergen, father, teacher, mentor and friend.

Chapter 1

Introduction

1.1　Background

Global concern over environmental climate change linked to fossil fuel consumption has increased pressure to generate power from renewable sources [1]. Although substantial advances in renewable energy technologies have been made, significant challenges remain in developing integrated renewable energy systems due primarily to the mismatch between load demand and source capabilities [2]. The output from renewable energy sources like photo-voltaic, wind, tidal, and micro-hydro fluctuate on an hourly, daily, and seasonal basis. As a result, these devices are not well suited for directly powering loads that require a uniform and uninterrupted supply of input energy.

Incorporating multiple renewable source types into the system design generally enhances resource availability (i.e., deployment of wind and solar or solar and micro-hydro etc) and aggregation of distributed renewable power generation mitigates short term (high frequency) variability [3]. However, practical renewable energy systems require an energy storage media to bank excess energy, when available, to buffer the output during periods where load demand exceeds the renewable input. Furthermore, different types of storage media are required to service short-term transients and long duration time scales.

In remote off-grid locations, operation from renewable resources traditionally requires large lead/acid battery buffers to address the issue of supply fluctuations. The physical size, limited life span, and initial capital cost of the battery bank coupled with transportation, maintenance, and battery disposal issues imposes significant limitations on the load capacity [4]. Significant improvements may be possible by storing the energy in the form of hydrogen instead of using batteries. During periods when the renewable resources exceed the load demand, hydrogen would be generated through water electrolysis. Conversely, during periods when the load demand exceeds the renewable resource input, a fuel cell operating on the stored hydrogen would provide the balance of power. Although considerable advances in hydrogen related technologies (electrolysers,

fuel cells, and storage media) have occurred during recent years, significant barriers in system integration must be overcome before the potential of renewable resource / hydrogen buffered energy systems can be realized.

The integration issues associated with the development of a hydrogen energy buffer are not well understood or documented in the literature. Experimental results detailing the energy balance within the system and quantifying the energy loss in various system components have yet to be reported in a unified manner. Furthermore, and perhaps more importantly the dynamic interactions between system components that occur while servicing real world loads remain unexplored. In general, a gap exists in experimental information available for validating the assumptions made in numerical simulations of renewable regenerative systems. Accurate data on the performance of the individual subsystems is required to inform and assist in the development of models to predict the performance of larger scale systems. A brief description of the challenges related to renewables, energy buffering and the history of hydrogen buffered renewable energy systems follows.

1.2   Renewable Energy and Resource Buffering

Definitions for 'renewable energy' vary depending on the context and scope of the energy system under investigation but this is generally understood as energy derived from natural, repetitive processes that can be harnessed for human benefit without consuming exhaustible resources. The source for most of this energy is from the sun, harnessed directly through solar heating or electricity generation, or indirectly through wind, waves, running water, and the ecosystem. Additional sources of renewable energy include tidal energy derived from gravitational pull and geothermal energy from heat generated within the earth. Renewable energy sources can be highly transient and exhibit strong short-term and seasonal variations in their energy outputs. Their variability poses problems for applications that require a continuous supply of energy. In addition, renewable resources typically have a low energy density, often large collection areas are required to generate modest power outputs.

Various agencies like the Department of Energy, the International Energy Agency, the UN International World Energy Assessment etc. the have generated estimates for the contribution that renewable energy sources provide to the total world energy usage. The estimates vary slightly, but in general, the largest contribution is from combustible renewables and renewable waste streams at approximately 10%, followed by hydro at approximately 2.2%, while all the other renewable forms combined contribute only 0.5% of the total world energy demand [5]. These percentages have remained fairly constant over the past 20 years; however, the total world energy usage has nearly doubled during that time to 11,435 Mega tones of oil equivalent (479 Exajoules) in 2005. While it is encouraging to see that the installed capacity of renewables has kept pace with the general increase in world energy demand, renewables still provide only a small fraction of our overall energy needs. Scenarios for energy consumption put forth by the various energy agencies all point to substantial growth in the total world energy consumption. A primary driver for the increase is due to the projected population growth coupled with increase in energy usage per capita as developing countries strive to improve there standard of living.

The exploitation of fossil fuels, specifically coal, oil, and natural gas, to supply the balance of our energy demand has created serious environmental issues. Each time a fossil fuel is consumed in a combustion process, the primary method for extracting the chemical energy in the fuel, a significant transfer of carbon (and other elements) takes place. Carbon dioxide emitted from combustion processes remains in the atmosphere as a green house gas for approximately 400 years. Although the argument can be made that fossil fuels were originally formed by natural processes that can ultimately be traced back to a renewable source - solar radiation - the time scales for production (thousands of years) versus the rate of consumption is certainly not sustainable and hence not 'renewable'. When viewed at a global level, the numbers associated with the overall energy usage are hard to comprehend. Values reported in Mega tones of oil, Terawatts, or Exajoules are difficult to relate to because we have little or no perspective for such large values. From an equilibrium standpoint, it is unreasonable to think that no balance shift will occur within the ecosystem when what nature took thousands of years to create is consumed over a hundred years. Yet this is the predicament we are faced with given

our predominantly fossil fuel based energy system. Many environmental scientists fear that if carbon dioxide emissions continue unchecked and unaltered, the ensuing climate change has the potential to threaten our very existence [6].

As environmental and sustainability issues arise with our current energy system, pressure is being applied on policy makers, governments, and the energy sector to provide the energy services we have grown accustomed to with less overall impact on the environment. In response, a variety of 'road maps' for the future of our energy system have been tabled which boldly state that energy from renewable sources will become a major contributor to the energy mix in the next 10, 20, 50 years. Countries like Denmark which have lead the way in incorporating renewable energy into their energy system have published energy plans which target 50 percent renewable by 2030 and 100 percent by 2050 [7]. In a recent state of the union address, the US president stated that new green energy technologies would be needed to secure the energy supply for the US and introduced a 22 percent increase in funding for clean-energy technology research [8]. The 'road maps' do not address in specific terms how the transformation to a green energy society will take place given that the current percentage of renewable power in the energy mix is so low. However, the common assumption is that if the goal is established, then new technologies will be developed to meet that goal. Timelines for such ambitious endeavours tend to drift far enough into the future that the immediate change is not required, but there is clearly a strong desire for renewables to supply a greater portion of the energy mix.

Two significant barriers impede widespread deployment of renewable energy; cost, and demand side servicing. While cost is an important factor, it must be evaluated relative to the true impact of the existing energy technologies. On the other hand, variability related to the inherent temporal mismatch between resource availability (sun shining, wind blowing etc.) and the load poses a serious technical issue for the deployment of renewable energy. Power from these resources may not be available when required. Although one can argue on a philosophical level that the demand side should be restructured to match the resource availability, history has shown that we place a high value on having energy available whenever and wherever we demand it. For renewables to assume a role as a primary energy source, the availability issue must be addressed.

One commonly quoted solution is to incorporate a broad mix of renewable sources, dispersed geographically, to improve the probability that one or more of the sources will be capable of meeting the demand [9]. While distributed generation has merit, there are often extenuating circumstances such as transmission capacity, lack of resource diversity, geographic constraints, etc., which limit practicality of this solution. In many situations, improving the availability of most renewable sources would require an energy buffer between the resource and the load [10]. With the exception of hydro and geothermal, the energy storage aspects have traditionally limited the deployment of renewable energy systems.

Many energy conversion devices exist or are under development which transform natural energy flows such as wind, tidal, geothermal, hydro, bio-mass, and solar into a more usable form, electricity and/or heat. While both output forms are challenging to store, heat energy is somewhat easier for two reasons; a variety of materials exist which are suitable for use as thermal reservoirs, and the time constants associated with heat generation and load demands are typically much larger. As stated previously, heat generation from biomass combustion is the single largest contribution that renewables make in our current energy system. However, with the exception of district heating and co-generation systems, storage of the biomass itself becomes the primary method for energy buffering as opposed to post combustion heat capture, storage, and utilization. Although heat is an important contribution from renewables, the current research is focused on electricity generation from renewable sources and the issues that arise in developing integrated energy systems.

Direct means for storing electricity once produced are limited to batteries, magnetic fields and super-capacitors. Of these, batteries are the only commonly used commercial devices but have low energy densities. Energy storage and power capacities (rate limits for charge/discharge) are inherently coupled. Batteries are also considered short-term storage devices since they typically loose 1 to 5 percent of their energy content per day through self-discharge [11]. Long-term energy storage requires a change in the storage media type to a time independent form such as compressed air, pumped hydro, and chemical compounds. The conversion efficiency, buffer capacity, and response times are key parameters used to characterize the performance of an energy storage system.

Compressed air and pumped hydro are technologies which favour large-scale implementation given the extensive infrastructure requirements. As such they can be built with large energy capacities and designed to provide load regulating capabilities (millisecond response rates) if required. The energy efficiency can only be assessed on a case by case basis since it is equipment dependent but corresponds fundamentally to that of standard turbo/electric machines optimized for energy input and extraction from the buffer media. Both compressed air and pumped hydro have been proposed to handle the buffer requirements for large-scale wind and tidal energy systems [1].

Water electrolysis is a convenient method for converting electrical energy into a chemical form, hydrogen. Hydrogen once generated can be stored as a gas or liquefied at low temperatures. Likewise it can be converted back into electricity in a fuel cell or used in a combustion process displacing hydrocarbons resulting in a substantial emissions reduction. Electrolysis is a scalable technology which has potential for use in a range of applications from remote monitoring stations (100's watts), off-grid residence (kW's), small wind farms (100's kW's), through utilities (MW's). Daily and seasonal time scales can be accommodated with appropriately sized hydrogen storage system. The minimum electrical and heat requirements for electrolysis are governed by the thermodynamics for water decomposition which is well defined and provides a baseline to gauge the performance of real electrolysers systems. Likewise, the maximum electrical energy available from regeneration of the hydrogen can be determined from the appropriate Gibbs energy functions [12].

The concept of energy buffering using hydrogen has been discussed in the literature for many years. In 1839, experiments conducted by Sir William Grove illustrated the energy storage potential of hydrogen in his gas voltaic battery, the first electrolyser / fuel cell system [13]. The technology for hydrogen generation through water electrolysis, primarily low pressure alkaline, evolved at a much earlier stage than the fuel cell. Commercial electrolysers have been available for over 100 years. However, electrolysis is an energy intensive process and cheaper alternatives for hydrogen production exist, namely steam methane reforming of natural gas (SMR), which is used extensively in industry today and in particular in processing of bitumen extracted from tar sands. Unlike SMR which emits CO_2, electrolytic hydrogen production has a low net

environmental impact provided the electricity is generated from a carbon neutral source. Historically, electrolysis has been limited to niche markets requiring low volume, high purity hydrogen production. As such, there has been little incentive to improve electrolyser efficiency. Development of the fuel cell was not seriously pursued until the 1960's during the Space Program. Since then, numerous advances in the technology have occurred to improve performance, reduce size, and lower cost.

During the late 1980's and 1990's a number of demonstration projects were performed to showcase evolving fuel cell designs. Some of these systems also included hydrogen production and storage. These systems were typically large (100's of kW), constructed from prototype components. Recent developments in proton exchange membrane (PEM) fuel cells and improvements to alkaline and PEM based electrolyser technologies have provided a new generation of components, suitable for implementing small-scale hydrogen energy buffers. Likewise, research in renewable energy converts and power conditioning devices has resulted in improved designs for the other elements needed to build renewable regenerative systems. Although the components exist, relatively little is known about the practical aspects associated with integrating these state-of-the-art elements into functional systems. The research presented in this thesis endeavours to directly address this issue.

1.3   Literature Review Summary

The main literature review covering the relevant modeling and experimental work for hydrogen based renewable-regenerative system is presented in Chapter 2. Included below is a brief summary of the prior research work.

A wide variety of theoretical models for hydrogen based renewable energy systems are presented in the literature, including models for isolated renewable energy systems with hydrogen storage [14, 15], methodologies for determining the performance of hybrid hydrogen systems [16], and exergy based simulation tools [17]. Sub-component models for hydrogen generation by electrolysis for renewable systems have been developed [12, 18], and high level models for stand alone and grid connected systems are reported in

[19-21].   High level models typically employ large time steps (hourly) and use average parameter values to represent the state of the system, an assumption that neglects system dynamics [22-25]. A better understanding of the real operating efficiencies, losses and dynamic interactions between system components is required to aid in the development of more accurate models.

Since the mid 1980's, a number of experimental renewable energy systems with hydrogen energy buffering have been developed. The first generation of systems demonstrated that hydrogen could be generated from surplus renewable resource power through water electrolysis and stored for both short term and seasonal energy buffering [26-28]. However, these systems also revealed that significant advances in electrolyser, fuel cells, hydrogen storage and power conditioning technologies were required before reliable operation could be achieved. At the present time, most of the initial demonstration projects are no longer in operation.

Several second generation residential scale systems have been developed using a combination of renewable input sources (solar and wind primarily), higher efficiency electrolysers, and PEM fuel cells [29-32]. However, most existing systems lack sufficient hydrogen storage capacity for long duration seasonal experiments. Research efforts with these test beds are focused primarily on developing control strategies.

General integration issues encountered during development of renewable-regenerative systems are outlined [27, 28, 33-36] but practical issues such as the influence of system architecture, criteria for energy transfer between short and long term storage, selection of energy storage media type, power flow management, communication interface etc., are not discussed in detail.

Experimental results for small scale renewable energy systems are not well documented in the literature. Where results are reported, they generally describe a "typical operational day" [26, 27, 35]. Basic system energy flows and efficiencies are reported for several systems [30, 37, 38] and power plots for various system components over a nine hour operating period are outlined [39]. An experimental analysis detailing the energy balance within the system and quantifying the long-term energy losses in various components has yet to be reported in a unified manner. Furthermore, the nature of the

dynamic interactions between system components remains an area of research that is not presented in the literature.

1.4   Objectives and Scope of Thesis

The following two objectives are addressed in the thesis:

1) To identify integration issues that pose barriers to the development of renewable-regenerative systems and devise solutions that will allow for the successful implementation of a system utilizing existing commercial products where possible.

2) To investigate the dynamic interactions that occur between system components and develop a database of experimental results that details the dynamic response, operating characteristic, efficiencies and losses within the system.

The objectives will be realized through the design, construction, commissioning, and experimentation with a new renewable energy test facility at the University of Victoria - Institute for Integrated Energy Systems. The hardware platform referred to as IRENE (Integrated Renewable Energy Experiment) is envisioned as a flexible distributed, laboratory-scale regenerative energy system comprised of commercial or pre-commercial components. A special design feature of this test-bed is the ability to accept inputs from, and provide loads to real devices as well as from simulated energy sources / sinks. The test-bed contains renewable input conversion devices, temporary energy storage, hydrogen generation, multiple forms of hydrogen storage, regeneration employing a fuel cell, and output load servicing devices.

The first objective stems from the need to understand the issues that pose constraints on the development of renewable-regenerative systems. The general perception among renewable energy advocates is that the development of hydrogen buffered renewable energy systems is relatively straight forward. However, the actual integration issues are not well understood or documented in the literature. Integration issues may indeed pose a significant barrier to the viability of deploying this technology. Identifying and documenting these issues will provide a knowledge base to inform future system

integrators of potential barriers in the development of renewable-regenerative systems. At present, most of the individual components required to develop a hydrogen based system are commercially available but are intended for alternate applications. As such, innovative solutions will be needed to address component compatibility issues. Outlining the implementation process, methods devised to overcome equipment limitations, and exposing the true state of the current technologies will aid future endeavours in the field.

The second objective is motivated by the need to develop an accurate knowledge of the system response under real operating condition and to provide experimental data for model validation. Each of the system components has time dependent characteristics which influence the operation of the combined system. In general, the dynamic aspects of system operation are not considered in the theoretical modeling of renewable-regenerative systems. Understanding the nature of the interactions and response characteristics for the combined system is essential for designing efficient regenerative systems.

Experiments with a variety of input perturbations on time scales that are relevant to renewable resources such as wind and solar power will be conducted to probe the dynamic interactions within the system. The response to high frequency transients as well as cyclic operation will provide valuable information to characterize operating regimes that a real system would experience. A detailed energy balance for the system will be conducted over a range of operating conditions to identify operating modes that minimize losses and conversely operating states which must be avoided if possible. A data base of experimental results detailing the actual system operation will provide a valuable resource for individuals engaged in model activities in the area of small scale renewable-regenerative system.

To accomplish the goals, a variety of practical issues will need to be addressed. The first is to develop a functional system from the individual components. Based on the literature review of the previous experimental endeavours in the field, the difficulty of this task must not be overlooked. The second is to equip the system with a broad range of instruments to measure the energy and mass flows. The third is to development data recording system capable of capturing the dynamic interactions between system

components (i.e., one that operates in the kHz range). The fourth is to create a centralized system controller to oversee the operation of individual components.

Once these tasks are complete, the experimental investigation can begin. The first series of experiments will be designed to characterize the response of individual system components. The second series will focus on the overall system response to coupled operation under conditions that are representative of the real demands that would be placed on a renewable-regenerative system.

The thesis is arranged in the following manner:

    Chapter 2 - relevant theoretical modeling and prior experimental work is reviewed

    Chapter 3 - IRENE component selection and implications on operation are discussed

    Chapter 4 - specific integration issues and associated solutions are presented

    Chapter 5 - dynamic response of the hydrogen energy buffer is explored

    Chapter 6 - coupled system response to a renewable input / demand load is examined

    Chapter 7 - conclusion and recommendations based on the finding are made

Chapter 2

Literature Review

The following review summarizes the theoretical modeling and experimental systems documented in the literature which utilize renewable energy sources coupled with hydrogen energy buffering. Numerous theoretical models have been presented in the literature which cover a broad spectrum of system sizes from a few kilowatts to a utility scale. This review does not cover the prior theoretical work in an exhaustive manner but is intended to provide a general overview into the types of models that are being proposed for IRENE-like systems. This information is relevant since experimental validation of the general modeling assumptions motivates much of the current research.

The experimental work documented in this review is restricted to systems which employ electrical based renewable resource conversion technologies, and contain components for hydrogen production and utilization for energy buffering. The systems are grouped into two categories; first generation proof-of-concept demonstrations, and second generation semi-functional systems. The overall system configuration, capacity and integration challenges will be highlighted.

The literature indicates that a significant effort has been devoted to demonstrating that hydrogen can be used to buffer intermittent renewable resources. However, a number of challenging issues remain in transitioning from the demonstration level to practical systems which have the potential to impact our power generation portfolio. The contributions and limitations of the previous experimental work will be discussed in order to place the current research in context.

2.1 Modeling of Hydrogen Buffered Renewable Energy Systems

A wide variety of theoretical models on combined hydrogen and renewable energy systems are presented in the literature. High level models deal primarily with the integration of renewable energy sources and the potential benefits of hydrogen energy

buffering at a national grid scale. Schenk et al. [40], Sorensen et al. [24], Da silva et al. [19], Conte et al. [41] and Rand and Dell [42, 43] present techno-economic analyses based on the assumption that existing hydrogen production, storage, and regeneration technologies can be deployed at utility scales. Simulations are conducted using annual energy flows, nominal operating efficiencies, and projected equipment lifetimes. Anderson and Leach [10] and Troncoso and Newborough [44] investigate the implementation of hydrogen energy buffering to allow high penetrations of renewable resources into existing power grids. While the results conclude that hydrogen and renewable energy technologies have potential to make significant contributions at a large scale, little consideration is given to practical aspects of implementing the systems. Models conducted at this level generally employ input data averaged over intervals that range from hours to days. This practice raises interesting questions regarding the accuracy of employing aggregate data to represent the actual response of a renewable-regenerative system.

Modeling of autonomous mini-grid systems has received considerable attention over the past decade. Young et al. [45] Shakya et al. [46], Ntziachristos et al. [47] and Isherwood et al. [48] discuss the technical feasibility of renewable systems suitable for small villages. Kasseris et al. [49], Chen et al. [50], Zoulias et al. [21, 51], Gosh et al. [11], Vosen and Keller [22], and Dienhart and Seigel [14] review hydrogen technologies for stand-alone power systems and draw comparisons against existing fossil fuel based solutions. Potential applications are evaluated on economics which assume stable long-term operation of the hydrogen systems.

Santarelli et al. [25, 52], Maclay et al. [53], and El-Shatter et al. [23] utilize basic component models to develop simulations for residential scale systems. Simulation are conducted for a variety of durations; yearly, weekly, and daily, with input data that ranges from hourly, 15 minute, and 30 minute averages respectively. System design guidelines and expected performance are established but model validation against experimental data was not conducted.

Santarelli and Macagno [17] developed an exergy based simulation tool to design stand alone energy systems and to evaluate the thermal and economic performance over a one

year period. Simplified component models are employed, and the analysis appears to over-estimate the component efficiencies, but the work is generally more focused on the economic aspects of the system.

Mills and Al-Hallaj [15] employed more sophisticated component models in their work on a residential hybrid renewable energy system. Multiple renewable sources, hydrogen generation and storage, fuel cell and inverter based load servicing were simulated using realistic resource and load data for a one year period. His work suggests that the battery capacity of a renewable regenerative system can be relatively small and still meet the load demands. Experimental validation is required.

Kolhe et al. [16] developed a methodology that extensively employs efficiencies to determine the performance of a hybrid hydrogen system. Model results are validated against data but are only reported for a 24 hour period. However, they clearly demonstrate that energy management in the system is intrinsically linked with the battery buffer state of charge.

Onar et al. [54] provides insight into the dynamic characteristics of a wind hydrogen hybrid system by conducting detailed 30 second simulations. The results indicate that system stability can be maintained if the hydrogen components react to rapid load shifts. The long-term implications on component lifetime and performance under dynamic operation are not addressed.

Deshmukh and Boehm [55] provides a detailed review of individual component models for renewable-regenerative systems but does not conduct a systems analysis. Many of the component models discussed in this excellent reference are more sophisticated then are employed in the bulk of the system models described thus far. Deshmukh et al. points out that further research is required to reduce the predominantly empirical nature of the models. Noteworthy is the absence of discussion or accounting for long term performance decline commonly observed with most components that constitute on operating system.

Dufo-Lopez et al. [56] addresses control system optimization in a renewable energy from an economic perspective. A strategy to minimize net present cost of the system is created and verified on hybrid renewable system with diesel back-up. Bilodeau and Agbossou

[57] addresses control issues by applying fuzzy logic to optimize system operational set-point. Simulations with real resource and load data are conducted but actual implementation was not conducted. Both models indicate that the control strategy employed in with the hydrogen energy buffer directly impacts system performance.

Three interesting sub-system models investigate hydrogen production from renewable resources. Sherif et al. [58] reviews the wind to hydrogen pathway and raises issues on intermittent operation of the electrolyser. Operating consideration, efficiency, coupling methods and thermal aspects are discussed; however, supporting experimental work is not referenced. Battista et al. [59] proposes a power conditioning method for matching wind turbine output to an electrolyser with reduced coupling electronics. The control scheme reduces the high frequency power fluctuations but the electrolyser is still subjected to low frequency variations. Performance is simulated by not verified experimentally. Finally, Ulleberg [12] and Roy et al. [60] develop detailed models for hydrogen production using an alkaline electrolysers. Models consider both electrical and thermal aspects and predict hydrogen production and associated efficiencies. Validation is conducted with experimental data collected from high pressure electrolyser employed in renewable energy test-beds. Several electrolyser operating strategies are discussed to improve hydrogen yield. Roy presents an analysis indicating that low pressure electrolysis is more efficient for renewable systems. However, the long-term impacts of variable current operation on electrolyser performance are not stated.

2.2   First Generation Hydrogen Renewable Energy Systems

During the late 1980's to mid 1990's nine renewable energy test-beds employing hydrogen energy buffering appear in the literature. The basic system architecture is similar to, or a minor variation of, the one presented in Figure 2.1. The scale of these projects range from small 1.3 kW proof of concept experimental platforms to large 270 kW multi million dollar corporate ventures. The projects mainly focused on fuel cell technology demonstrations but also showed that hydrogen could be employed to buffer the daily and seasonal variations of an intermittent renewable energy source. A summary of the basic system parameters for the various projects is given in Table 1. An overview of each system is presented in the following sections.
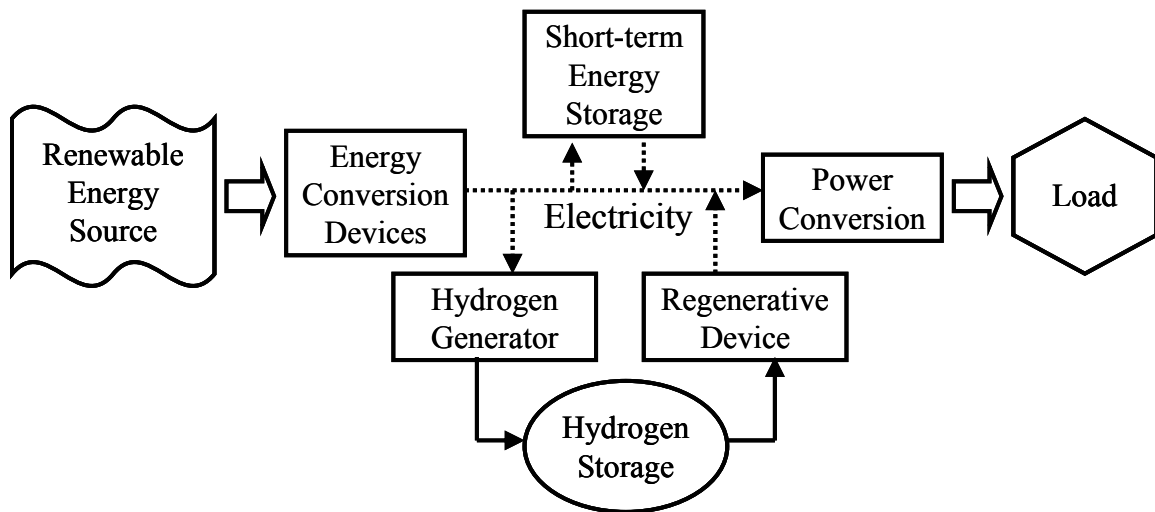
Figure 2.1 Typical First Generation Renewable-Regenerative System Architecture

First Generation Renewable Hydrogen Energy Systems

	Solar-Wasserstoff-Bayern	Helsinki Hydrogen Energy Test-bed	Schatz Solar Hydrogen Project	Freiburg Solar House	University of Oldenburg	INTA Solar Hydrogen Facility	Friedli Solar Hydrogen House	PECS Energy Conversion System	PHOEBUS
Year Initiated	1986	1989	1989	1989	1990	1990	1991	1992	1993
Location	Germany	Finland	USA	Germany	Germany	Spain	Switzerland	USA	Germany
Solar Input	370 kW_p	1.3 kW_p	9.2 kW_p	4.2 kW_p	6.2 kW_p	8.5 kW_p	4.5 kW_p	0.15 kW_p	43 kW_p
Wind Input	none	none	none	None	5 kW_p	none	none	none	none
Battery Storage	none	14 kWh @ 24 VDC	5 kWh @ 24 VDC	19 kWh @ 24 VDC	size not specified	none	38 kWh @ 24 VDC	none	303 kWh @ 220 VDC
Electrolyser	211 kW_{el} @ 1 bar 100 kW_{el} @ 31 bar	0.8 kW_{el} @ 25 bar	5.8 kW_{el} @ 8 bar	2 kW_{el} @ 30 bar	0.8 kW_{el}	5.2 kW_{el} @ 6 bar	10 kW_{el} @ 2 bar	0.095 kW_{el} @ 6 bar	26 kW_{el} @ 7 bar
H_2 Storage	5000 m^3 @ 30 bar	200 Nm^3	5.7 m^3 @ 30 bar	15 m^3 @ 30 bar	30 Nm^3	8.8 m^3 @ 200 bar + 24 m^3 MH	0.5 m^3 @ 29 bar MH	2.6 Nm^3 MH	27 m^3 @ 120 bar
O_2 Storage	500 m^3 @ 30 bar	none	none	7.5 m^3 @ 30 bar	size not specified	none	none	none	20 m^3 @ 70 bar
Fuel Cell	6.5 kW_{el} AFC 10 kW_{el} PEM 79 kW_{el} PAFC	0.5 kW_{el} PAFC	1.3 kW_{el} PEM	0.5 kW_{el} AFC	0.6 kW_{el} AFC	10 kW_{el} PAFC 5 kW_{el} PEM 2.5 kW_{el} PEM	none	size not specified	6.5 kW_{el} AFC 5 kW_{el} PEM 2.5 kW_{el} PEM
Load	public grid	0 – 0.5 kW DC resistive	0.6 kW AC	0.35 kW combined	size not specified	public grid	stove / mini van	size not specified	15 kW local grid
Notes	Industrial size system - US$ 80 million investment	Direct Bus connection (no dc-dc converters)	Long-term continuous operation	Solar heating systems employed	Limited system data available	Direct PV electrolyser connection	Project funded by home owner	Limited system data available	Large-scale high visibility demonstration project
Primary Reference	Szyszka 1998, 1992	Vanhanen 1998,1997	Lehman 1997	Goetzberger 1993	Haas 1991	Schucan 2000	Hollmuller 2000	Hollenberg 1995	Ghosh 2003

Table 2.1 Component Data for First Generation Renewable-Regenerative Systems

SWB: Solar-Wasserstoff-Bayern GmbH Test-Bed

Szyszka [28, 33] outlines the development of the first large-scale solar-hydrogen-fuel cell demonstration project located in Neunburg Vorm Wald, Germany, which commenced in 1986. The project was a joint venture between the German government and a conglomerate of companys, (notably Bayernwerk AG, BMW, Linde AG and Siemens AG) with a mandate to develop and test industrial scale hydrogen energy system components. The array of first generation prototype equipment assembled for this project was both impressive and diverse. The total reported capital investment over the 13 year project was approximately 80 million US dollars.

A block diagram for the overall plant is given in Figure 2.2. Solar collectors of monocrystalline, polycrystalline, amorphous silicon, and advanced monocrystalline were employed in multiple fields connected to a common DC bus by various styles of power conditioning modules. In addition, several collector fields were tied directly to the three phase grid via DC-AC inverters. A variety of electrolyser technologies were tested including both low and high pressure alkaline and low pressure membrane types. Hydrogen production was controlled by limiting electrolyser input power. Extensive purification and compression stages were implemented for both the hydrogen and oxygen streams. Primary storage was in compressed form at 30 bar. Multiple fuel cell technologies were tested including alkaline, phosphoric acid and proton exchange. The fuel cell electrical output was used locally or coupled to the grid via appropriate DC-AC inverters. In addition, hydrogen and oxygen was also utilized in various boilers, catalytic heaters and absorption refrigeration technologies under investigation.
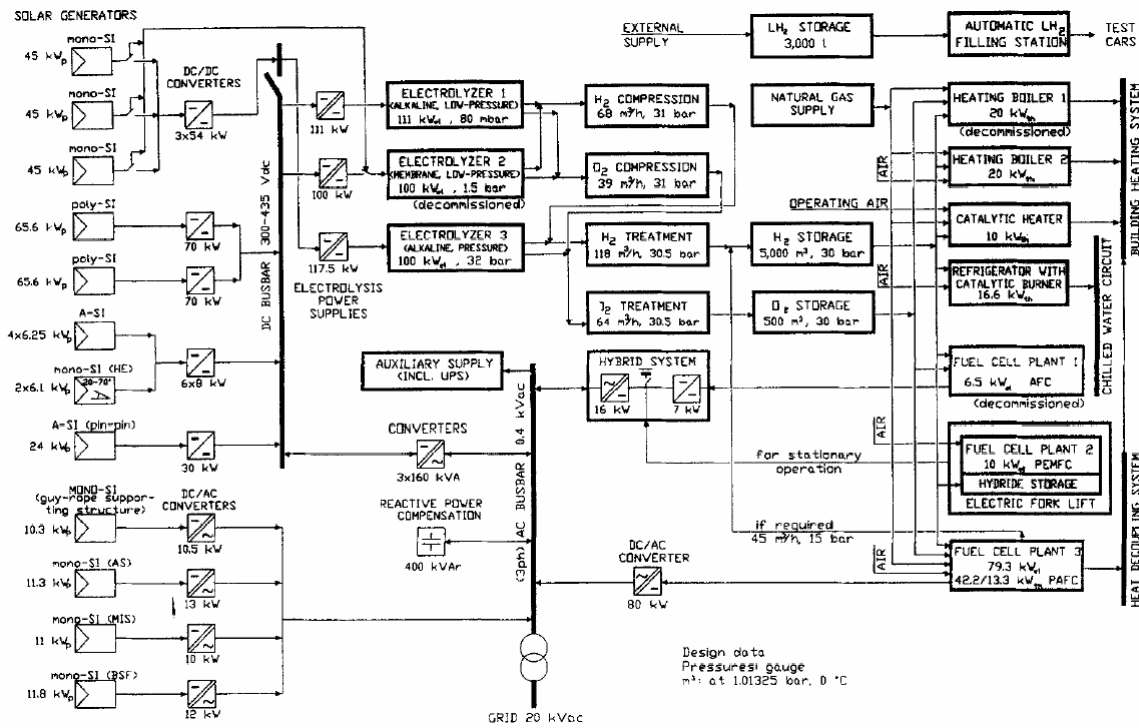
Figure 2.2 SWB Solar Hydrogen Facility Block Diagram

The experimental program at SWB generated a significant database of information for the industrial partners involved, but limited results are reported in the public domain. The technical aspects benefited component manufacturers involved unfortunately many are no longer active in the field of hydrogen energy systems. Papers by Szyszka indicate that considerable delays in commissioning sub-systems was a common occurrence and that components often required complete redesigns.

The SWB project reinforced the fact that significant advances in component reliability and performance were required before hydrogen systems for energy conversion could be realized on a commercial scale. It also illustrated that integration of hydrogen components was often more difficult than commonly believed.

University of Helsinki Hydrogen Energy Experiment

Kauranen et al. [34] and Vanhanen et al. [61, 62] report on the development of a small photovoltaic hydrogen energy test-bed at the Helsinki University of Technology. The test-bed, initiated in 1989, consisted of a 1.3 kW PV array, a 12 kWhr lead acid battery

bank, an 800 W alkaline electrolyser, a 500 W phosphoric acid fuel cell and a variable 500 W load, outlined in Figure 2.3. The electrolyser is referred to as a pressurized type and no additional compression capabilities are mentioned. Conventional compressed hydrogen storage is assumed.

A notable feature of this test bed is the absence of power electronics to interface the components to the DC bus. The component characteristics were carefully matched allowing direct connection to the DC bus, thus eliminating the need for power conditioning converters. Furthermore, the load is a simple DC resistive type so the typical inversion step is forgone. The power flow between system elements is directly linked to the state of charge of the batteries which determines the bus voltage. The experimental flexibility of the system is therefore restricted to a limited operating envelope.

The system was designed with the belief that the round-trip efficiency of the hydrogen storage loop would be too low for daily use and applicable only to seasonal storage. Adequate short-term battery storage was therefore a necessity. Numerical models for the system components were developed and evaluated against experimental data. Simulation results showed good agreement with test data and a round-trip efficiency of 25 percent for the hydrogen storage system was demonstrated. Details regarding the fuel cell performance are omitted from the publications.

A conclusion drawn from the research was that a PV array has to supply approximately three times the load energy for 100 percent self-sufficiency when operating in Helisinki's climate using the technology of the day. However, given the relatively large battery storage capacity, idealized load, and lack of power conversion devices (i.e., low parasitic loses) this result many not be applicable to practical size systems. It would be interesting to know the ratio for a fully integrated renewable energy system using present day components.
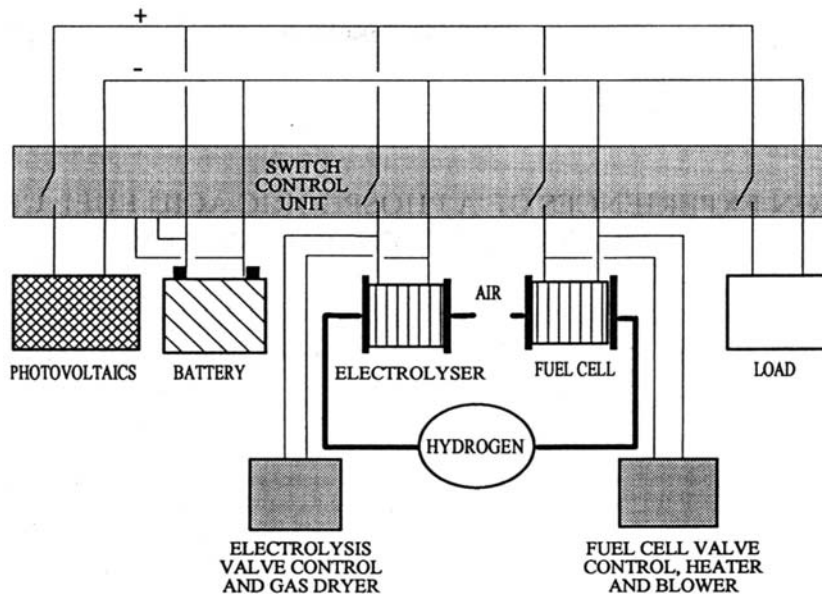
Figure 2.3 University of Helsinki Hydrogen Energy Test Facility Schematic

Schatz Solar Hydrogen Project

Lehman et al. [27] discussed the Schatz Solar Hydrogen Project initiated in 1989 at Humbolt State University. This project began with the goal of demonstrating that hydrogen was a practical storage media for solar energy. The system in its final form consisted of a 9.2 kW solar array, 5 kWhr battery bank, 12 cell 6 kW bipolar alkaline electrolyser, 8 bar compressed hydrogen storage, a prototype 1.5 kW PEM fuel cell, DC-AC output inversion, and a 600 watts aquarium air compressor load. A system schematic is given in Figure 2.4.
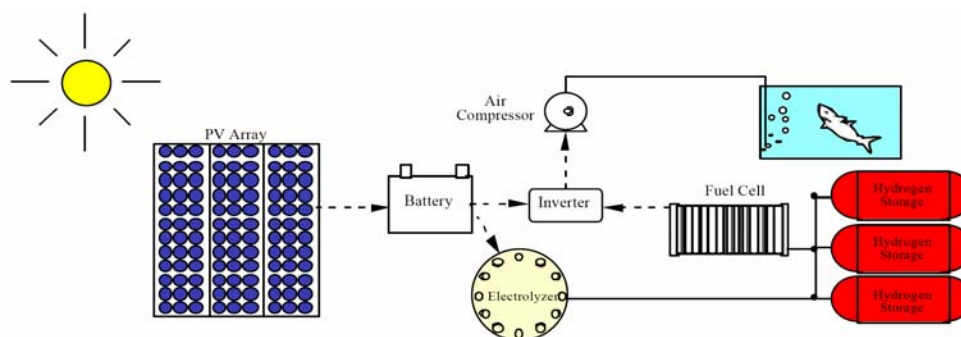
Figure 2.4 Schatz Solar Hydrogen Project Schematic

System reliability was a key design parameter given that the load was a primary life support system for the aquarium. A fail-safe power transfer system was incorporated to return the air compressor to local grid power in the event of a failure in the hydrogen energy system. Although the solar collectors, electrolyser, hydrogen storage and inverter worked reliably, problems with the fuel cell led to limited system utilization. The original commercial fuel cell manufacturer was unable to provide a working unit during the first two years of the experimental program. The poor fuel cell performance led to a university research initiative to develop fuel cell technologies.

The system was not energy self-sufficient due to the control system and auxiliary components loads (electrolyser makeup water pump, cooling systems, safety monitors etc). As such, accurate figures on the overall system efficiencies are not available. However, an efficiency of 34 percent can be estimated based on the ratio of power to produce and subsequently recovered from a given volume of hydrogen. Other efficiencies are quoted for the electrolyser and fuel cell, but are somewhat dubious since they do not take into account the parasitic loads. This work reinforces the need for accurate accounting of all system loads when evaluating the real world efficiency and utility of an energy system.

Another technical challenge identified was the difficulty in matching the electrolyser and PV array characteristics. The direct connection topology between the electrolyser and the DC bus introduced control issues during electrolyser start-up and illustrated the need for power conditioning between DC bus elements. Similar problems were not mentioned in the Helsinki test-bed but they had over 15 times the relative battery capacity. This raises questions on the minimum short-term energy buffer requirements to maintain system stability.

Freiburg Self-Sufficient Solar House

Goetzberger et al. [63] outlines the renewable energy system of a self-sufficient solar house designed to use only solar radiation to supply heat and electricity for the inhabitants. The house, located in Germany, incorporated many novel technologies including: transparent insulation, solar space heating, advanced flat plate solar hot water heaters, 4.2 kW solar array, 19 kWhr battery storage, 2 kW alkaline high pressure

electrolyser, compressed hydrogen and oxygen storage, a 500 watt alkaline fuel cell, power inverters, and energy efficient hydrogen powered appliances. A brief description of the energy systems utilized in the house is provided in Figure 2.5.

1: windows, 2: TI wall, 3: PV generator, 4: thermal collector, 5: control and data acquisition, 6: battery, 7: inverter, 8: electrolyser, 9: fuel cell, 10: H_2 and O_2 storage tanks, 11: heat exchanger, 12: water storage tank, 13: mains water, 14: ventilation heat recovery, 15: heater, 16: earth heat exchanger, 17: fresh air, 18: exhaust air, 19: return air.
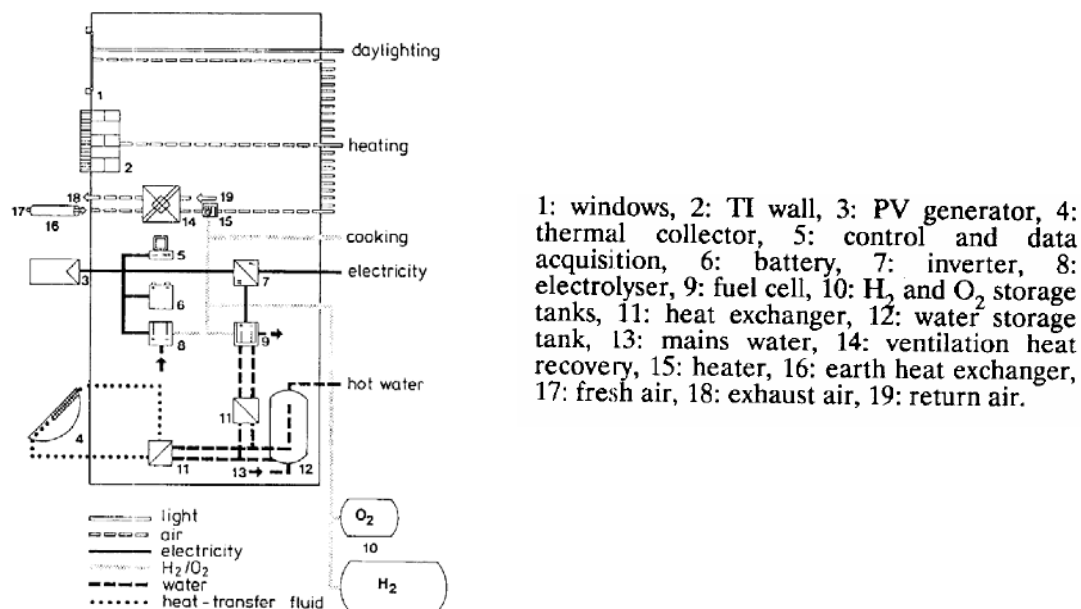
Figure 2.5 Freilburg Self-Sufficient Solar House Energy System Diagram

The primary design focus was on the thermal aspects considering that 80 percent of the energy demand of a conventional German residence is for space heating. Seasonal thermal self-sufficiency was achieved, but the electrical demand was under estimated. The installed PV capacity was insufficient to supply the electrical load under real operating conditions. Fuel cell reliability proved to be a serious issue for completing the project. A stack life time of less the 100 hours was obtained leading to very short demonstrations of house in self-sustained operation. Initial publications indicate that a replacement fuel cell was planned for the future, but follow up reports detailing performance improvements of the house were not found.

This project demonstrated that the photovoltaic system must supply much more energy than required for the basic household electrical appliances alone. For example, the energy requirements of the control, conversion, and emergency systems for the hydrogen related equipment was equivalent to the electrical energy demand of all the common household appliances. Considerable thought must be given to the design and integration of the hydrogen buffers peripheral support systems.

University of Oldenburg Renewable Energy Project

Limited information on the University of Oldenburg experimental system is available. A brief overview of the system is given by Snyder [36], who reports that the system began operation in 1990 and included both wind and solar power generation components, see Figure 2.6. The system employed a 6.2 kW PV array and a 5 kW wind turbine, a battery bank of unspecified size, an 800 W electrolyser, compressed hydrogen storage, a 600 W fuel cell, and an undefined load. It is noted that the system was designed for seasonal energy storage inferring that significant hydrogen storage capacity was implemented.

This is the first experimental renewable energy test-bed reported to have both wind and solar input sources. However, it is likely to have encountered fuel cell reliability issues that plagued other experimental studies conducted at that time period.
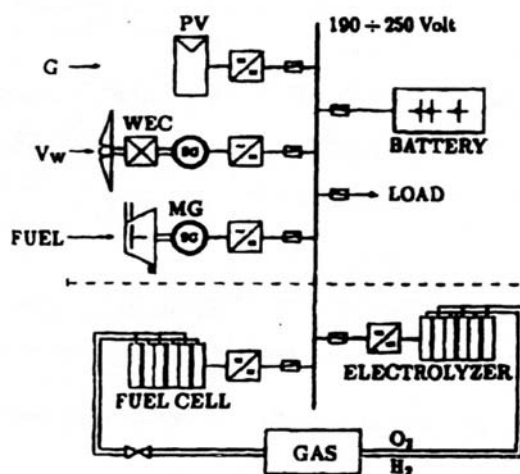
Figure 2.6 University of Oldenburg Renewable Energy Test Facility

INTA Solar Hydrogen Project

Schucan [35] summarizes a demonstration project for non-centralized electric generation using hydrogen and fuel cells conducted at the Instituto Nacional de Tecnica Aeroespacial (INTA) in Huelva, Spain. Work on the project occurred primarily between 1990 and 1994. Detailed experimental results are not reported in the literature. The basic system outlined in Figure 2.7 consists of an 8.5 kW photovoltaic field, a 5.2 kW alkaline electrolyser, metal hydride and compressed hydrogen gas storage, a 10 kW phosphoric acid fuel cell, and an AC inverter tied to a local grid load. A methanol reformer was

included as a secondary hydrogen source to improve the overall flexibility of the experimental system.

An alternate system architecture was employed where the renewable input was tied directly to hydrogen generation. Short-term battery storage of PV power was not included. The number of functional electrolyser cells could be varied based on the available solar power. During periods with high solar radiation 24 cells were used to draw 90-120 A from the PV array. By adding more cells in series, the effective electrolyser load decreases for a given PV array voltage. The current draw for 25 and 26 cells was 60-90 A and 30-60 A respectively. This simple control method dispensed with the need for a DC-DC matching converter to maximize power transfer from the PV array.
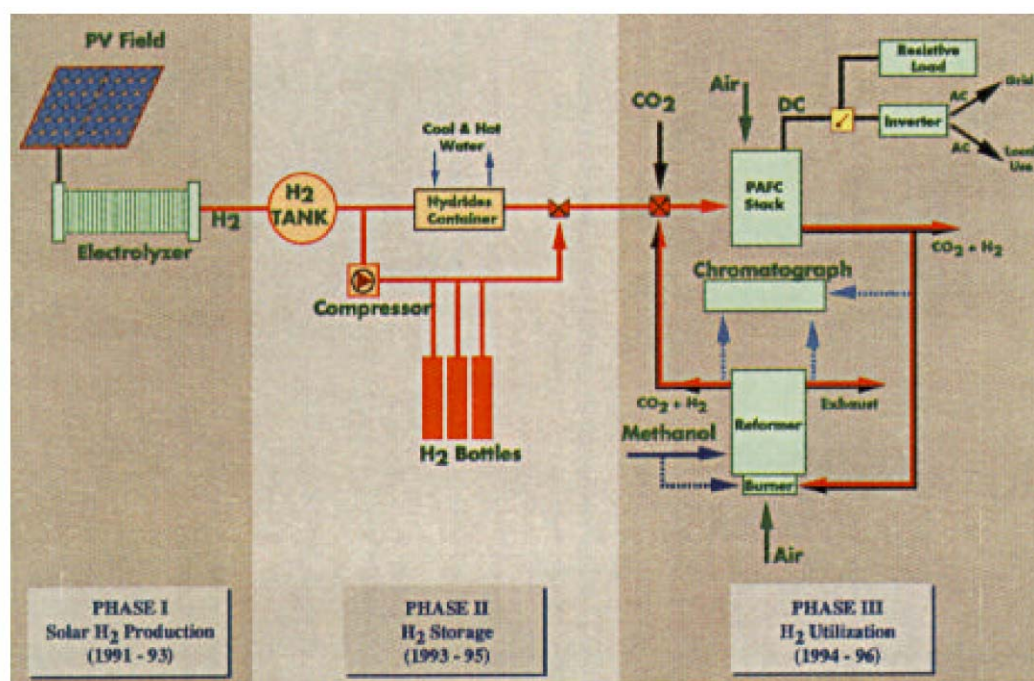
Figure 2.7 INTA Solar Hydrogen Energy Test Facility Block Diagram

The system was in operation for three years and worked satisfactorily in direct connected operational mode. Integration issues typically encountered in systems employing a common DC bus were avoided by fully decoupling production and utilization using hydrogen buffering. However, the global efficiency of this system architecture was shown to be less then three percent. This work illustrates that the hydrogen system

architecture can have a significant impact on performance and that direct comparisons between various configurations would be valuable.

Friedli Residential Solar Hydrogen

Hollmuller et al. [26] outlines a photovoltaic hydrogen production and storage installation in a private residence in Switzerland that began operation in 1991. This system is unique in the sense that it was built by the owner Markus Friedli for domestic use without major support from public funds. It was constructed primarily from commercial components and operates without an elaborate control scheme. The system consists of a 4.5 kW photovoltaic array, a 38 kWhr lead acid battery bank, a 10 kW alkaline electrolyser, and a metal hydride hydrogen storage system, see Figure 2.8. Domestic AC power is supplied exclusively from the battery bank via DC-AC inversion. An option to export AC power to the grid exists. A converter for battery charging and electrolyser operation from the grid is included for backup. Grid power is also used for the electrical control circuits. Hydrogen is consumed in several household appliances as well as a converted mini bus with a separate metal hydride storage system.

Gas purification and storage system were the reported weak points in the system implementation. The hydrogen purification unit consists of a water bath, condenser and dryer. The condenser filled with noble metals catalytically removes oxygen, but required regeneration by heating and reverse flow consuming up to eight percent of the hydrogen produced. An intermediate compressor increased the hydrogen pressure to 29 bar required by the metal hydride storage system. The regeneration and compression processes were power intensive and as such utilize the grid. The storage capacity of the hydride system was compromised by the hydrogen purity and failure to use a thermalizing circuit. In the original configuration, the system did not contain sufficient hydrogen storage for seasonal sustainability. A ten fold increase in capacity would be required given the reported consumption levels.

Several peripheral issues that arose given the residential nature of the project were the high water consumption (in excess of 40 L/hr) required primarily for electrolyser cooling and the lack of an automated control system to select the storage mode

(batteries/hydrogen/grid). For safety reasons, the system was only operated when the inhabitants were at home leading to low overall efficiency.

Although this project did not include a regenerative fuel cell, the work is relevant to the current research since it demonstrates a real world implementation of a residential scale renewable energy system. It illustrates that individuals are seeking alternative solutions for powering their households. However, also reveals how difficult it is to implement hydrogen based solution without the grid for backup or partial assistance. The fact that the project was completed without the resources and assistance of a research organization specializing in hydrogen system development is impressive. The only reported interaction was system characterization and performance studies conducted after the installation was complete.
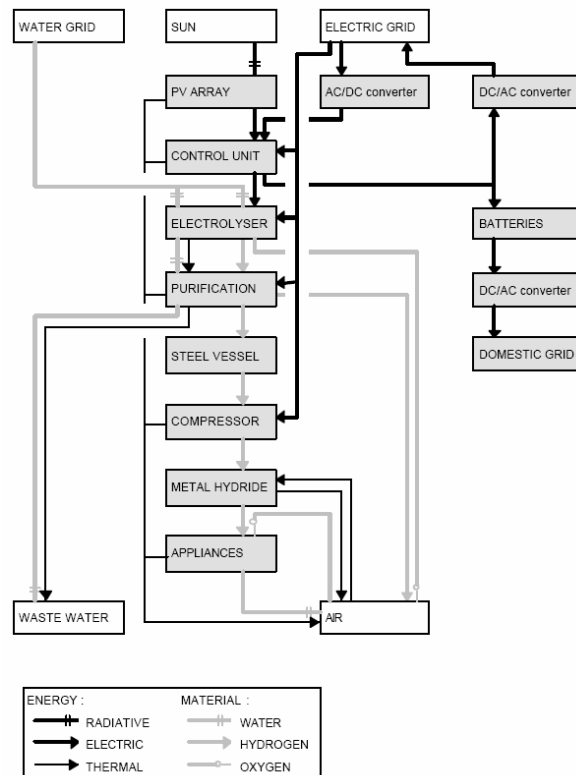
Figure 2.8 Friedli Residential Solar Hydrogen House Energy System Block Diagram

PECS: Photovoltaic Energy Conversion System

Hollenberg et al. [64] describes a small photovoltaic energy conversion system constructed at The Cooper Union engineering school in 1992. This system consisted of a

150 W solar array, a 95 W electrolyser, metal hydride hydrogen storage, and a PEM fuel cell outlined in Figure 8. A significant portion of the work centered on the development of a load matching device between the PV array and the electrolyser. Once this was constructed, experiments were conducted that studied the effect of unsteady insolation on hydrogen production. They concluded that the hydrogen generation did not exhibit the same unsteady behaviour as the insolation and that significant smoothing in hydrogen production occurred.

Detailed results for the fuel cell and combined system operation are not reported hinting that the test capabilities were never fully developed. The reported electrolyser operating behaviour is desirable from a system implementation perspective but the experiments were conducted using low power devices. Duplicating these results with larger system components is required to validate that the smoothing effect is scale independent.
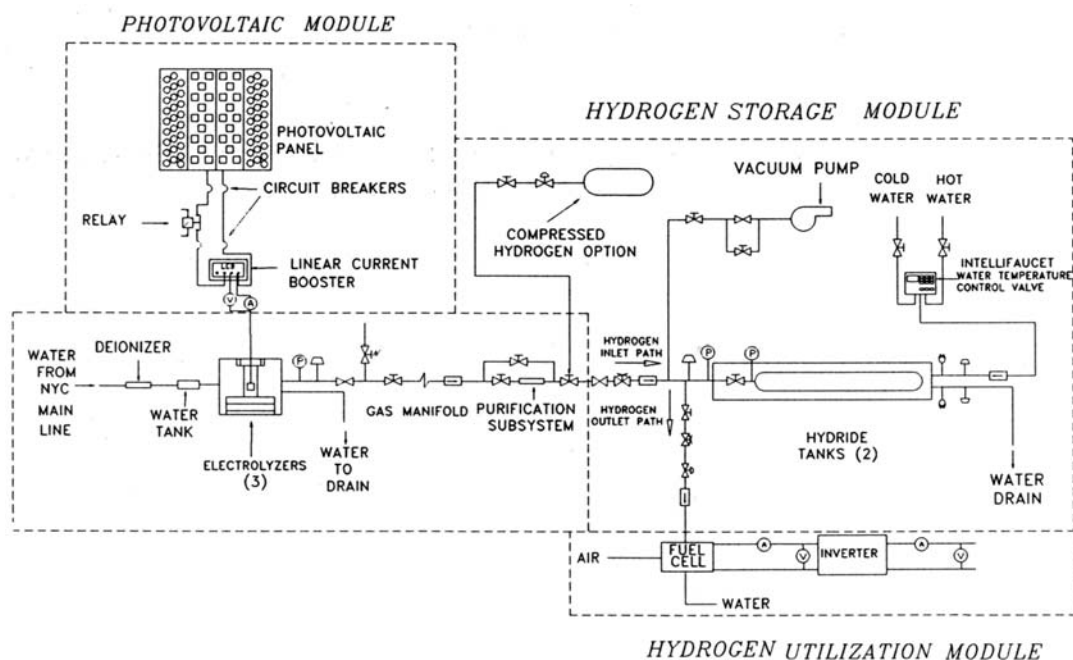
Figure 2.9 The Copper Union Hydrogen Energy Test Facility Schematic

PHOEBUS: PHOtovoltaik, Elektrolyseur, Brennstoffzelle Und Ststemtechnik

The German PHOEBUS plant located at Central Library in Forshungszentrum was a large, high visibility demonstration project for solar hydrogen energy buffering. Ghosh et al. [20] summarizes the equipment used and operating experience gained though this ten

year project. The equipment included four photovoltaic arrays totalling 312 m^2 with combined output of 43 kW, DC-DC matching converters, 303 kWhr of lead acid battery storage, a low-pressure 5-26 kW 35 V alkaline electrolyser, high-pressure hydrogen and oxygen storage, several different fuel cells, and a 15 kW inverter feeding a local grid, see Figure 2.10. The system was built around a high voltage bus (200-260 V) in an effort to reduce system ohmic losses.
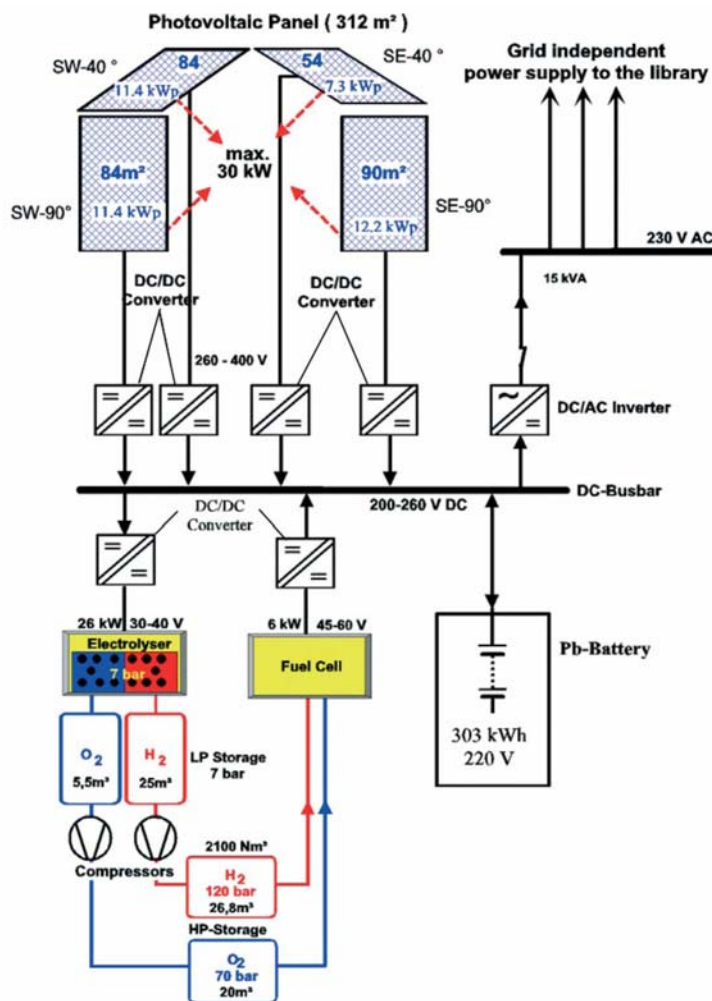
Figure 2.10 PHEOBUS Block Diagram

At the start of the project pneumatic driven piston compressors were used, but reliability issues and the high input energy required to compress the hydrogen and oxygen to 120 and 70 bar respectively (more than 100 percent of the energy stored in the gas) led to replacement with high efficiency metal membrane compressors. Problems encountered with the original compressors also led to the development of a smaller 5 kW high-

pressure (120 bar) electrolyser and a two stage solar thermal metal-hydride compressor. During the course of the project, both of these units were tested and integrated into the system. However, the original electrolyser remained the main hydrogen generator for the system.

A 6.5 kW Siemens alkaline fuel cell was used in the first phase of the project, but was found to be too unreliable. Efforts were made to develop two replacement 2.5 kW PEM fuel cells. These first PEM fuel cells were also plagued with operational problems and finally in 1999, a reliable 5 kW unit was installed which functioned until the end of the project. An AC-DC converter 'fuel cell simulator' was extensively used as a proxy to allow continued operation of the system during periods where the fuel cell power was unavailable.

One of the main goals behind PHOEBUS was to show that a high level of energetic reliability could be achieved in a renewable energy system with very low battery capacity. Although the battery bank consisting of 110 lead acid 1380 Ahr cells appears large, it could only fulfil the energy demand of the system for 3 days. Operational results indicated that the hydrogen system could store sufficient energy to offset seasonal fluctuations in solar input. A sensitivity analysis of photovoltaic array position to the long-term system energy balance was conducted. Average efficiency associated with the hydrogen buffer loop was calculated at only 22 percent.

In the original plant design, the electrolyser and the photovoltaic array output were of equivalent power ratings. During the course of operating, it was determined that sufficient hydrogen for long-term storage could be produced with a smaller electrolyser without sacrificing the energetic reliability of the system. However, a reduction factor is not specified. Additional research is required to determine the relative scaling factors between system components. Energy management schemes based on the battery state of charge were conceived during this project that warrant further development.

2.3   Second Generation Hydrogen Renewable Energy Systems

A renewed focus on energy systems with hydrogen buffering started in the late 1990's marked by the deployment of second generation projects built with significantly improved components. The systems are typically smaller in size and designed as research tools to study renewable energy systems in comparison to the first generation systems which were built as dedicated demonstration projects. A summary of the basic system parameters for the various projects is given in Table 6.2.

ENEA - Wind-Hydrogen Research

Dutton et al. [65] summarizes the results from a project at ENEA's Casaccia Reseach Center in Italy designed to examine the potential of wind power to generate hydrogen. The goal of the work, which commenced in 1996, was to determine the effect of fluctuating power, indicative of wind generation, on electrolyser operation. The system consisted of a 5.2 kW Riva wind turbine, 36 kWhr battery bank, a 2.25 kW alkaline electrolyser and two dump loads, see Figure 2.11. A DC-DC converter was used to match the bus and electrolyser voltages, but typically operated in a transparent manner generating a linear transformation of bus voltage. Hydrogen storage and regenerative components were not incorporated so the system is incomplete from a full hydrogen energy buffer standpoint. However, research conducted on the electrolyser operation is enlightening and warrants discussion.

Second Generation Renewable Hydrogen Energy Systems

	ENEA-Wind Hydrogen Project	ENEA- SAPHYS	Hydrogen Research Institute	Desert Research Institute	Grimstad Renewable Energy Park	PVFC-SYS
Year Initiated	1996	1996	1999	1999	2000	2000
Location	Italy	Italy	Canada	USA	Norway	France
Solar Input	none	5.6 kW$_p$	1 kW$_p$	2 kW$_p$	20 kW$_p$	3.6 kW$_p$
Wind Input	5.2 kW$_p$	none	10 kW$_p$	3 kW$_p$	remote data link	none
Battery Storage	36 kWh @ 110 VDC	51 kWh @ 36 VDC	42 kWh @ 48 VDC	8.4 kWh @ 24 VDC	none	1.9 kWh @ 24 VDC
Electrolyser	2 kW$_{el}$ @ 20 bar	5 kW$_{el}$ @ 20 bar	5 kW$_{el}$ @ 7 bar	5 kW$_{el}$ @ 6 bar	50 kW$_{el}$ @ 15 bar	3.6 kW$_{el}$ @ 10 bar
H$_2$ Storage	None	300 Nm^3 @ 20 bar + 24 m^3 MH	3.8 m^3 @ 10 bar	2.2 m^3 @ 6 bar	8 m^3 @ 15 bar	0.4 m^3 @ 10 bar
O$_2$ Storage	None	none	1 m^3 @ 8 bar	none	none	0.2m^3 @ 10 bar
Fuel Cell	None	3 kW$_{el}$ PEM	5 kW$_{el}$ PEM	2 kW$_{el}$ PEM	2.5 kW$_{el}$ AFC	4 kW$_{el}$ PEM
Load	None	5 kW variable load	12 kW DC 3 kW AC	5 kW AC load bank	8 kW local grid	5 kW AC load
Notes	Fluctuating RE input hydrogen generation experiment	Residential load profiles were simulated	Integrated system with matching converters (10kW power source)	Direct electrolyser – Bus connection limits system flexability	Diverse solar heating system interconnect	Pre commercial venture with two demonstration projects

Table 2.2 Component Data for Renewable Energy Systems - Late 1990's to 2003
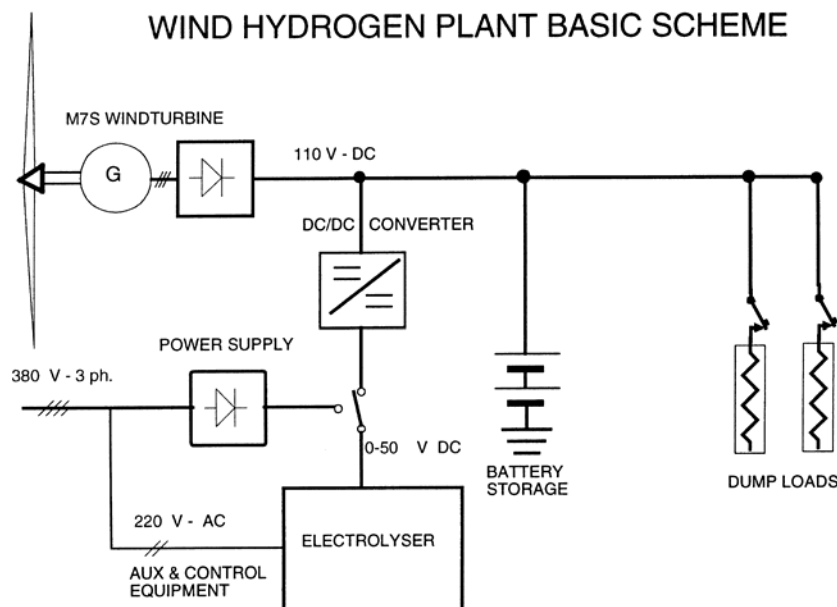
Figure 2.11 ENEA Wind Hydrogen Plant Schematic

An investigation of the electrolyser response to rapid input fluctuations was conducted using 1 second power data from the wind turbine and with 10, 60, 150 second averages. Results were benchmarked against constant operation for a 24 hour period. No significant performance differences were observed other than a small decrease in volume and gas purity (both less then 2.5 percent). The decline in gas purity appeared to be affected by power variations on the scale of a few minutes rather than a few seconds. Furthermore, simulation work conducted in conjunction with the experimental program suggest that a higher overall efficiency (and hence increased volume of hydrogen produced) can be obtained by systems with additional energy storage (i.e., batteries) where the electrolyser is operated continually at partial load.

Independent verification of these results would form an important contribution since the general characteristic of power smoothing without performance degradation is a common assumption applied to electrolyser operation in a renewable-regenerative system.

SYPHYS: Stand-Alone Small Sized Photovoltaic Hydrogen Energy System

SYMPAS was a joint Italian, Norwegian, and German undertaking conducted in tandem with the ENEA wind project discussed above. The focus of work, which started in 1996, was to assess hydrogen energy storage potential for a small stand-alone system utilizing solar input. Galli and Stefanoni [30] describes the system targeted at a residential scale with 5.6 kW PV array, 51 kWhr battery storage, a high-pressure electrolyser, compressed hydrogen gas storage, a 3 kW PEM fuel cell and an integrated control system, illustrated in Figure 2.11. The electrolyser and fuel cell were connected to the common bus using separate DC-DC converters. An electronic load was used to simulate the energy demand of an isolated house with typical domestic summer and winter electrical loads. While the primary components performed satisfactorily, frequent failures of auxiliary components (mostly related to the electrolyser) resulted in poor system reliability and limited experimental results in continuous operational mode.

Development of control strategies was a major aspect of the experimental study. The initial control algorithm was based on the battery state of charge. However, it was determined that discrepancies between the calculated and the actual energy stored in the batteries resulted in control stability issues. A control algorithm based on the bus voltage and load profile was subsequently developed but required periodic battery recharging indicating that an accurate system balance is hard to obtain.
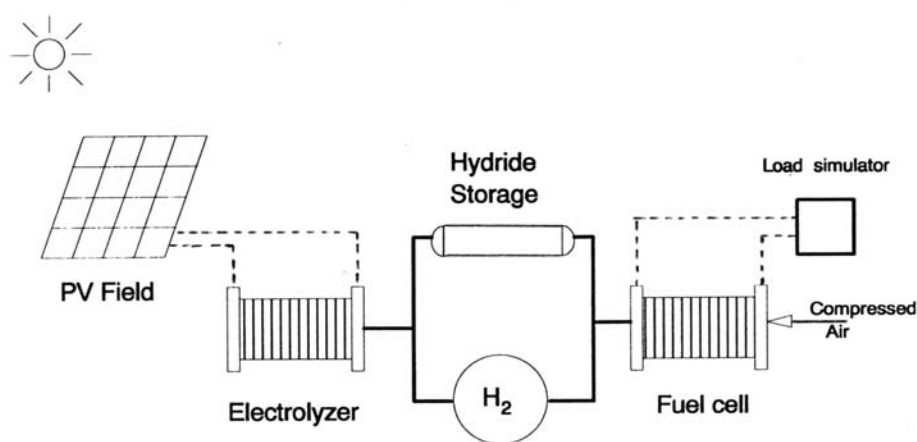
Figure 2.12 SYMPHYS Schematic Diagram

The time required to make the basic system operational was longer then expected and as a result, funding for the program ended before long-term operational data could be collected. The general conclusions from this study were that the high cost, complexity and reliability issues pose significant barriers against widespread adoption of hydrogen buffered energy systems. Control issues present additional operational challenges that must be addressed.

Hydrogen Research Institute Integrated Renewable Energy System

Hydrogen Research Institute at the University of Quebec, Trois-Rivieres, started development of experimental platform in 1999 to test and optimize control strategies for renewable energy systems with hydrogen buffering. Agbossou et al. [29] describes the system which consists of a 10 kW wind turbine, a 1kW PV array, a 42 kWhr battery bank, a 5 kW electrolyser, compressed hydrogen storage, a 5 kW PEM fuel cell and an AC output inverter, see Figure 2.13. Adjustable output DC-DC converters are used to match the VI characteristics of the individual devices to the common DC bus. A 10 kW power supply is used to supplement input power during periods of low renewable source availability.

Agbossou et al. [39] reports that the facility is operational and outlines the systems performance for a typical day. The control algorithm is based on the battery state-of-charge. Threshold levels for diverting power to the electrolyser or operating the fuel cell have been determined experimentally. The energy management system maintains the batteries at nearly full charge and only allows a short discharge cycle before engaging the fuel cell. In this mode, the batteries provide bus voltage regulation and take care of short term transients while the hydrogen leg provides the energy storage function.

Published results indicate that successful system operation in a stand-alone mode has been achieved. Significant effort has been devoted to the development and implementation of control strategies for generic renew-regenerative systems. Research on fast switching loads has shown that stable system operation can be achieved with the proper control strategy.
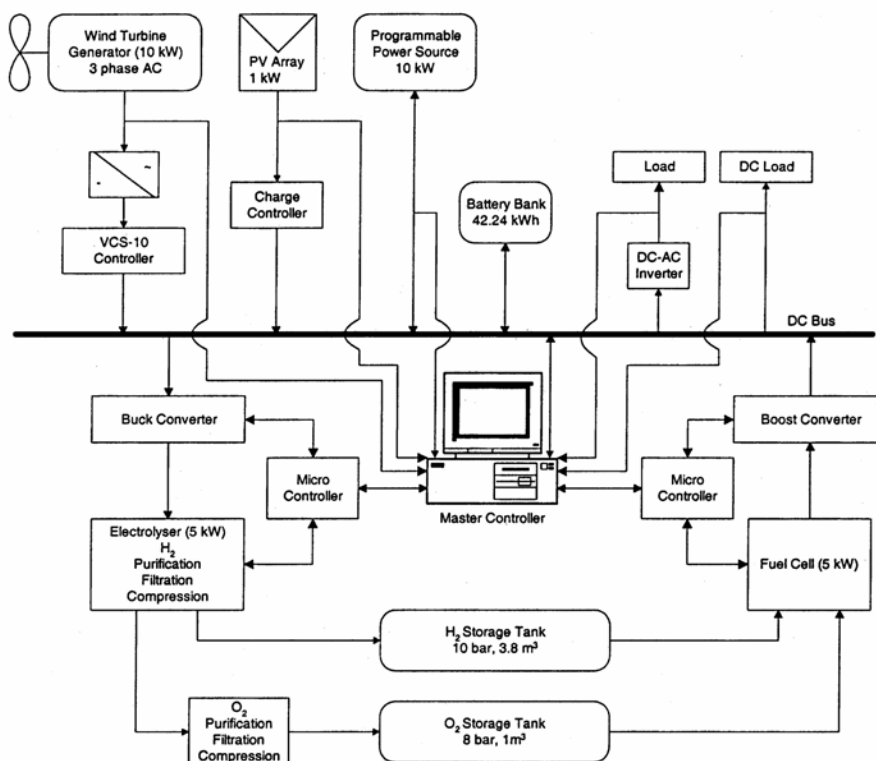
Figure 2.13 Hydrogen Research Institute Test Facility Block Diagram

Unlike the systems covered thus far, reliability issues with the fuel cell have not been reported. This is an encouraging sign indicating that the present generation PEM fuel cells may be robust enough for integration into real world stand alone renewable energy systems.

Desert Research Institute Hybrid Energy System

Desert Research Institute started development in 1999 of a prototype residential scale stand-alone power system based on wind and solar inputs with hydrogen energy buffering. Rambach [31] and Jacobson et al. [37] describe the system which includes two 1.5 kW wind turbines, a 2 kW PV array, 8.4 kWhr battery storage, a 5 kW alkaline electrolyser, compressed hydrogen storage, a 2 kW PEM fuel cell, and a 5 kW programmable load, see Figure 2.14. Modified commercial charge controllers have been used to deal with the voltage mismatch between the common bus and PV arrays, wind turbines and fuel cell. This method of control dissipates the excess voltage as heat and

results in a moderate loss in system efficiency. Furthermore, the electrolyser has no power conditioning and is directly connected to the bus. When in use, the current draw is a function of the bus voltage and stack temperature which leaves little room for system control. A DC-DC converter is under development to address this problem.

The system is intended as a platform for testing generic control algorithms to provide reliable power from temporal sources. As of the start of the IRENE project, publications from DRI have been limited to a master's thesis [36] describing the system and several Department of Energy briefs. They state that the system is functional and outline plans for future development of advanced control software to handle more complex (real world) operating conditions. An experimental program to collect data for various load profiles representative of remote locations is included.
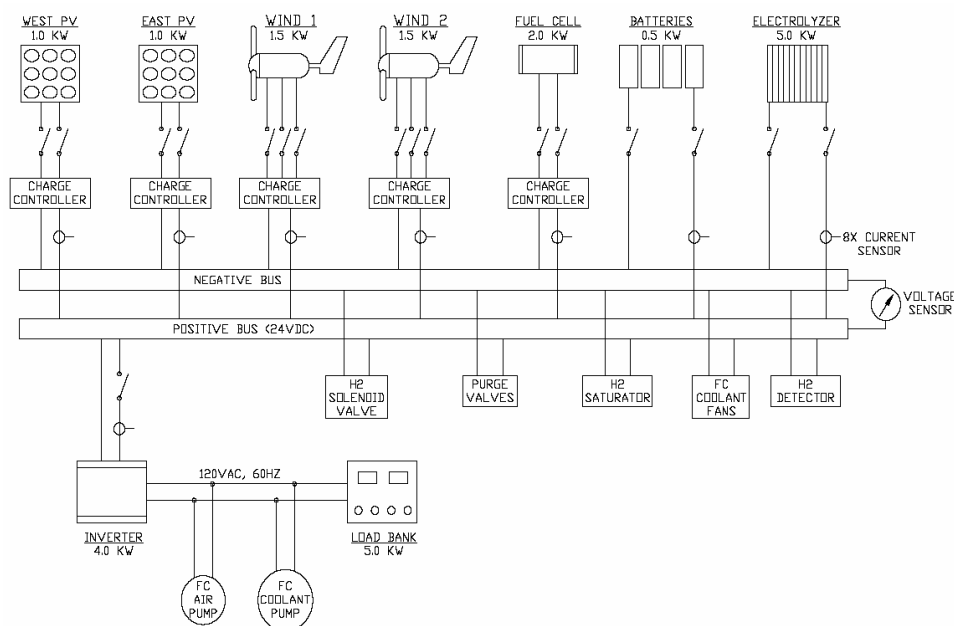
Figure 2.14 Desert Research Institute Hybrid Hydrogen Energy Facility Schematic

Grimstad Renewable Energy Park

Valand et al. [32] describes the Energy Park located in Grimstad, Norway, which opened in 2000. This integrated energy demonstration project incorporates a wide assortment of renewable energy technologies including thermal, biological, and electrical, see Figure

2.15. Solar collectors, heat exchangers, heat pumps, hot water storage tanks, deep boreholes, and a heat delivery system are showcased in the thermal system. Energy crops such as reed canary grass and short rotation coppice of willow have also been planted to study the energy content of the plants under Norwegian conditions. The electrical system consists of 20 kW photovoltaic array, a 50 kW high-pressure alkaline electrolyser, compressed hydrogen gas storage, a 2.5 kW alkaline fuel cell, and an AC inverter tied to a local grid load. Battery storage is not implemented. Although a wind energy converter is not located on site, wind energy data is available via a direct data connection to a windmill park located in southern Norway.

Numerous sensors distributed throughout the park are tied into a central control and data acquisition system. The park intends on broadcasting real-time data via the Internet so that researcher's around the world can participate in monitoring and analyzing the performance of the various systems. Security issues have to be resolved before data transmission will commence.

The energy park is reported as functional and collecting data but experimental results where not published in the literature at the onset of the IRENE project. System characterization and analysis work is currently in progress by several Ph.D. candidates. Results are pending.
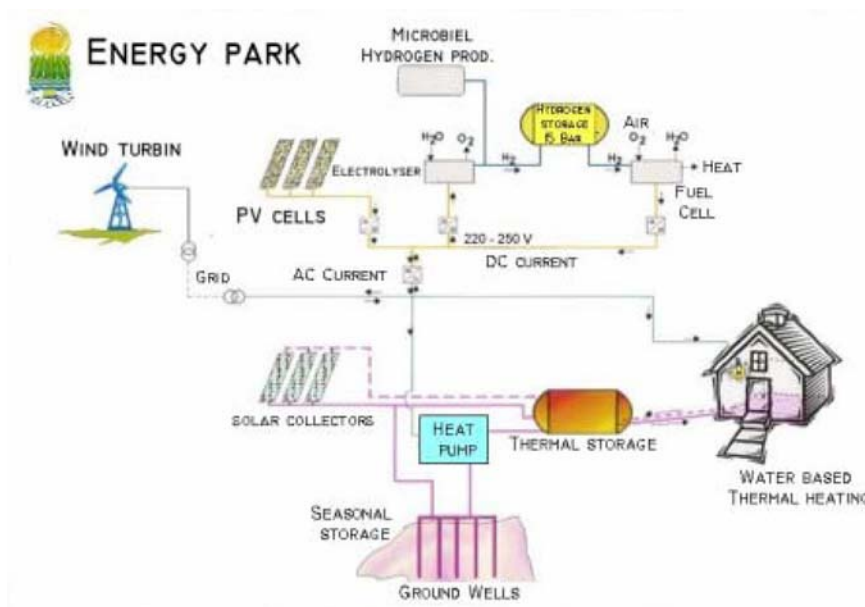
Figure 2.15 Renewable Energy Park Component Diagram

PVFC-Systems

The PVFC-SYS is a joint industrial / academic project started in 2000 with a focus on developing renewable energy systems with hydrogen technology to service 5 to 10 kW remote applications.   The first stage of the project entailed the development of two experimental platforms, one at a research institute at Sophia Antipolis, France and one in an industrial setting at Agrate, Italy.   Busquet et al. [66] describes the basic experimental system composed of a 3.6 kW PV array, 1.9 kWhr battery storage, a 3.6 kW electrolyser, compressed gas storage, a 4 kW PEM fuel cell and 5 kW load, see Figure 2.16.   During the initial phase of the project, the power management unit was not functional so experimental results were not published.   Preliminary modeling results are reported and indicate that seasonal operation of the test rigs will not be possible given the limited hydrogen storage capacity.   Further results have not been reported in the literature so it is not known if the systems are currently functional.
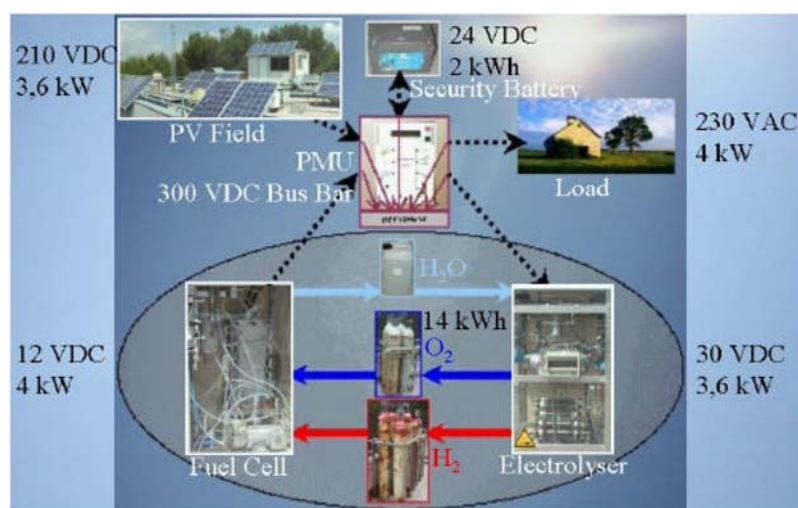
Figure 2.16 PVFC Hydrogen Energy System Conceptual Diagram

Recently Developed Systems

Since the start of the IRENE project, several renewable-regenerative systems have been or are in the process of been developed at other research institutes. The HaRI project at West Beacon Farms, Leicestershire, UK utilizes an assortment of renewable conversion devices, loads and storage technologies as reported by Little et al [67]. Gazey et al [68]

reports on the PURE project, an integrated wind hydrogen renewable energy project on the remote Island of Unst, UK. The system is designed to supply renewable energy to five small businesses.

A similar type project called Utsira was initiated in 2004 to supply 10 households with renewable power on the Island of Haugesund off the coast of Norway. Both of these projects incorporate hydrogen generation, storage and utilization to buffer the variability of the renewable resource. Nakken et al. [69] briefly describes the operational experience with the Utsira project thus far and indicates that the high number of device interfaces within the system created major development challenges. The wind resource was also underestimated in the pre-studies. The most difficult operational issue encountered has been the control and regulation of the autonomous grid during times with large power generation and low demand. The system generates substantial surplus energy which is not currently used due to the limited electrolyser capacity.

The research institute Riso in conjunction with the Danish Technical University are developing SYSLAB, a platform for research and testing of decentralised energy resource. This system incorporates a variety of renewable energy technologies. However, the main research is focused on system control for distributed and decentralised systems. Publication of the current research is pending [70].

2.4   Summary

A wide variety of articles focusing on the theoretical modeling of hydrogen based renewable energy systems are presented in the literature. These models to predict the performance of a renewable-regenerative energy system servicing a given load on a seasonal basis but typically employ large time steps and assume that system response can be predicted from average parameter values. High level models often treat the energy buffer as a black box with an efficiency factor defining the input / output relationship. The dynamics of the system within the box are ignored. These models tend to be for large scale systems where other factors, like the physical size of the renewable input devices, storage, cost etc., are not contemplated.

Lower level models divide the energy buffer into functional blocks, applying separate efficiencies for the hydrogen generation, storage, and regeneration stages. These models have the potential to more accurately predict the response of a real IRENE like system but still often neglect the dynamic interactions between system components. A common assumption in the modeling the hydrogen generation stage is that the electrolyser can respond to rapid changes in the input power and, as such, function as a load-leveling device, absorbing any excess energy that may be present.

While the theoretical studies provide insight on system issues, they fail to address practical concerns that arise from the integration of real components.

A number of experimental renewable energy systems with hydrogen energy buffering have been developed since the mid 1980's. The first generation of systems demonstrated that hydrogen could be generated from surplus renewable input power through water electrolysis and stored for both short-term and seasonal energy buffering. They illustrated that a continuous supply of power can be derived from an intermittent renewable energy source coupled to the appropriate hydrogen conversion devices. However, the test-beds were constructed primarily from custom components, often one-off prototypes, and were plagued with reliability issues. Energy self sufficiency was for the most part not obtained due to the limited energy generated from the renewable sources coupled with poor component efficiencies and large parasitic system loads. All

of the demonstration projects report major operational problems with the fuel cells used in the regenerative subsystem. They revealed that significant advances in electrolyser, fuel cells, hydrogen storage and power conditioning technologies were required before reliable system operation could be achieved.

A renewed focus on energy systems with hydrogen buffering started in the late 1990's marked by the deployment of second generation projects built with significantly improved components. These systems are typically smaller in size (targeted at the residential scale) and designed primarily as research tools. The reported reliability of these systems is better, due mostly to improved fuel cell module. However, these systems remain complex, expensive and lack sufficient hydrogen storage capacity for long duration seasonal experiments. Research efforts with these test beds are focused primarily on developing control algorithms for generic renewable-regenerative systems.

Although a significant amount of research work has been conducted in the development of renewable regenerative systems, detailed experimental results of the operating characteristics of these systems are not well documented in the literature. If results are published, they are typically for short durations (i.e., a single operational day) and report the average operating efficiencies. Experimental results detailing the energy balance within the system and quantifying the energy loss in various system components has yet to be reported in a unified manner. Furthermore, experimental evaluation of the dynamic interactions between system components remains an area of research that has received little attention.

PART I :

IRENE System Development

Chapter 3

IRENE Component Selection and Implications

3.1   IRENE Design Criteria

General design criteria for the IRENE test-bed were established following the review of existing experimental systems presented in Chapter 2. Several key criteria differentiate IRENE from systems built and investigated to date. The first is that IRENE was to be constructed from commercial components where possible. During the review process it became evident that in the majority of systems built thus-far, key system components that were highly specialized research prototypes were used. However, the intent with the IRENE test-bed is to investigate the integration and operational issues of renewable-regenerative systems, not the development of a particular component. Given the recent advances in renewable energy converters, electrolysers, fuel cells, power conversion devices, etc., it is *possible* to assemble a system from commercially available components. Evaluating how *practical* the hydrogen energy buffering concept is given these technologies is an important aspect of the current research. By using commercial devices the current state of the technologies will be probed and the obstacles impeding development of market ready systems will be exposed.

The second key design criterion for IRENE is the emphasis placed on hydrogen as the primary energy storage medium for the system. This represents a significant departure from many of the previous systems which utilize the grid or conventional storage devices for primary energy buffering. The intent with IRENE is to utilize the minimum battery capacity needed to maintain system stability, and generate hydrogen with any excess renewable input.

Flexibility in the configuration of power sources and sinks is the third key design criterion for the IRENE test-bed. The input side of IRENE must be capable of utilizing a variety of standard renewable energy converter technologies or hybrid combination. The output from the system must be capable of servicing real loads with a variety of demand profiles. The system should be designed in a modular fashion to allow testing of newly

developed components. In addition, the system layout should include a grid tie to maximize experimental options.

The fourth key criterion for IRENE is that the entire system be fully instrumented with a high speed data acquisition system (i.e., in the kHz range) capable of resolving the dynamic interaction between elements. Currents, voltages, mass flows, temperatures, etc., must be accurately measured and recorded for analysis. Furthermore, the system controller must be implemented in a modular fashion to allow experimentation with alternate control strategies. Appropriate safety features must also be incorporated to facilitate continuous long duration experiments.

Additional criteria for IRENE center on performance aspects and logistics. To reduce parasitic losses, system components with high overall efficiency should be selected where possible. They should be sized to minimize the need for power conditioning elements. The physical and electrical layout must include provisions for future system expansion. The initial system is to be developed at the University of Victoria, with the hydrogen related components situated in the Fuel Cell Laboratory. However, the system should be developed with future relocation to a remote site in mind.

3.2   IRENE System Sizing and Initial Configuration

The overall system capacity and configuration were not specified in the initial design criteria. During the project planning stage, sizing issues were considered, taking into account a range of practical constraints including: project budget, available laboratory space, size and capacity of relevant commercial components (renewable energy converter, fuel cells, electrolysers, inverters etc.), and the scale of systems typically modeled in the literature. The outcome was the selection of a target system capacity in the three to four kilowatt range. This capacity is similar to the typical electric demand of a Canadian residence [71].

A smaller system, in the one kilowatt range, would be easier to implement given the availability of components. However, the bulk of the simulation work referenced in Chapter 2 is conducted on larger scale systems, so the experimental results would not be

as relevant. At the other end of the spectrum, utility scale systems are often modelled but are beyond the resources and scope of the current project. A residential scale system is a good compromise, with a power demand and service requirement that the average person can relate to. Research conducted on candidate hydrogen technologies at the proposed scale will directly inform developments targeted at the residential market, particularly in the areas of distributed power generation and renewable energy integration. Likewise, the experimental work will directly benefit ongoing modeling efforts in the area of small renewable systems by providing accurate data for model validation.

In the early system design stage, it became clear that powering IRENE directly from a renewable energy conversion device would be cumbersome and provide only marginal benefits. The laboratory space designated for the project combined with the build design does not lend itself to the physical implementation of standard renewable energy conversion devices (solar panels, wind turbines etc). Although alterations to the building could be achieved, the cost is prohibitive given the marginal renewable resources available. In addition, installing real devices directly ties the experimental parameter space to the local conditions. From an experimental viewpoint, it is beneficial to decouple local conditions from the operating envelop of the system to allow investigation of broad and more generally applicable environmental conditions.

Given the physical limitations and budget constraints, an alternate approach to supplying the input power has been adopted. A controllable power supply of suitable size acts as a proxy for the renewable energy source and conversion devices. Accurate performance data and transfer functions are available for a wide variety of renewable energy conversion devices. Simulations of renewable energy sources such as wind, solar, micro hydro, tidal etc (or hybrid combinations) will be conducted by processing representative time series data with suitable transfer functions. During an experiment, the power supply will be programmed to deliver the correct amount of power at a given time step. The ability to drive IRENE from a variety of virtual input sources allows for greater experimental flexibility and compression of time scales for long duration experiments. An additional benefit of the simulated source is the ability to turn off the input when experiments are not being performed. A real renewable energy converter would require a dump load to dissipate power under these conditions.

The basic system schematic for the initial IRENE configuration is illustrated in Figure 3.1. The main components are: the proxy renewable input power source, battery bank, power conversion elements, AC load devices, and the electrolyser / hydrogen storage / fuel cell system. Control and data collection devices are not shown. Electrical components are linked via a common DC power bus. Manual fused disconnect switches provide a means for isolating individual system components. A local hydrogen distribution system links the electrolyser and fuel cell to the hydrogen storage system.
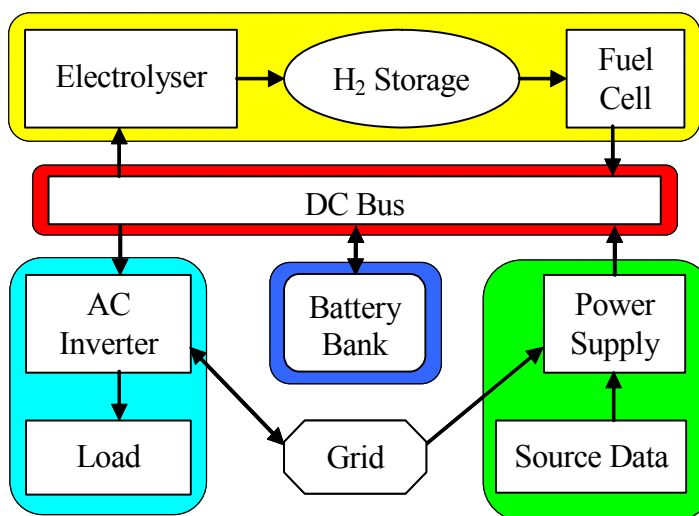
Figure 3.1 IRENE Test Platform Schematic

3.3 Commercial Component Overview

The major components obtained for the IRENE system are designed for other applications. As such, the operating characteristics are not optimized for a hydrogen energy buffering system. The specifications, design features and original design intent of the commercial components acquired are presented below.

3.3.1 Input Power Supply

A Lambda EMI ESS 15 kW grid connected power supply (Lambda Americas Inc., New Jersey) provides the primary DC input power to IRENE's nominal 48 V bus, see Figure 3.2. The output is adjustable from 0 to 60 VDC with adjustable current limiting to 250 A.

The supply was designed for industrial power applications and requires a 3 phase 208 volt grid connection. The unit operates primarily as a voltage source supplying up to the set-point current. If the load demands a higher current than available, the output voltage is automatically reduced to a level that tracks the current limit. Regulation is based on average RMS measurements at the output.

Figure 3.2 Main 15 kW Lambda Power Supply

The power supply is equipped with an optional control interface that allows for remote programming via a standard RS232 link. Power-up default mode is for manual operation based on the front panel settings. Once communication is established, remote programming of voltage, current, and mode settings is enabled. The control module can also be polled for the measured current and voltage outputs. OEM interface software was not available at the time of purchase; however, the communication protocol was included with the device documentation to allow for development of a custom user interface.

3.3.2   Short Term Energy Storage

The battery storage bank consists of 24 GNC Absolyte IIP deep cycle AGM cells (Exide Technologies, Alpharetta) arranged in series for a nominal bus voltage of 48 VDC, see Figure 3.3. These batteries are an advanced lead acid design used extensively in telecom applications. A key design features is the electrolyte confinement within glass mats surrounding the plates. This allows horizontal mounting of the batteries reducing the density stratification issues associated with standard wet cell technologies. The mechanical structure of the unit cell has been optimized for repeated deep discharging and carries a 1200 cycle rating to 80 percent depth-of-discharge (DOD). This is significantly greater than standard lead acid batteries which typically suffer capacity degradation if discharged below 80 percent [20].

Figure 3.3 IRENE Battery Bank

As with any battery, energy storage capacity depends on the history, maintenance, and immediate operating parameters, (charge / discharge rate, temperature state-of-charge etc). The batteries employed in IRENE carry an 8 hour discharge rating of 272 A-hrs. Working voltage at 80 percent DOD is approximately 46.5 VDC and are considered fully discharged at 42 VDC. The maximum charge rate is only 17 amps and the maximum charge voltage is 56 VDC. The life expectancy under optimal conditions (54 VDC float operation and regular maintenance) is ten years.

The battery capacity is relatively small and does not represent a significant energy store for the system. The battery's primary function is to stabilize the bus under transient loading and as such provide the system reference voltage system. Hence, the battery state-of-charge (SOC) directly affects the working voltage of components attached to the bus (a 42 – 56 VDC window).

3.3.3 AC Inversion Hardware

Two Xantrex SW4840 4 kW 110V AC output inverters (Trace Engineering Inc., Arlington) handle the main DC-AC inversion, see Figure 3.4. The converters were designed for backup power applications and have a number of advanced features. They can be configured to operate in isolation from each other (i.e., no correlation between output phase) or in a synchronize manner, creating 110 V (parallel configuration) or 220 V (series configuration) output. The inverters require a DC source voltage ranging from 44 to 62 VDC. The design point is 50.4 VDC at 100 amps. Internal low voltage

monitoring can be programmed to disable conversion if the DC input voltage falls below a prescribed value, thus protecting battery sources from excessive discharge.

Figure 3.4 AC Output Inverters

The inverters have grid and generator inputs on the AC side and default to these sources when present. Provided the AC source meets the prescribed frequency and voltage criteria, the inverters lock in-phase with the AC input and provide an uninterrupted output in the event of a loss in the AC connection. In this situation, the unit can initiate start-up of a backup generator. The ability to track an AC source also allows for grid assist modes. If the load demand exceeds the capacity of the AC source (i.e., supplying the in-rush current for an electric motor from a small generator) the inverters automatically transfers power from the DC source to make up the shortfall. Likewise, the inverters can also be programmed to 'sell' surplus DC power back to the grid at prescribed times.

The wide range of features incorporated in the inverters provides additional experimental capabilities to the IRENE test-bed such as load levelling and peak shaving using hydrogen or renewable power. Although a single inverter is capable of meeting the 4 kW target output capacity for the system, two units were purchased to allow flexibility in configuration. For example, one inverter can be coupled to the fuel cell on the DC side and act as 'generator' to the second inverter which in turn supplies the main AC load. In the initial system configuration the two inverters operate independently, servicing individual AC loads.

3.3.4   AC Load Devices

The primary AC load device is a NHR 4600 3kW 110V programmable load bank (NH Research Inc., Irvine) commonly used by manufacturers of power electronics for testing and verification, see Figure 3.5. The load bank contains an array of configurable power resistors linked to a sophisticated control system. Advanced features like reactive load simulation are achieved by manipulating the phase angle at which individual load elements are applied or removed.

The load bank does not have a manual user interface. All configuration, set-point, and measurement information must be accessed remotely through the RS232 communication link.   An OEM software tool was included with the unit to provide control and monitoring functions.   In addition, LabView subVI's were provided as a resource for building custom control applications.

Figure 3.5 AC Load Bank

The load is only rated at 3 kW which is less than desired system load but was the maximum available in a single air cooled unit. Higher loads can be achieved by adding parallel load banks configured in a master / slave arrangement or by incorporating fixed output loads into the system. The second option is more attractive because inductive and capacitive devices could be used to create more complex transient load profiles. Simulation work rarely addresses the peak demands placed on a system, but rather assumes average load conditions. A system designed around these simulations may fail to service the in-rush demands of real load devices.   Experimentation with various common residential load devices will provide insight into the capacity factors that must be applied to account for the different load scenarios.

3.3.5 Hydrogen Generation

The device purchased for hydrogen generation is a Stuart SRA 6 kW alkaline electrolyser (Stuart Energy Systems, Mississauga), see Figure 3.6. It was one of three electrolysers built explicitly for Small-scale Renewable energy Applications (hence the SRA designation). The basic platform was an adaptation of technology developed to generate hydrogen for weather balloons at remote meteorological stations.

Figure 3.6 Stuart Electrolyser

The cell stack is a low pressure alkaline design with a maximum 900 L/hr H_2 production capacity. The control system allows hydrogen production provided the input voltage is between 42 and 56 VDC. According to the manufacturer, hydrogen production is roughly linear with respect to input power. Standard equipment includes inlet water purification, hydrogen gas purification, compression to 17 bars, and an integrated safety monitoring system. Oxygen recovery and purification was not included.

The user interface consists of several simple connections for water, power, hydrogen and control. A ModBus communication interface and custom OEM software provides remote monitoring capabilities. However, direct control of the unit is not available over the remote data link.

3.3.6 Hydrogen Storage

Both compressed and metal hydride storage components are utilized in IRENE. The compressed hydrogen storage system includes three composite 150 L (water volume) storage tanks (Dynetek Industries Ltd., Calgary) dedicated to low pressure storage operating at the electrolyser output pressure. Excess hydrogen is compressed via a PDC 3-6000 diaphragm compressor (PDC Machines, Warminster) and stored in a fourth composite tank, see Figure 3.7. All tanks are rated for 200 bar operation to allow for future revision of the system. The compressor, powered by a 5 hp 3 phase 208 VAC motor, is rated at 0.3 Nm^3/Hr at 400 bar. A minimum inlet pressure of 10 bar is required for proper operation of the intake check valves. The tanks and compressor are standard industrial components. A local control system for compressor operation was not furnished with the compressor.

Ovonics 58250 (Ovonics Hydrogen Systems LLC, Michigan) and Palcan 300 (Palcan Power System Inc., Vancouver) metal hydride canisters are employed in the alternate hydrogen storage module. A Julabo Fcw 2500T chiller (Julabo Labortechnik GmbH, Seelbach) coupled with a water bath provides canister temperature control which is the primary mechanism driving hydrogen absorption and de-sorption by the hydride material.

Dynetek Composite 150L
Storage Tanks

PDC Diaphragm
Compressor

Ovonics
Metal Hydrides

Figure 3.7 Hydrogen Storage Components

Hydrogen storage is integral part of the overall IRENE system, so the appropriate solenoid valves, pressure regulation, temperature and flow meters have been acquired to implement a control interface for both systems.

3.3.7   Hydrogen Regeneration

A Ballard Nexa 1.2 kW fuel cell (Ballard Power Systems Inc., Burnaby) is employed as the regenerative component. It was the first commercial Proton Exchange Membrane (PEM) fuel cell system offered by Ballard, see Figure 3.8. Although marketed as product, the first generation Nexa was developed mainly as a fuel cell demonstration tool for universities and research institutes. Subsequent versions included refined packaging and additional hardware that made it a more practical power source for OEM applications.
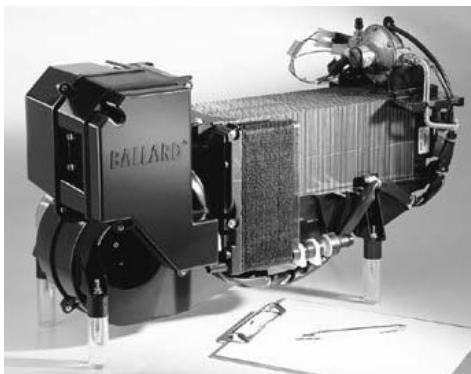
Figure 3.8 Nexa Fuel Cell

The Nexa's power rating is smaller than the nominal design rating for IRENE but is reasonably sized based on the hydrogen production capacity of the electrolyser. Hydrogen consumption at the peak rated output of 26 VDC at 46 A is 1100 L/hr. Hydrogen quality must contain less than 15 ppm CO and meet two 9's purity. Delivery pressures ranging from 2 to 15 bar are acceptable. The output voltage is unregulated and spans a significant range, 46 to 22 VDC, depending on the demand current and stack condition. Lifetime rating of the stack is only 1000 hours but reports from Nexa users have shown this to be a conservative estimate with actual lifetimes exceeding 3000 hours.

The Nexa is outfitted with the basic balance-of-plant systems required for operation. It is an air breathing design which uses a small compressor to distribute inlet air to the 46 Membrane Electrode Assemblies (MEA's). Moisture, recovered from the cathode exhaust stream through a membrane process, is used to humidify the hydrogen stream. The hydrogen side is a dead-head design with purging at intervals determined by the fuel cell control module. Stack temperature is regulated by a separate blower forcing cooling

air through designated passages in the plate and frame structure. A dedicated control module monitors the stack and adjusts parameters accordingly to ensure proper operation. Monitoring of the system is possible using an OEM software tool and a RS232 data link.

3.3.8 Data Acquisition

IRENE's data acquisition and control system is PC based using a Dell workstation (Dell Inc., Round Rock) and LabView software (National Instruments Corp., Austin). A National Instruments 333 kHz PCI-6052E DAQ card operating in conjunction with an external SCXI expansion system handles analog and digital I/O signals. Two Amplicon cards (Amplicon LiveLine Ltd., Brighton) provide sixteen additional channels of electrically isolated RS232 for communication with external devices. A full array of instruments including insertion shunts, voltage probes, mass flow meters, pressure and temperature transducers are employed for process monitoring. A custom software interface is required to manage data acquisition, processing, file I/O, control and safety monitoring.

3.4 Initial Component Testing

During the initial development stage, individual component tests were conducted to verify device operation and to expose hardware limitations that would pose challenges to system integration. This was a valuable exercise as a number of issues were uncovered. However, this was also a discouraging exercise due to the high rate of device failures and instances where the expected performance and actual operating characteristics differed.

In general, component reliability has been disappointing. Every device acquired for this project, apart from the batteries, has had manufacturing defects and/or significant functional omissions that required repair. Brief reference to the types of component failures encountered will be made in the subsequent discussion. Many hours were invested resolving technical details. Based on this experience, the quality of the individual sub-systems would need to be substantially improved for commercial success of an IRENE like system to occur.

A summary of findings from the initial trials follows.

3.4.1   Power Supply Trials

The main power supply was tested as per the manufacturer's recommended procedure for voltage and current verification. In manual mode, the voltage and current outputs were within specification. However, the optional control and communication interface required service and recalibration before it functioned properly.

Several noteworthy observations were discovered during the initial experiments. First of all, the actual output current may be larger than expected due to the supply's internal output capacitors. Therefore, the real power delivered during transient operation depends on the frequency characteristics of the load. High frequency current measurement is required to determine actual power transferred to the IRENE system.

The second observation is that the current regulation is more stable than voltage regulation. In voltage limiting mode, the output tends to hunt about the average set-point by approximately 100 mV while the deviation is less than 10 mV in current limiting mode. The internal design appears to favour current feedback control.

The third observation is that the supply is not equipped with a feature to disable the output section. Consequently the supply outputs power during the transition period from power-up to the acknowledgement of remote data. The time delay is long enough that serious damage could occur to devices attached to the power supply if proper manual set-points are not maintained.

The fourth observation is that the supply's output section topology is unable to buffer reverse currents so direct connection to IRENE's DC bus could easily destroy the unit. If the output voltage is set lower than bus voltage, the supply appears as a short circuit across the batteries resulting in large reverse current. An adequately sized blocking diode with fast response time to transients is required between the supply and the DC bus. At the supply's maximum output, the diode insertion loss could exceed 250 watts, so heat dissipation as well as electrical isolation must be considered. In addition, the IRENE system controller will need to compensate for the diodes non-linear voltage drop in scenarios where the bus voltage is derived from the supply.

The final issues encountered during initial testing relate to the remote programming features. A write limitation on the software selectable mode (remote/local) control, programmed voltage limit, and programmed current limits was discovered. The EEPROM memory fails after approximately 10,000 updated cycles. While this is adequate for most applications, care must be taken in the communication coding to ensure that these parameters are only accessed when changes are required. An improperly executed control program could easily blank out the memory in less than two minutes. The regular voltage and current settings do not share this limitation and can be updated in a typical continuous looping structure.

Dynamic control of the voltage and current set points via the RS232 interface was much slower than desired. Data communication combined with the internal command processing results in a time delay of approximately two seconds. This presents a significant challenge for implementing local closed loop control.

3.4.2   AC Inverter and Battery Trials

AC inverter tests were conducted with the battery bank supplying the required DC input power. Extensive repairs were required to correct an output section failure that occurred in one of the inverters during the first five hours of testing.

Initial experiments revealed several issues with the inverters that complicated system integration. The user interface is an inherent weakness of the inverter design. Programming the manual presets required for operation using the four button interface is possible but the menu system is cumbersome to navigate. External control and monitoring employs an even more cryptic and extremely slow interface. The RS232 module plugs into the proprietary signal bus used to synchronize multiple inverters. It allows access to the system presets but requires a command sequence which mimics the actions of a user during manual parameter entry. Furthermore, all parameter set-points are lost when DC power is removed from the unit, a frequent event given the experimental setup. Remote interface source code was not provided with the RS232

module and the executable can not be adapted for use in IRENE system controller. A custom user interface is needed.

The second weakness in the inverter design is the DC side input filtering, or lack of filtering, to be more precise. The inverter imposes large current demands on the DC source, easily in excess of 200 amps, at frequencies that match the AC load. For simple resistive AC loads, current ripples occur at 120 Hz (i.e., the zero crossing frequency of alternating output waveform). However, if the inverter is servicing a more aggressive load, say a switching power supply, the current demand may have frequency components in the kHz range. Typical inverter designs have input filtering to smooth out the current demand on the source side. The particular units obtained for this project have limited filtering. The manufacturer expects that sufficient battery capacity exists to service the current demands.

In the IRENE system, the battery capacity is minimized in keeping with the main project theme 'to utilize hydrogen as the primary energy storage media'. Having observed the demands placed on the batteries during the initial experiments, it is clear that the lack of capacity leads to operating scenarios that exceed the batteries design point. The actual bus / battery voltage varies considerably based on the instantaneous current demands. In this mode of operation, IRENE's battery life expectancy will be much shorter given the frequent deep discharge cycles. Given the research context of the work, it is important to probe the boundaries of system design. However, it is unlikely that the minimalist approach taken to electrical energy storage would be feasible in a commercial implementation of an IRENE-like system. Related issues surrounding bus stability, transient behaviour and the imposed operational constraints will be addressed subsequent chapters.

The third observation concerning the inverters deals with the battery charge mode. When connected to an AC source, the inverters automatically default to battery charging, pushing current into the DC system. Charge mode can not be disabled. Care must be exercised in parameter programming because the default charge rate is significantly higher than the battery's allowable charge rate. Furthermore, the charging parameter is based on AC current input, not the DC output. Before connecting to an AC source, the

charge rate parameter must be adjusted to a value less than six amps. The minimum set-point is one amp.

The final observation made about the inverters during the initial testing deals with the accuracy of the current control during grid assist modes. Set-points established for the grid and generator contribution to the total AC output current are not tightly adhered too. Actual currents from these sources may vary by two amps from the target values. While this level of control is adequate, the variation is large enough that external measurements will be needed to form an accurate picture of the power transferred from each source.

3.4.3   AC Load Bank Trials

The AC load bank was subjected to a detailed review. Changes were made to resolve device input connectivity issues. Operation was subsequently verified over the working range of the device.

The useful dynamic range of the load bank is more restricted than expected. Although it is capable of applying an updated load setting on each successive input cycle, the memory mapping is limited and requires extensive programming prior to the load pattern execution. Duration of the variable load is relatively short at approximately two seconds. In general, the programming overhead is not warranted, so the load bank's effective dynamic response will be governed by the remote set-point update rate. The actual AC load will appear uniform on a cycle-to-cycle base.

The main problem encountered during initial testing was with the RS232 interface. The software supplied with load bank allows the user to select the active communication port. However, repeated attempts to control the load failed when using any of the computers sixteen expansion ports. The problem was traced to the load bank's software routines which place rigid constraints on the host computers communication port configuration. The load bank only responds on COM 0, a non-isolated port. Furthermore, omissions in the port handling subroutines cause the computer to freeze if a strict power-up / port initiation sequence is not adhered to. Options for communicating with the load are limited to the OEM's library of subroutines. Manual entry of configuration data during

port initialization is unavoidable. Careful development of the master IRENE system controller is required to circumvent computer lock-up.

3.4.4 Electrolyser Commissioning

Initial electrolyser commissioning efforts revealed a number of problems that present barriers to the development of IRENE. According to the manufacturer, the electrolyser was configured as a 'black box' solution for hydrogen generation requiring only a tap water connection, power from a renewable energy converter, and a high pressure line for the product hydrogen. Our experience differed somewhat.

Validation of the electrolyser performance curves was not completed during the initial commissioning phase due to the problems encountered. Electrolyser issues are categorized as operational concerns or equipment sub-system deficiencies. They are addressed separately as follows.

Operation Concerns

The first issue is that provisions for controlling the electrolyser power draw were not made (other than the main stack disconnect). Power draw is therefore governed by the electrolyser's VI curve combined with the auxiliary loads (hydrogen compression, control system, stack cooling circuit, etc). For moderate bus voltages, the electrolyser appears as a 5 to 6 kW load. In IRENE, the electrolyser is intended to convert *excess* power to hydrogen production. However, the probability that the excess will exactly equal the electrolyser's unconstrained power draw is small. The lack of current control has a major implication on the control methodology for the IRENE system and significantly impacts the experimental space that can be explored.

The second issue is the extensive purging requirements on start-up. The control system utilizes normally open valves that vent the hydrogen system to atmosphere when control power is removed. The manufacturer intended that the electrolyser would be operated on a regular basis, hence power would be maintained. In the IRENE system, a consistent supply of power to the electrolyser is not guaranteed increasing the purging frequency.

Purging is a complicated manual procedure that involves injecting low pressure inert gas into the hydrogen system. However, the piping layout, injection points, and venting

design are not conducive to direct purging of entrained air. In order to circulate the inert gas, the compressor must run. This only occurs when the stack is powered and generating hydrogen. Consequently, a temporary safety hazard is created where both hydrogen and oxygen co-exist within the system. Once the addition of purge gas has ceased, product hydrogen must be vented for an additional two hours to ensure purity is sufficient to avoid contamination of the downstream system. The required operator intervention, potential safety issues, and losses are unacceptable within the context of IRENE.

Hydrogen Compression Sub-System

Five undesirable operational characteristics were observed with the OEM's hydrogen compression system. The first characteristic is that the compressor cycles on and off more frequently than required, consuming excess energy. Oscillations in control are due to inadequate dead-band in the control set-points, pressure measurement sensitivity, and relative expansion volumes of the compressor's bypass circuit.

The second issue is the high compressor in-rush current at start-up which nearly doubles the effective electrolyser load. In an IRENE-like application with limited renewable input, power may be available to sustain the nominal electrolyser operation but not the high in-rush demands.

The third issue is the operating temperature which is higher than desired. In an effort to reduce the power consumption, a large reduction ratio was implemented between the drive motor and the compressor. As a result, the compressor is driven below the optimal speed range, limiting the effectiveness of the splash lubrication and flywheel cooling systems. Additional cooling is required for long duration experiments.

The fourth issue is the unsteady flow of hydrogen delivered to the user. Although hydrogen generation in the cell stack is a continuous process, the delivery of purified hydrogen from the unit occurs in bursts. An operating pressure of approximately 15 bar is required for the electrolyser's hydrogen purification system to function properly. Pressure is maintained by a spring loaded back pressure regulator which inherently generates an unsteady output flow. This is undesirable from an experimental perspective

because of the time delays and added complication involved in accurately measuring the volume of hydrogen in each burst. Furthermore, adjustment of the regulator setting is required to balance plant pressures / flow rates with the user's downstream process. The variability in conditions alters the net power required for compression which in turn affects the overall electrolyser efficiency.

Finally, numerous compressor failures had serious implications on the reliability and operation of the IRENE system. The majority of the reliability issues stem from materials compatibility issues with the feed stream compounded by the operating approach. A brief process description is required to outline the constraints on the compression process and conditions that have led to the various compressor failures.

Hydrogen and oxygen gas bubbles, generated in the electrolysis process, carry trace amount of potassium hydroxide out of the cell stack. The KOH is scrubbed through contact with the liquid seal water located in the bottom of the respective low pressure buffer tanks. Oxygen is subsequently vented to atmosphere while the hydrogen is collected in the buffer tank (provided the vent solenoids are closed). The height difference between the two water columns sets the pressure in the hydrogen buffer. Since this is physically limited to 150 mm, the pressure at the compressor inlet is only 1.5 kPa gauge. At such a low inlet pressure, serious sealing issues develop in the compressor's intake check valves due to the low cracking pressure constraint. Clearance volumes are also critical since the gas will compress into local voids resulting in low net flow. Furthermore, the inlet gas is fully saturated with water vapour from the liquid seal. Since the relative vapour content decreases with increasing pressure, excess water condenses within the compressor. Moisture traps are included but have limited effect on the water droplets that pool in the check valves.

The electrolyser's supplier elected to equip the device with a compressor intended for dry oxygen service since a suitable unit for hydrogen compression was not available. This unit was selected because the sealing requirements for oxygen are much higher than in a standard compressor (due to the inherent combustion issue between compressed oxygen and the lubricating oils). However, the materials in contact with the feed stream are mild steel sealed with paper gaskets. The OEM oversized the unit to account for the molecular

size difference between hydrogen and oxygen, and retrofitted the crankcase vent with a buffer tank return line to recycle blow-by.

Problems were not detected during OEM electrolyser trials because the unit was new and run in a continuous manner. Both the condition and operating mode are significant because the performance evaluation occurred while the check valves were still able to form a seal, and the steady flow of gas removed excessive moisture. Once the trials were complete, the compressor was disassembled, serviced, and prepared for shipping by covering all exposed surfaces with a light coat of oil.

In the IRENE system, the electrolyser is utilized in a significantly different manner from the continuous mode for which it was primarily designed. During periods with marginal excess power, the unit will be subjected to frequent start/stop cycles as a method of regulating the average power draw. Furthermore, it may be inactive for days or weeks if excess power is not available. These conditions promote corrosion of the internal components. The OEM's recommended solution was to disassemble the compressor, and to clean and wipe all surfaces with oil after each use. This procedure takes approximately four hours to complete and is an unreasonable level of maintenance to perform on a frequent (daily) basis. During the electrolyser commissioning period the check valves, which rely on knife edge surfaces to generate a seal, became sufficiently pitted that pressure could no longer be developed. The required operator intervention and resulting electrolyser down time impose serious constraints for conducting an experimental program with IRENE.

Power Distribution Sub-System

Deficiencies in the electrolyser's power distribution system constitute an operational safety hazard. An electrical fire which occurred during electrolyser commissioning illustrates the serious nature of this problem. In general, the main DC wiring is poorly organized and implemented. Inadequate space is allocated for the high current components and the heavy interconnect cabling. Unnecessary wire junctions are included that result in additional ohmic losses and hot spots. Operational issues with the main stack disconnect relay were also noted. It frequently remains latched after the control is toggled off. In this instance, the stack continues to generate hydrogen but the control

system does not respond appropriately. Extensive damage to both the stack and the peripheral equipment could result. Revision to the power distribution system is required to address these issues.

Control and Instrumentation Sub-System

Intermittent failure of the electrolyser control system power supply was observed. The DC/DC converter used to step-down the main 48 V input to the control system voltage was found to be undersized and is unable to supply sufficient current to support the control system load during recharging of the backup batteries or during prolonged operation of the stack cooling pump (typically five minutes or greater).

Hardware modification of the electrolyte level control tank is required to address safety issues. During electrolyser commissioning, leakage of concentrated potassium hydroxide electrolyte occurred causing damage to electrical wiring and sensors. This incident highlighted the need for careful containment and sealing of the electrolyte employed in alkaline based electrolysers.

Excessive electromagnetic noise is present in the electrolyser's instrumentation due to the power and ground schemes implemented. Fly-back protection for inductive loads has not been included resulting in voltage spikes when these control devices are switched. Furthermore, measurement quality is compromised since instrument signals utilize only a few percent of the controller's available input range. Scaling factors used in measurement conversion are inaccurate and result in poor quality data. In addition, data exchange with the host computer utilizes a Modbus protocol which is slow and requires the use of hardware handshaking lines.

A major upgrade was required to raise the performance of the control and instrumentation system to an acceptable level for inclusion in the IRENE system.

3.4.5   Hydrogen Storage

Individual tests of the compressed hydrogen storage components were not conducted in advance of sub-system integration. However, safety issues were investigated and several constraints were established that had an impact the integration of IRENE. Given the volume of hydrogen to be stored it was necessary that these components be located in a

secure outdoor compound adjacent to the building. This imposed constraints on the design of the overall IRENE control system. A dedicated local control system at the compound is required to supervise compressor operation. A direct communication link to the main IRENE system controller is needed to coordinate compressor activity and transfer data.

Development of the metal hydride storage system was conducted as a separate research project and will not be addressed in this dissertation apart from noting that provisions are made to include this module into IRENE's hydrogen system. For further discussion, readers are referred to [72].

3.4.6 Fuel Cell Trials

Initial experiments with the fuel cell revealed that several key components are required for integration. Although the Nexa has an extensive balance-of-plant, the auxiliary power source, output relay and blocking diode were not included.

An auxiliary power source capable of supplying 5 A at 20 to 30 VDC is required to operate the controller, blowers, fans, and solenoids during start-up and shutdown modes. During operation, the auxiliary source is not needed as these devices are powered directly from the fuel cell stack. Auxiliary power must be referenced to the stacks cathode voltage (i.e., a floating supply). The voltage range is suitable for series connected 12 V batteries but no provision for recharging is made.

An output relay is required to disconnect the Nexa from the user's load if the controller observes a fault condition (e.g. excess current, low cell voltage, high stack temperature, flooding, low hydrogen pressure etc.) or during start-up and shutdown periods. Power for the peripheral loads mentioned above is extracted prior to the output relay.

A blocking diode is required in applications where the fuel cell stack could be subjected to reverse currents. Given the common bus configuration of IRENE, the potential exists for back driving the fuel cell stack from the bus. A suitable fast response diode must therefore be used.

Verification of the Nexa's VI characteristics was limited to tests at several discrete points on the curve due to limited availability of appropriate loads. Results were lower than the

manufacturer's published data. However, stack performance may recover after the automated conditioning cycle which occurs during longer duration operation.

The most significant information gathered during initial Nexa experimentation relates to the current sourcing potential. The maximum allowable current ripple is limited to 25 percent of the delivered current at a given point on the VI curve. Experiments conducted with the AC inverters, mentioned in Sections 3.4.2, generated a 100 percent current ripple on the DC side. The Nexa is unable to directly service this type of dynamic load. The current ripple limitation greatly restricts the options for incorporating the Nexa into the IRENE system.

The fuel cell monitoring software presents another integration issue as the OEM supplied only executable code. Documentation for the communication protocol is not available and the low level data transfer does not occur in a discernable pattern. Significant effort would be required to reverse engineer the software interface in order to construct a custom module compatible with the IRENE system controller.

3.4.7 Data Acquisition and Control Trials

Initial experiments with the data acquisition components were conducted to clarify device capabilities. Operation was considerably different then expected. The DAQ card is capable of sampling a single input channel at 330 kHz; however, the analog multiplexer limits the rate to 100 kHz. In addition, the multiplexer only samples from multiple channels if they are grouped in sequential order with identical sample rates and gain settings. The original intent was to acquire data at a sufficient rate to capture the dynamic interaction between system components. To achieve this, parameters like currents and output voltages need to be sampled at a much higher rate than the hydrogen flow rates, temperatures, pressures etc. The requirement for uniform channel sampling diverts resources away from the primary inputs and will result in lower resolution data. Furthermore, the requirement for a single input gain setting dramatically increases system complexity. External signal conditioning is required on each channel to adjust the output level to a common voltage range. These limitations impose significant constraints on the design of the data acquisition system.

Another issue that was not anticipated prior to testing is the intensity of the electrical noise generated by the power supply, inverters, and main interconnect cabling. The DC system radiates noise giving the high amplitude current pulses flowing between system components. Transmission of high impedance instrument signals to the DAQ system is not feasible in this environment. To achieve the desired signal quality and frequency response, extensive analog signal conditioning and shielding is required.

Preliminary experiments with LabView were conducted to ensure that the RS232 port handling routines could support simultaneous communication with multiple devices. Issues were noted with the data collection routines which halt program execution while data read events transpire. This represents a major issue in constructing the control software which must manage data flow with all the devices while maintaining data acquisition, processing and file management operations.

3.5   Summary

Design criteria for the IRENE system were established based on the project goals and review of prior research. The key requirement was that commercial products be utilized for all primary system components. System sizing considerations narrowed the test-bed development to a residential scale system. Commercial components selected for IRENE were reviewed and the integration issues noted. A broad range of challenges exist in the development of a unified system.

Chapter 4

System Integration

Developing an integrated system with the commercial components outlined in Chapter 3 was a more challenging task than originally anticipated. Each of the devices, with the exception of the batteries, required service work, modifications and/or custom equipment in order to function within the context of the IRENE system. The project goals were re-evaluated in light of the number of issues raised during the initial validation experiments. The vision was narrowed from the development of a generic readily reconfigurable system to a fixed system architecture that could support preliminary research efforts.

Many innovative hardware and software solutions were required to address the integration issues identified. Detailed development work involved aspects of both mechanical and electrical engineering. A description of the system integration methods and creative enabling solutions is presented in the following sections.

4.1   General Component Integration

Assembling the individual components into a functioning system required a physical framework for the devices. Items like the battery bank, power supply, inverters and load bank are heavy devices and for obvious safety reason require semi-permanent mounting in an indoor location. The only specific installation requirement for the electrical devices was mechanical bonding of all case grounds to provide protection for stray currents.

Special consideration was given to the location of hydrogen related components due to the inherent safety hazards associated with gas leaks. The electrolyser was rated as a free air device provided the access panels remained closed and the vent lines were connected to outdoors. However, laboratory procedures limit testing of hydrogen components to the confines of the fume hood until safe operation is confirmed. This policy is well advised given the problems encountered with the electrolyser during validation experiments. The electrolyser has thus remained a permanent fixture in the fume hood. The fuel cell

performed satisfactorily during initial fume hood trials and was subsequently moved into the main laboratory. A backup safety system monitors hydrogen gas concentrations within the laboratory, and is capable of isolating all power sources within the room should a gas leak occur. As mentioned in the Section 3.4.5 preceding discussion, compressed hydrogen storage components are located in a secure outside compound.

Aspects considered while designing the physical layout of the IRENE system included available laboratory space, ease of access for maintenance, DC bus cabling lengths, user accessibility to disconnect devices, location of instrumentation, and heat dissipation requirements. To minimize the cable length to the electrolyser, electrical components were located in small corridor immediately adjacent the fume hood. A custom free standing metal frame was fabricated to house these items, employing the battery bank as ballast weight, see Figure 4.1. Given the tight confines of the corridor, the entire assembly is portable and can be moved into the main laboratory for service work. Furthermore, the unified design facilitates future relocation of the system with minimal disassembly. Components are arranged for easy access to the manual control interfaces. To minimize heat transfer to other system devices, the air cooled AC load bank is located at the top of the rack. Other items have sufficient air gaps to allow for heat dissipation. A simplified DC bus schematic is illustrated in Figure 4.2.
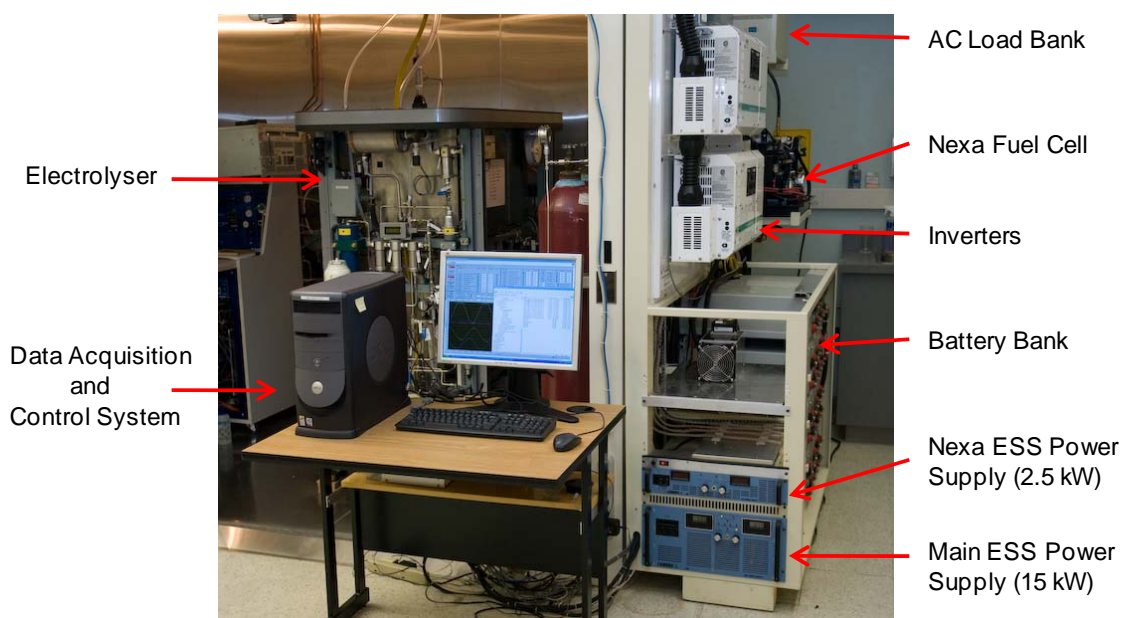
Figure 4.1 IRENE System Installation
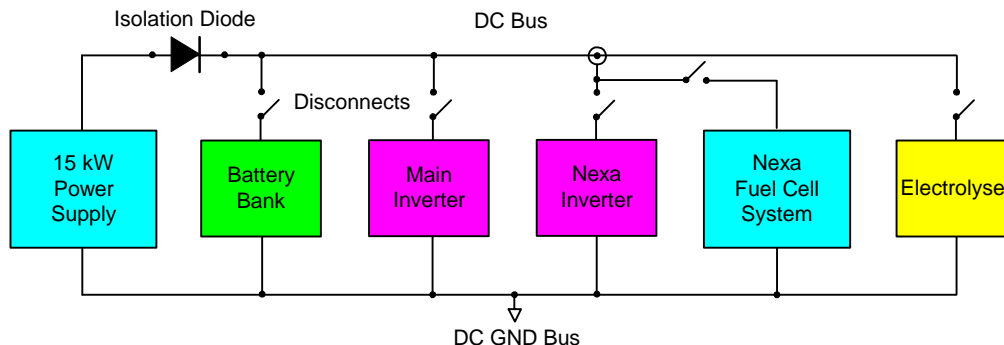
Figure 4.2 Simplified DC Bus Schematic

The junction box, originally furnished with the inverter modules, was retrofitted with the main DC bus bar and isolation devices, see Figure 4.3. The overall physical layout minimizes cable lengths between DC devices and places the disconnect switches in a prominent location. Removable panels limit physical access to the battery posts and other high side DC connection points. The main power supply is not equipped with a DC disconnect device. Isolation is afforded by the blocking diode, illustrated in Figure 4.4. The diode is a full-brick, high current unit rated for 250 amp continuous duty that meets the requirements outlined in Section 3.4.1. Forced convection cooling of the heat sink is required to maintain acceptable diode junction temperature. From a system perspective, the diode is considered part of the power supply. Therefore, the diode power drop and cooling fan loads are not included in the IRENE energy balance. Calculations are based on actual current delivered at the measured bus voltage.

A removable bonding point incorporated in the DC bus allows the fuel cell system and one inverter to be isolated from the other units, illustrated in Figures 4.2 and 4.3. The ground side remains common with the other devices to ensure proper referencing for measurement purposes. This feature allows the fuel cell system to directly service an AC load under strictly controlled conditions that will be discussed in a subsequent section. Under normal operating conditions, the inverters require battery buffering so the copper bridge must remain installed and the battery disconnect closed. A naming convention of "Main" and "Nexa" inverter is adopted to differentiate the two inverters.

Figure 4.3 DC Bus Bar and Disconnects

Figure 4.4 Power Supply Protection Hardware

All AC wiring is physically separated from the DC system. An AC wiring schematic is presented in Figure 4.5. Breakers for the local inverter grid connections and load bank crossover selector are located above the inverters, see Figure 4.6. Solid state relays, installed in series with the inverter grid connections, provide a means for computer control over these sources. Two additional relays control power to the AC receptacles tied to the output side of the inverters. These receptacles have been incorporated to allow

real loads to be added to the system. The ability to apply appropriately sized base loads, in conjunction with the programmable load, will allow for direct simulation of a residential demand profile. A final relay controls the AC connection between the Nexa inverter output and the Main inverter generator input.

Figure 4.5 AC Wiring Schematic

Figure 4.6 Optional AC Load and Configuration Points

The main AC grid tie for the power supply, inverters, and auxiliary 110 V power receptacles is routed through disconnect relays, located in a dedicated service panel fixed to the fume hood. Flexible cap-tire wiring is used on all interconnects between frame mounted components and external termination points to allow for frame movement. If the need should arise, external power to the system can be removed by tripping the

emergency stop circuit, see Figure 4.7. This precaution was taken to provide an effective shut down mechanism for personal unfamiliar with system operation.

Figure 4.7 Emergency Shut Down Interface

4.2　Electrolyser Integration Phase 1

Electrolyser integration presented one of the largest challenges in developing the IRENE system. Extensive modifications were required to address the equipment failures and omissions discovered during initial validation experiments, outlined in Section 3.4.4. Several iterations of development work were required as new issues arose while addressing the original problems.

The first phase of modifications addressed critical operational and safety concerns. A new electrolyte level control tank was fabricated to replace the leaking unit, see Figure 4.8 (a). To rectify deficiencies in the original design, the new unit was constructed from thicker material with enlarged sensor bosses. The mounting location was modified to reduce stress on the connection points and reposition the unit to a more protected area.

The entire high current power distribution system was relocated and rewired to minimize the possibility of another electrical related fire. The revised design simplified the layout considerably and insured proper isolation of the DC system from chassis ground, see Figure 4.8 (b). In the process of relocating the high current wiring, the stack current

sensor was upgraded with custom interface to improve signal stability and maximize output range. Safety concerns with the main stack disconnect relay were also addressed. Bench test with the relay revealed that both mechanical binding and electrical drive issues contributed to the intermittent latching issues. Modifications to the internal transfer mechanism were made and the entire drive circuit was redesigned. Together, these changes eliminated the switching problems.

Alterations to the venting system were made to address the frequent nitrogen purging requirement. Several solenoid valves were replaced and a pressure balancing circuit was installed, see Figure 4.8 (c). A small positive pressure now remains in the hydrogen system when controller power is removed. These changes minimize the operator intervention, time requirements, and lost hydrogen production following a plant shut down. Venting capabilities have been maintained in the event that excessive oxygen crossover is detected or an emergency condition exists. Furthermore, a dedicated nitrogen regulator, control valves and injection point has been added to facilitate purging when required.

(a) Custom Electrolyte Level Tank   (b) Simplified High Current Wiring   (c) Revised Hydrogen Venting and Integrated Nitrogen Purge

Figure 4.8 Electrolyser Safety Modifications

Efforts were made to address the hydrogen gas compression issues. The intent was to implement interim solutions to enable IRENE characterization work to commence while a permanent compression solution was developed. The compressor was reoriented to provide easier access during routine maintenance. In the original layout, servicing the valve plates required removal of the entire compressor since access to both compressor heads was obstructed. Replacement OEM valve plates were installed with new check valve assemblies. Control stability was improved through revised set-point values and

delay constants. An electric fan was added to increase air flow across the compressor heads and cylinders. Connecting-rod splash plates were modified and crankcase oil level raised in an effort to increase lubrication. And finally, a prototype DC soft starter circuit was developed to reduce the compressor in-rush current.

Once these modifications were implemented, a brief series of experiments were conducted in an attempt to verify basic electrolyser operation over the full rated input power. Unfortunately the compressor suffered irrecoverable damage from corrosion and gouges in the cylinder walls due to heat and lack of lubrication, see Figure 4.9. Stuart elected to use this compressor because a suitable hydrogen rated unit was not readily available. Small off-the-shelf compressors designed for hydrogen service with low inlet pressures do not exist. Several companies claim to make devices but they are custom design / build units that are prohibitively expensive.

(a) Valve Plate and Check Valve Corrosion   (b) High Pressure Cylinder Damage
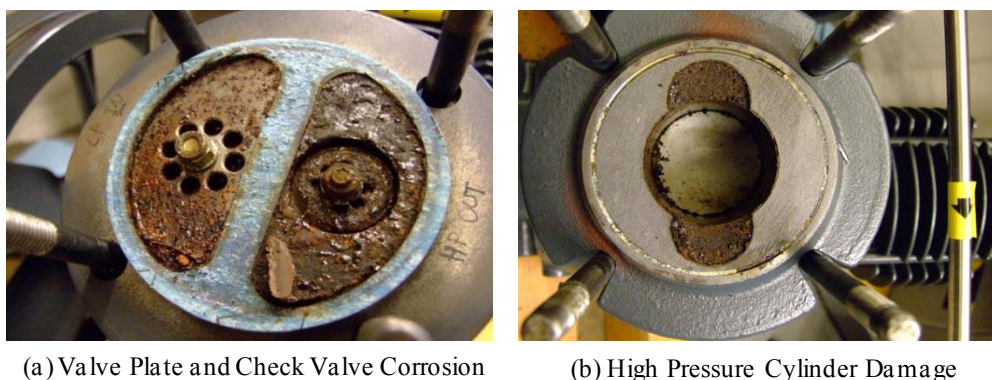
Figure 4.9 Compressor Damage

To proceed with the IRENE project, a new strategy was developed to deal with the electrolysed hydrogen. Given the research setting, some latitude was available to alter the system configuration. The solution involved measuring the quantity of hydrogen produced and injecting a similar amount of bottled hydrogen into the storage system, thereby creating a virtual compressor. The electrolysed hydrogen is vented into the fume hood exhaust stream after measurement. (The dilution factor is sufficiently large to minimize the safety hazard.)

From a system perspective, the fundamental reason for compression is to reduce storage volume. The fuel cell is inherently a low pressure device, operating with internal pressures near one atmosphere, so the compression work is not utilized. Therefore, the

only immediate penalty introduced by virtual compression is the cost of the mass flow control equipment and bottled hydrogen. If a more elaborate energy system balance is required, the compression work can be estimated based on the mass flow rates and pressures.

To implement the virtual compression scheme, accurate measurement of the hydrogen production rate is required. However, this presents a non-trivial problem since standard gas measurement techniques are not compatible with the process constraints (low flow rate, 0-15 L/min; low inlet pressure, 1.5 kPa gauge) or gas composition (hydrogen saturated with water vapour). Furthermore, the measurement must not alter the stack operating conditions or control methodology. Since a suitable commercial device was not available, a custom instrument was developed, the inverted bucket flow meter, illustrated in Figure 4.10.

Left - Physical Installation   Top - Flow Controller   Right - Flow Diagram
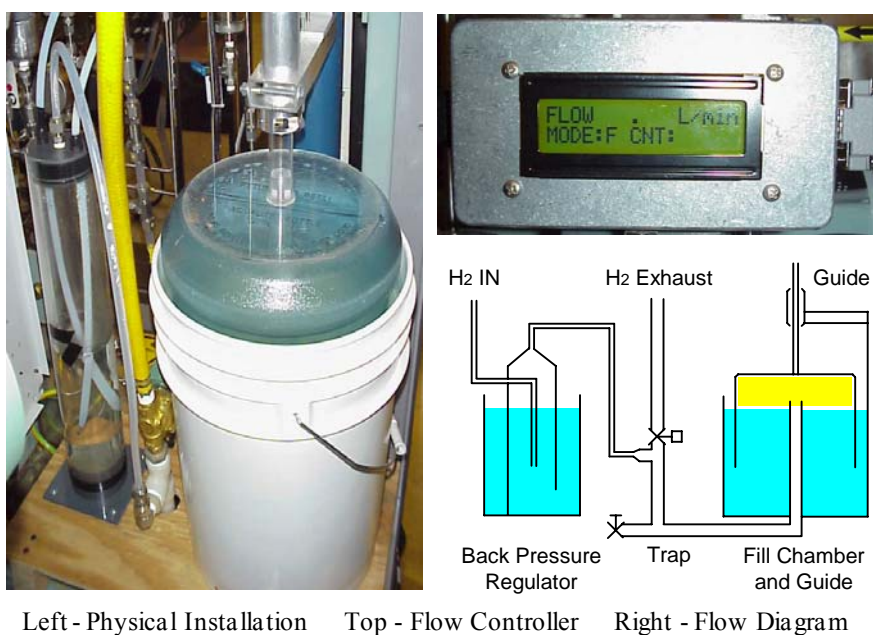
Figure 4.10 Inverted Bucket Flow Meter

This device allows flow rate measurements based on the time required to fill a fixed volume. Hydrogen gas is piped into the center of an inverted cylindrical shell placed in a water bath. The cylinder rises out of the bath as it fills, and the time between two fixed heights is measured. Once full, a solenoid valve releases the hydrogen, the cylinder returns to its original position, and the cycle repeats. Fill volume was selected to achieve a suitable balance between measurement accuracy and cycle rate.

The prototype unit was constructed from basic components, hence the relatively large size. To create sufficient space for installation, the original hydrogen compressor was removed and the stack water purification system was relocated. Although the prototype looks primitive, it performs well and further refinement has not been necessary. An added bonus of the flow meter design is the visual indication that the electrolyser is functioning and the intuitive sense of gas volumes generated.

As indicated in the cycle description, cylinder buoyancy is slightly negative so a positive pressure, equivalent to a 5mm water column, is required for proper operation. This pressure is so low that the hydrogen gas must first pass through a separate water column to maintain the electrolyser stack operating conditions. To obtain an accurate volume measurement, the cylinder must be guided as it rises out of the water bath. A guide tube and low friction roller bearing support assembly have been developed to ensure smooth motion. Furthermore, it is critical that cylinder movement cause minimal disturbance to the water bath or a bobbing action will result, leading to premature indication of the full state. To aid in this, the top of the cylinder is not allowed to plunge below the water line on the return stroke. In the lower most position, the cylinder rests on the hydrogen inlet stand pipe with the liquid level maintained slightly below this point. Swept volume is therefore decoupled from the bath level. Automation of the cycle is achieved using a single limit switch to detect the full position and the pressure release solenoid valve. A dedicated micro-controller controls valve timing, measures fill time, calculates flow rate, drives a local led display, and reports data to LabView via RS232. Since the error between the actual measurement temperatures and pressures and standard conditions (STP) is negligible, correction factors are not required.

Periodic addition of makeup water is required to compensate for evaporation. Level adjustment is recommended in the final portion of the exhaust cycle when the cylinder rests on the stand pipe and the solenoid value is open. During sustained operation, moisture condenses in the low portion of the stand pipe and must be drained. Disruption of data collection can be avoided if the trap is emptied during the exhaust cycle. This also aids in expelling condensate. (Note: prolonged contact with the condensate should be avoided as it may contain traces of potassium hydroxide.)

4.3   Electrolyser Integration Phase 2

The successful implementation of phase 1 modifications enabled electrolyser operation over the full input power range. Tests conducted at moderate to high input power settings (60-100 amps) revealed a serious deficiency in the stack cooling system that had not been observed in previous experiments.   The stack is designed to operate at 60 °C. Temperature is maintained by circulating water from the oxygen liquid seal (approximately 30 L) through cooling coils located in the electrolyser stack end plates. A thermo-couple, immersed in the electrolyte, provides temperature feedback to the control system which operates the cooling pump on a simple 5 °C threshold control scheme.

Figure 4.11 illustrates the onset of thermal run-away after two hours of operation at the upper current limit of 100 amps. A reduction in slope of each successive cooling cycle indicates that the liquid seal was unable to reject sufficient heat. After four cycles, the temperature differential between the cooling water and the stack is inadequate to cool the unit. This is not surprising considering that the liquid seal is essentially a metal container with little air flow over the surface operating with a total temperature differential of only 35 °C. The perplexing question is how such a serious problem went undetected by the manufacturer during design and commissioning phases.
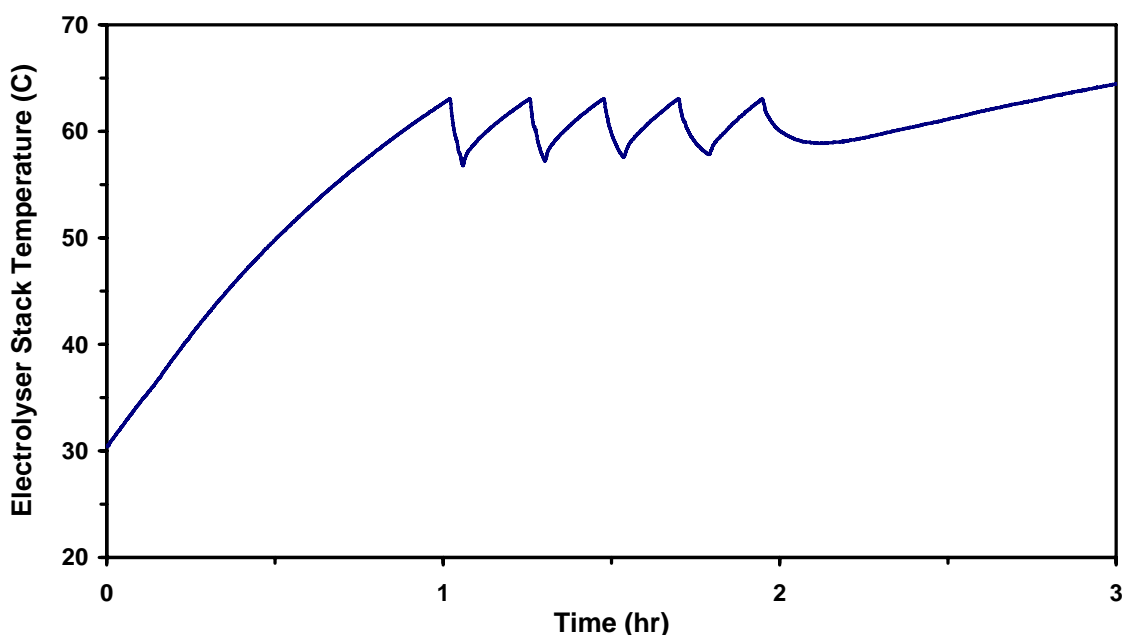
Figure 4.11 Electrolyser Stack Temperature Response at 100 A Input Current

A closed loop system utilizing a custom three core industrial radiator with shroud and forced air circulation was developed, see Figure 4.12. To further aid in cooling, the electric fan is positioned to draw air over the electrolyser stack surface, improving convective heat transfer. A custom support frame and relocation of the cooling pump and associated piping was required for installation. The new system does not circulate the oxygen liquid seal water due to compatibility issues between the seal water's residual potassium hydroxide and the radiator materials. Distilled water is used to minimise the risk of contamination should a leak develop. With the new system, stack temperature swings have been reduced by an order of magnitude and sustained operation at maximum power is possible. A safety shutdown at 68 °C remains in place to safeguard stack operation.
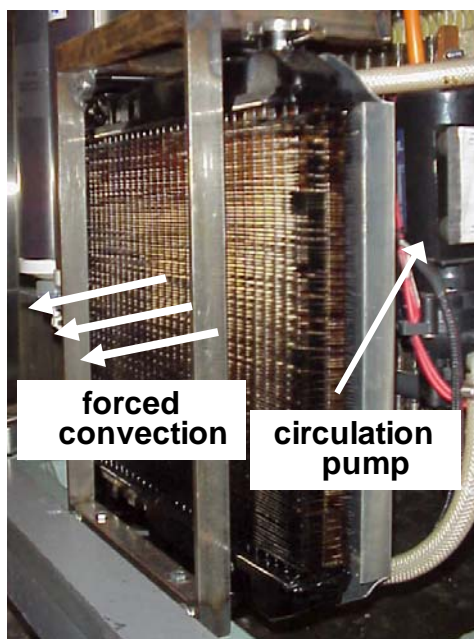
Figure 4.12 Electrolyser Cooling System Upgrades

Extensive upgrades to the electrolyser's instrumentation and control system were implemented to address deficiencies in the original design. The entire system was rewired to separate control circuits from measurement instruments, see Figure 4.13. Proper star grounds were created for each group to reduce current induced noise on the instrument channels. A custom interface board was developed to allow manual override capability and proper switching / fly-back current protection of the control devices. Analog signals levels were increased and an analog-to-digital converter with higher

accuracy was installed to improve signal resolution. A high capacity DC/DC converter with an enlarged heat sink and additional output capacitance was installed to provide stable power for the control system. Finally, the entire 80 page ladder logic program was rewritten to work with the new I/O parameters, address safety features that were omitted, expand reporting to LabView, and incorporate remote control features. These changes greatly improved performance, accuracy, and reliability of the control system.

(a) Original Control System Layout   (b) Revised Version
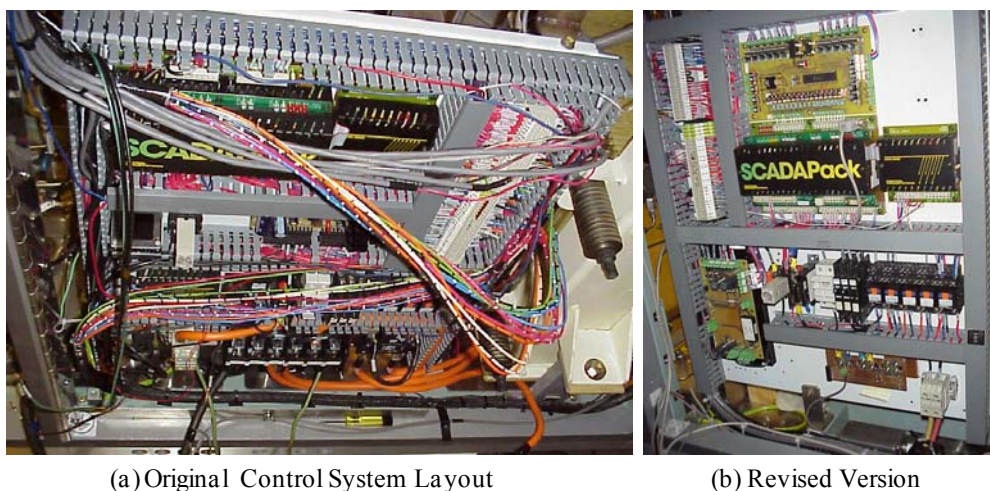
Figure 4.13 Electrolyser Instrumentation a Control System Upgrades

The final electrolyser integration task addressed the need for active control over the stack power consumption. A short-term and long-term strategy was required given the unique power conditioning issues encountered. The long-term objective was to develop a DC/DC converter to handle the near unity matching condition that exists between the electrolyser and the DC bus. Standard converter topologies are configured for a single conversion direction, step-up (boost) or set-down (buck). To control the electrolyser current, a relatively small adjustment in voltage is required from the nominal bus level. However, the adjustment may be in either direction depending on the battery state of charge, instantaneous current demands, and desired electrolyser current draw. Multi stage conversion is required to handle the general matching constraint. A commercial device with appropriate ratings is not available.

A joint project to develop an efficient converter topology to handle these situations was undertaken with members of the Electrical Engineering department. The electrolyser will

serve as a test-bed to evaluate various designs, ultimately leading to purpose built converter tailored to the needs of the IRENE system. An extensive review of the design requirements, relevant converter topologies, and a proposed initial design for a converter unit has been conducted [73]. Further development is pending.

The short-term strategy was to develop a passive device to limit stack current by reducing the effective input voltage. The rationale behind this approach is that under most operating scenarios, the need is to limit electrolyser power draw, not augment it. The only condition where voltage step-up is required is in the event that low bus voltage coincides with a period of high renewable input. In that case, the bus voltage may be insufficient for the electrolyser to absorb all of the renewable input power based on the VI transfer characteristics. In the IRENE system, the bus voltage is easily manipulated due to the limited capacity of the battery bank. In the scenario described, the excess power would result in battery charging, increasing the bus voltage and raising the effective electrolyser operating point.

The device constructed provides discrete voltage steps by employing 12 high power diodes connected in series with shunt relays across each element, see Figure 4.14. Additional shunt relays have been installed across groups of diodes to lower the net contact resistance of the system if minimal power dissipation is required. Diodes were chosen over pure resistive elements because a minimum voltage drop exists regardless of current. Mechanical relays were used due to the requirement for low shunting resistance at high currents. Contact arcing is not significant since the diodes inherently limit switching voltage to less than one volt. The mechanical relays provide the electrical isolation needed to allow for voltage adjustment on the positive side of the stack without requiring a floating control scheme. This insertion position is preferred since it does not interfere with other electrolyser instrumentation. The diodes, which are electrically isolated from the mounting surface, require substantial cooling to dissipate the heat generated during continuous forward conduction. (Diode capacity factors must be de-rated substantially given the 100 percent duty cycle.) Two large fan cooled heat sinks are used, illustrated in Figure 4.15. Custom interconnects, machined from solid copper, allow for compact mounting of all power components while minimizing resistive losses.

Insertion loss at 100 A is less than 50 mV. A span of approximately 8 V can be generated with all diodes in-circuit.
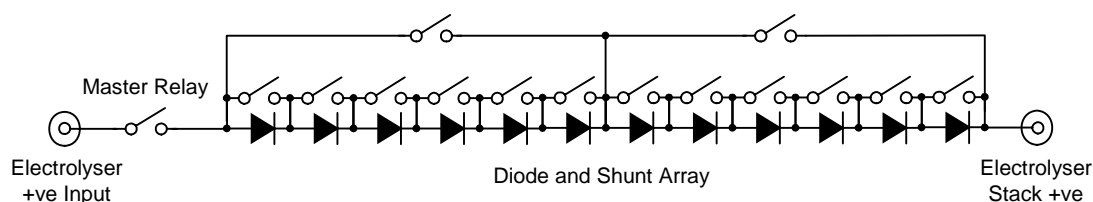
Figure 4.14 Electrolyser Diode Power Conditioner Schematic

Custom Diode Controller   Diode Bank and Heat Sinks
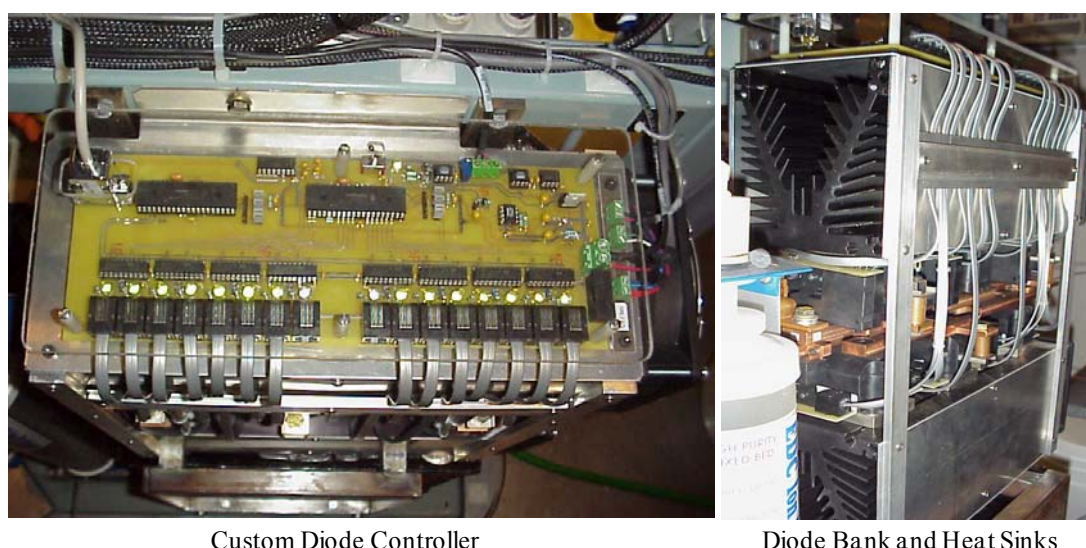
Figure 4.15 Electrolyser Stack Power Conditioning Module

A dedicated micro-controller coordinates the number of diodes in use at any given instant. The physical distribution of diodes is taken into account to distribute heat as evenly as possible. The primary control input is the stack current. The control module receives a target stack current (in one amp increments) and attempts to maintain a time averaged current at that level by adding or removing diodes. The control algorithm is error driven so switching rate is dependant on the deviation from the actual current. Current swings of four to six amps are typical per power increment. If the controller is unable to track the desired current, it resorts to the best default to achieve the operational goal (i.e., all diodes in-circuit or out as the case may be). Discrete LED's indicate which shunts are applied. The manual user interface is limited to an override switch which applies all shunts. The RS232 link provides access for set-point adjustment and feedback

of power level, error count, and actual stack current. The diode drop device provides sufficient range to maintain the target electrolyser current over a five minute window given normal variation in the bus voltage levels.

4.4   Hydrogen Storage System Integration

Due to the limited infrastructure, the compressed hydrogen storage system is intended to service both the IRENE system and the laboratory's fuel cell test station. Hydrogen supplied to the test station is metered and accounted for in the event that simultaneous experiments are conducted. The new hydrogen system was to utilize the existing building piping system and retrofit either ends. The piping system required refit work and re-certification for the elevated working pressure of 17 bar (29 bar test pressure).

A hydrogen distribution system with appropriate flow control solenoid valves, check valves, manual bypass circuits, mass flow meters, pressure gauges, purge points, and pressure regulators for the Nexa and fuel cell test bench was installed in the fume hood, see Figure 4.16. Node points for the hydride system were incorporated for future integration of this sub-system. Two buffer tanks were added with a throttling valve between stages to smooth the hydrogen flow from the electrolyser.

The compound was extensively modified to incorporate the new equipment, see Figure 4.17. The composite storage tanks, high pressures compressor, compressor cooling system, power distribution, interconnect piping, and instrumentation was added. A custom compressor control system was developed that has both local and remote control capability [74]. A dedicated data link between the laboratory and compound allows the main IRENE control system to oversee compressor operation. A backup hydrogen supply with five standard 'T' cylinders and appropriate interconnect piping was installed to ensure that the requirements of the fuel cell test station are met at all times. All systems were leak tested during installation but limited service testing has occurred due to the subsequent issues with the electrolyser.

Figure 4.16 Fume Hood Hydrogen Distribution System

Hydrogen Compressor Installation   Bottled Hydrogen Backup System

Figure 4.17 Hydrogen Storage Compound Equipment Installation

4.5 Fuel Cell Integration

Integration of the fuel cell presented another difficult problem given the significant variation in output voltages and limitations on transient currents as outlined in Section 3.4.6. Since the Nexa is unable to directly service an AC load without an intermediate energy buffer, the fuel cell power must be transferred onto the DC bus and effectively act

as a battery charger. Under these conditions, a current profile with acceptable ripple could be maintained. The preferred solution is to use a DC to DC converter but a commercial product that was tailored specifically to the Nexa's output characteristics was not available. However, several consumer devices, developed for alternate applications, showed potential if particular operational constraints could be met. The most promising was a stackable 500 watt boost converter model APC-F501 (Powerstax PLC, Hampshire).

The converter specification indicated that multiple units could be operated in series or parallel configurations. The devices utilized a high primary switching frequency of approximately 330 kHz. So with moderate input capacitance, the Nexa would be subjected to relatively smooth loading conditions. The converters were voltage output regulated devices, nominally rated at 48 V, but a trim feature allowed for 15 percent adjustment in range. A circuit was envisioned to dynamically adjust the output level to track natural variations in the IRENE bus.

Tests conducted with a single converter illustrated that power transfer from 50-500 W could be achieved. However, experimentation with multiple converters in parallel revealed that the Nexa's output impedance was not low enough to suppress oscillations between converters. Use of a single converter marginalized the fuel cell's potential contribution to the overall IRENE energy balance.

An alternate approach was implemented that involves floating the Nexa on an external current limiting power supply, see the circuit schematic Figure 4.18. The supply operates primarily as a current device, applying the required voltage to maintain the set-point current. At low currents, below 5 amps, the fuel cell generates approximately 75 percent of the total required voltage and hence power output. As the current increases, the fuel cell voltage decreases to roughly 55 percent of the total nominal voltage required to transfer power onto the bus. Therefore the contribution of the external supply increases with increasing current. The implementation utilizes the fuel cell's full VI curve so the benefit of high efficiency at low power settings is retained. A 2.5 kW, 50 V 50 A Lambda EMI industrial power supply (Lambda Americas Inc., New Jersey) similar to the main ESS supply, visible in Figure 4.1, was employed. However, the "Nexa supply"

only requires a single phase 208 V grid connection. The manual and remote control functions were similar but not identical between units so subtle modifications to the program interfaces are necessary.
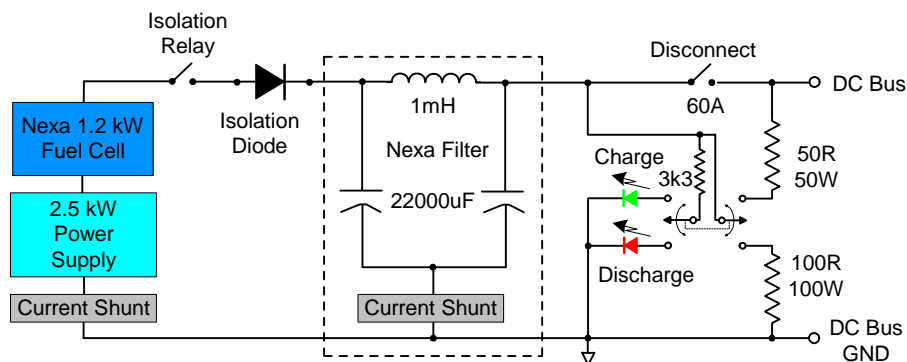
Figure 4.18 Nexa Integration Schematic

The power contribution of the supply and fuel cell are monitored so the appropriate accounting can be conducted. The hybrid system can be viewed as a higher capacity fuel cell where the hydrogen required to develop the equivalent net power can be estimated from the measured Nexa consumption versus the proportion of total power supplied. Or the contribution from the power supply can offset some of the 'renewable input' that would otherwise be applied by the main ESS power supply. Either method can be adopted within the framework of the overall IRENE system controller. The benefit with the integration approach taken is that the net fuel cell power transferred to the DC bus can be adjusted for virtually any bus operating voltage.

Additional components are required to complete the installation because the power supply is unable to dynamically track high frequency variations in bus voltage (it has output capacitance similar to the main power supply). A large passive LC filter, installed between the hybrid fuel cell output and the bus, isolates the fuel cell system from bus transients, see Figure 4.19 (a). Filters are typically employed to smooth noisy source signals. This one simply works in reverse. The filter's time constant is sufficiently large that the load imposed on the fuel cell is within OEM specification. The phase shift generated by the filter on the DC bus is significant enough that the dynamic filter currents must be taken into account when conducting the instantaneous IRENE energy balance.

(a) Passive LC Filter Components   (b) Custom Fuel Cell Integration Hardware
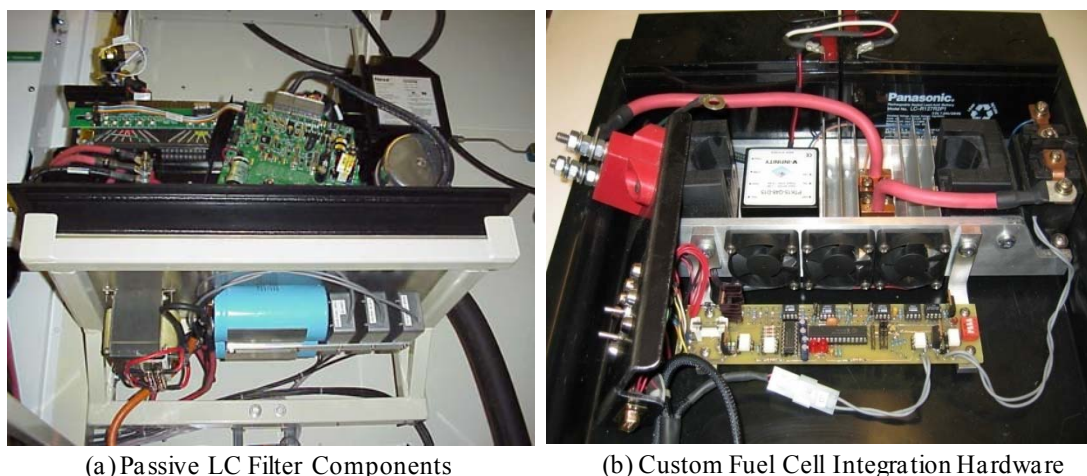
Figure 4.19 Nexa Integration Components

The drawback with employing large passive elements is the additional circuit management issues introduced. The capacitors require pre-charging to 80 percent of the bus voltage prior to operation of the fuel cell system. Likewise they must be discharged during shut-down. A manual control system has been developed that utilizes the DC bus for charging (using resistive element to limit current draw) and applies a suitable resistive load for discharging. Kick-back voltage from the inductor under field collapse posed another concern mandating the use of clamping diodes in parallel with the inductor to limit maximum voltage swing.

A more serious situation develops during operation which requires a dedicated local controller to actively monitor capacitor voltage. For safety reasons, the main circuit breaker for the fuel cell system is located between the bus and the filter output pole. If the breaker trips during operation the effective fuel cell current drops to zero and operating point shifts to a high output voltage. At the same time, the power supply generates a higher voltage in an effort to achieve the desired output current. As a result, the combined output voltage could easily reach 75 V which exceeds the voltage rating on the electrolytic filter capacitors. Electrolytic capacitors have a low tolerance to over-voltage conditions and fail catastrophically.

To ensure that over-voltage is avoided, a custom hardware monitor is implemented that can open the fuel cell output relay if a critical situation is observed. Several other monitoring features were incorporated to ensure other safety states were observed including minimum capacitor pre-charge, minimum supply voltage, and delays before

relay closure. The local control circuit is integrated with the auxiliary power batteries, battery recharge circuit, disconnect relay, blocking diode, heat sink, cooling fans, and output terminals that were added to address omissions in the original Nexa offering, see Figure 4.19 (b). The control panel has manual switches to initiate the Nexa power-up sequence and to activate run mode. LED's provide visual indication of system power, output relay state, and error status. Power for this local instrumentation and for recharging the auxiliary start-up batteries is extracted directly from the fuel cell stack and therefore appears as a parasitic load. However, the average power draw is less than 15 watts under normal operating conditions.

4.6   Instrumentation and Control System Integration

IRENE's data acquisition and control system is complex and highly integrated. Since the value of the research work that can be conducted with IRENE is intimately linked to the quality of the measurements, significant effort was put forth to create a comprehensive and accurate instrumentation system. Specialized hardware and software solutions are generated for each sub-system. A circuit schematic indicating the measurement nodes is illustrated in Figure 4.20.
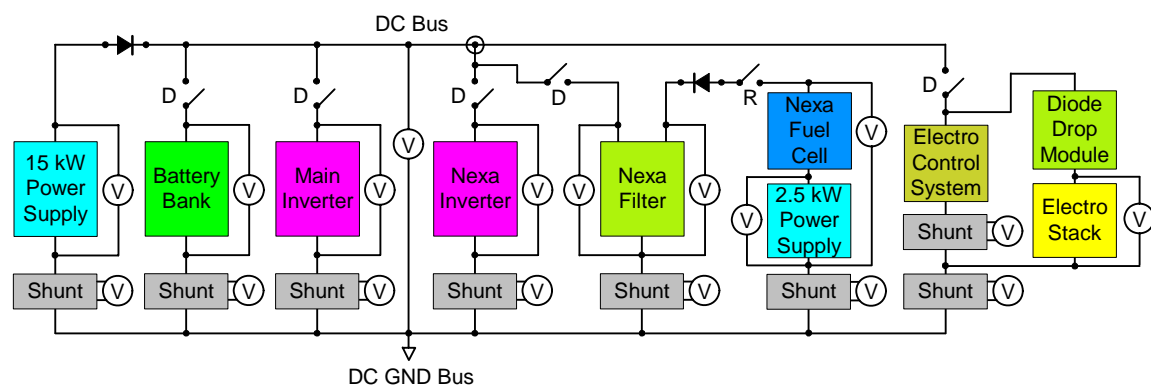
Figure 4.20 IRENE Instrumentation Node Schematic

Current is the most difficult parameter to measure accurately. Non-intrusive Hall-effect based sensors exist that are able to measure AC and DC currents without insertion losses but have long-term drift, linearity, and saturation issues. The alternate approach is to install resistive shunts and measure current as a function of voltage drop. Shunts

introduce losses and have limitations on sensitivity, thermal stability, and bandwidth. However, given the magnitude of currents and desire for accurate DC and AC measurements to 10 kHz, shunts are a better alternative [75]. The insertion point within the electrical circuit is important because absolute voltage on the shunt terminals must be considered, not just the differential. Fortunately, all of the electrical components used in the DC system are floating devices so shunt insertion on the ground side is possible. A star ground is developed to ensure all currents would pass through the shunts (i.e., no bypass routes through chassis ground paths). To minimize voltage induced between shunts due to interconnect cabling resistance, all shunts are located in close physical proximity.

The original installation is highlighted in Figure 4.21 (a). The shunts, which are electrically isolated from their mounting bases, were attached to two large heat sinks to ensure uniform operating temperature. The layout proved to be unsatisfactory because stray coupling effects induced voltages in shunts that were not actively passing current. This is mentioned to highlight the fact that analog instrumentation in such a challenging environment is as much art as a science. Extensive tests were conducted to develop a new shunt layout that would produce accurate measurements. The resulting design, shown in Figure 4.21 (b), is very unconventional. The shunts are all aligned in a row in a common plane. Cabling carrying the input and output currents are paired and attach to the shunt body at right angles. Each shunt is mounted to custom box section aluminium heat sinks, which are electrically isolated from each, and held in position via non-magnetic side rails. Air is blown through the center of the heat sinks to aid in cooling. Custom Mu metal shields surround the shunts. The signal conditioning modules are placed at right angles to the shunts in a plane slightly behind the shunt. The entire assembly is located as far away from the inverters as power supply as possible. With the physical layout established and the custom signal conditioning units developed, measurements of 10 mA in 300 A is achieved. If any of these apparently arbitrary parameters is altered (like moving one of the shunts by 10 mm with respect to the others) substantial noise is introduced.

(a) Original Current Shunt Installation   (b) Revised Version
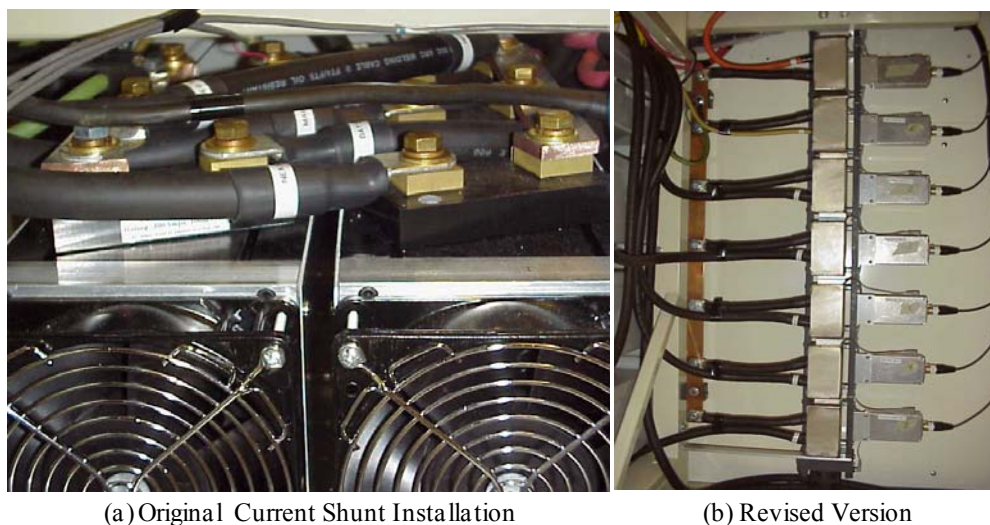
Figure 4.21 DC Bus Current Measurement Configuration

Custom signal conditioning units, mentioned above, facilitate integration of the raw transducer signals to a the common DAQ interface, see Figure 4.22. Each unit is fully shielded to allow mounting directly at the signal source. The common circuit layout can be populated in three different ways to accommodate shunt conditioning, voltage monitoring and flow meter buffering. Each module provides local amplification, offset and balancing of the raw signals. The ability to apply precise DC offset adjustments greatly improves the resolution of voltage measurements for bus devices because the active range can be mapped to the DAQ system. The effective voltage range of the DC bus is 40-60 V which is well beyond the allowable input range of the DAQ system (-10 to 10 V). The signal conditioning modules effectively shift the measurements by 50 V and allow bus voltage resolution of 0.3 mV to be achieved. The signal conditioners employ high current balanced output drive sections enabling the input impedance of the DAQ system to be reduced, improving noise rejection. To minimize power supply induced noise, each unit contains local rectification and regulation to generate the amplifier rail voltages relative to the local signal reference. A floating two wire low voltage AC source is needed for each signal conditioning module. In all, 23 modules were deployed throughout the IRENE instrumentation system.
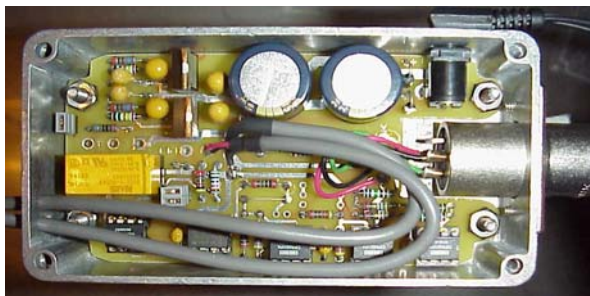
Figure 4.22 Custom Signal Conditioning Modules

Physical modifications to the DAQ system is limited to the addition of a manual patch bay for input signals and a gain adjustment in the multiplexer buffer stage to improve signal response. However, extensive code manipulation is employed to achieve an acquisition rate suitable for capturing the dynamic response of the IRENE system. The SCXI interface is the primary bottleneck in the acquisition system. The low level software drivers impose an arbitrary acquisition limit of 100 kHz due to the settling times of the amplification stages. In the IRENE application, all signal amplification occurs in the dedicated conditioning modules so the SCXI device runs at unity gain and the settling constraint does not apply. The multiplexer interface is capable of higher switching rates but the LabView software prevents the standard DAQ VI's from utilizing the potential. This limitation is overcome by tricking the DAQ card into thinking that it is reading from a single channel while the multiplexer coordinates actual channel selection. Management of the data stream is much more involved because samples are not associated with the appropriate input channels. An efficient algorithm was developed to coordinate data parsing and apply the appropriate scaling values. In the end, an acquisition rate of 9 kHz per channel was achieved.

Integration issues with the control system revolve mainly around serial port communication limits. The two Lambda power supplies and the electrolyser require a hardware based solution in the form of dedicated microprocessor communication module, see Figure 4.23. Custom interfaces were developed to conduct the low level data exchange with the remote devices in accordance to the strict timing and bit protocols. The microprocessors translate the data and interact with the computer using a data structure that LabView can deal with efficiently. In addition to solving the communication issue, the hardware interface provides a means to implement a watchdog

to ensure the LabView controller was operating. If communication ceases due to a computer crash, the interface modules take action to return the system to a safe operating mode.
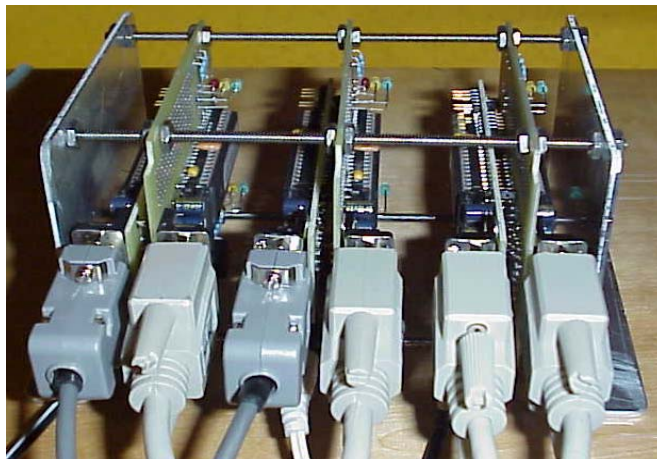
Figure 4.23 Custom Control Interface Devices

Extensive LabView programming was conducted to implement the data capture and control system for IRENE. Code development represents a major component of the integration effort. A master control virtual instrument (VI) supervises the high level control and data monitoring activities. Under this umbrella, individual sub VI's communicate with, and ensure the proper operation of each device. Data files containing time series information on specific load and renewable energy profiles are read and executed by the main control VI. Appropriate parameters that characterize the system response are logged for post experiment analysis. Data based on average values for a specified interval (typically 3-6 seconds) is recorded on an ongoing basis. Snapshots of all data points acquired for an interval can also be captured to reconstruct the exact system response for transient analysis. The user interface displays all relevant information in a multi-page format, see Figure 4.24. The real time display functions similar to an oscilloscope to allow the operator to observe current, voltage, and mass flows between any system components at the appropriate scale and time base. The code is structured in a modular fashion to allow for implementation of alternate control algorithms. The control schemes are tailored to the individual experiments and will be outlined in the discussion of results presented in Chapters 5 and 6.

Figure 4.24 LabView Bases IRENE System Controller

In general, the data acquisition and control program consumes all of the computing resources available. Additional programs can not be executed while running the master control VI. Code stability has been demonstrated during multi week experiments. Operation for longer durations is limited only by the stability of the Windows operating system. Any future modifications to the code must be mindful of the overall loop execution rate that must be maintained to avoid buffer overflow.

4.7 Summary

Developing a unified IRENE system from the commercial components purchased was a challenging task. The following integration aspects were addressed through a number of creative component modifications and design of custom devices; including: development of a user configurable bus interface; electrolyser limitations related to control, thermal response, hydrogen compression, measurement, and input power conditioning; hydrogen storage and delivery; fuel cell power utilization; and system level instrumentation and control.

Component reliability has been an ongoing issue that has introduced additional barriers to integration. Several temporary solutions were required to make the system operational while long-term answers were sought.

Creating a unified data acquisition and control system has introduced a number of complications in both hardware and software due to variations in standard used by the device manufacturers.

Overall, the integration process has demonstrated that significant advances in the core technologies are required before systems employing hydrogen energy buffering can be readily assembled from commercial components.

PART II :

Dynamic Operation of the IRENE System

Chapter 5

Hydrogen Buffer Response to Dynamic Operation

The experimental work conducted with the IRENE test-bed examines fundamental modes of operation that a renewable-regenerative system would encounter on a day-to-day basis. In a real system, the hydrogen energy buffer must respond to a full range of dynamics imposed by the temporal nature of the renewable input, bus component interactions, and loads. System stability can only be maintained if sufficient power transfer occurs at every instant. The ability to absorb power from the input source is as critical as the ability to service the load. The underlying notion generally applied in the modeling of renewable-regenerative systems is that the transfer characteristics between devices are well matched enabling stable operation.

From a conceptual viewpoint, coupling wind turbines, solar arrays, and other devices that generate electricity to an electrolyser, which consumes electricity to generate hydrogen, is straight forward. In the prevailing operating methodology proposed for renewable-regenerative system, the electrolyser functions as a load levelling device, absorbing excess input power when available, and is the first load shed when a power deficiency exists. This represents a significant departure from the steady-state operating mode that electrolysers are commonly subjected to and for which data on power consumption, hydrogen production, gas purity etc., is available [58]. However, in an IRENE-type application, the electrolyser transition characteristics may have a significant impact on the overall system performance. The first series of experiments probes the basic electrolyser response during the start-up transition period under conditions which are representative of the operating limitations due to the common bus system configuration.

The electrolyser's response to dynamic variations of input power is a critical aspect influencing the functionality of a real IRENE system. The instantaneous power profile available for hydrogen production is dictated by the variability in the renewable source coupled with the actual service demands of the load. Some inherent smoothing takes place in systems with multiple renewable inputs and loads. However, practical

limitations on generation capacity coupled with peaking demands from real loads will inevitably subject the electrolyser to both low frequency and high frequency events. The actual electrolyser response under variable operation is not well documented in the literature. Models employed in high level renewable-regenerative system surveys neglect dynamic operation by assuming that average values for power input and efficiency are sufficient to characterize the electrolyser. More in-depth theoretical work includes temperature and pressure affects, but operating history is not accounted for. The second series of experiments probes the electrolyser response to short duration transient events that would occur during operation from an unsteady resource such as wind power.

The third series of experiments is designed to investigate the electrolyser's response to operation on time scales that are representative of predictable resources like solar or tidal power. The response to cyclic operation will help inform design of the energy buffer sub-system which employs electrolysis in a non-traditional manner.

Data analysis is not conducted in an exhaustive manner but is intended to expose trends that were observed during the experimental program. While the operating efficiencies, hydrogen production rates etc., are interesting, they are specific to the hardware implementation. However, the trends and operational considerations gathered during the execution of the experimental program are more generic in nature and applicable to a broad range of small-scale renewable energy systems.

5.1   Electrolyser Temperature and Transition Characterization

Renewable-regenerative systems, like IRENE, rely on the electrolyser to absorb excess power whenever it is available. Theoretical system models assume that the electrolyser is capable of sinking the rated name-plate power input at any instant. The operating characteristics of a real electrolyser may differ considerably if a large change in set-point is introduced. A worst case scenario is envisioned when the electrolyser transitions from an inactive state to the maximum input setting.

Thermodynamic analysis of the electrolysis processes indicates that both heat and electrical input energy is required [76]. Process efficiency increases with increasing temperature.   In actual operation, the heat evolved due to electrical inefficiencies is sufficient to cover all of the process heat requirements and additional cooling is required to remove the surplus. Thus, the thermal aspects of electrolyser design focus primarily on heat removal not addition. Small electrolysers, like the SRA used in IRENE, rely on natural self heating to reach the desired operating temperature of 60 to 80 °C. However, electrolyser cell stacks have significant mass and associated thermal inertia, so temperature changes do not occur instantaneously.

Modeling efforts commonly neglect thermal effects by assuming that a constant electrolyser temperature is maintained. While this may be reasonable in a large-scale renewable-regenerative system implementation, the parasitic load would need to be carefully evaluated in a small-scale application. If the electrolyser is not used for an extended period, the energy consumed to heat the stack may be unwarranted. A trade-off exists between the potential performance losses associated with the start-up period and the energy required to minimize that loss.

5.1.1   Step Function Experiments

A set of step function experiments were conducted to assess the electrolyser's transitional behaviour. Although the power input profile is idealized, the intent is to evaluate the most extreme case that the electrolyser would be subjected to in actual operation. The step profile is not unreasonable for a renewable system based on solar input. Figure 5.1 illustrates the results of a numerical simulation for a solar based renewable-regenerative

system during a period with favourable insolation [77]. In this system, the solar array was sized to meet the winter load and excess energy is available for hydrogen production during the summer months. The simulation assumes that energy produced during the early morning is used to recharge the batteries to a 100 percent state-of-charge (SOC). Thus the excess energy available for hydrogen generation between 9:00 to 15:00 hrs includes a large initial step change and is the basis for the electrolyser input power profile.

In a real system, bus voltage is the dominant control parameter that drives energy exchange between system components and is also an indicator of battery SOC. The working range of bus voltages for the IRENE system is 46 to 54V. The electrolyser response at the various voltage levels is required to map the transitional behaviour.
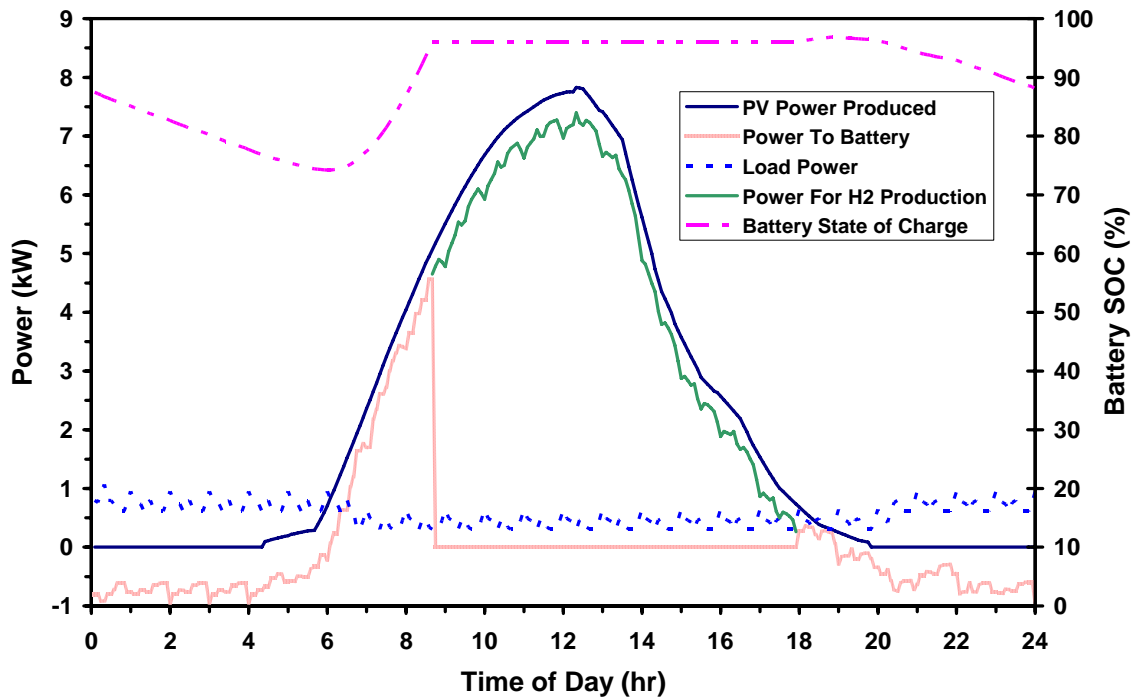
Figure 5.1 Input Power Profile Reference Data – NRCan Model

Data Courtesy of M Mottillo, NRCan, Ottawa [77]

The step function experiment entails electrolyser operation for a six hour duration at a steady input voltage level. Following this, sufficient off time is allocated to allow the electrolyser to return to ambient temperature (typically 24 hour). The cycle is repeated

for an alternate input voltage level, spanning a range from 46 to 54 V in roughly 0.9 V increments. The stack current, temperature and hydrogen production rates are observed.

A family of curves for the basic electrolyser response to the six hour step function input is illustrated in Figure 5.2. To account for minor variations in the initial electrolyser temperature, the t_0 start time is corrected for a stack temperature of 28 °C. In each case, the net power draw increased until the stack temperature reached the 60 °C operating point. The total hydrogen produced, energy efficiency, and key thermal parameters are summarized in Table 5.1.

Figure 5.2 Electrolyser Six Hour Step Function Response

Electrolyser Operating Point (volts)

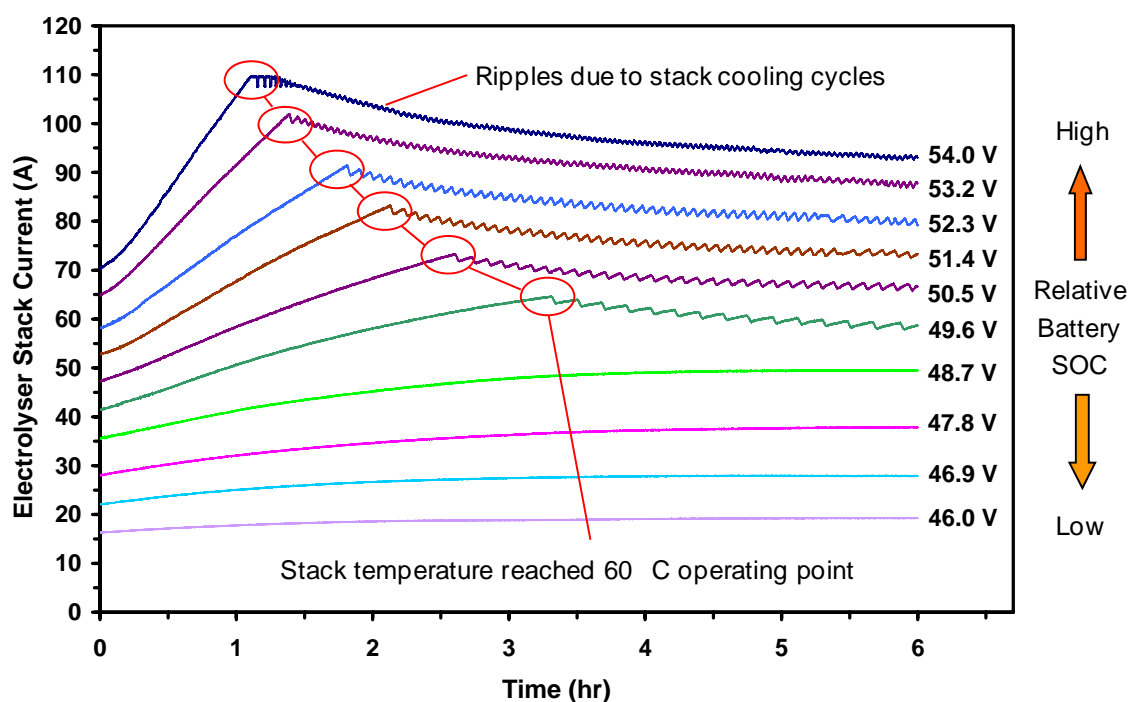|	54.0	53.2	52.3	51.4	50.5	49.6	48.7	47.8	46.9	46.0
Total H_2 Produced (L) *	5922	5500	4911	4432	3924	3326	2729	2031	1488	984
H_2 Energy Value (kW·hr) **	16.5	15.3	13.7	12.4	10.9	9.8	7.6	5.7	4.2	2.7
Input Energy (kW·hr)	31.3	28.7	25.4	22.6	19.8	17.1	13.4	10.1	7.5	5.1
Average Energy Efficiency (%)	52.7	53.4	54.0	54.7	55.4	57.7	56.8	56.1	55.5	53.6
Time to 60 °C (min)	77	83	109	127	156	199	na	na	na	na
Final Stack Temperature (°C)	60	60	60	60	60	60	56.6	49.6	43.3	37.7

* H_2 measured at 25 C, 1 Atm   ** Based on Lower Heating Value

Table 5.1 Electrolyser Six Hour Step Function Results Summary

In reviewing the data, several observations are made. The most notable is that the thermal response of the electrolyser has a significant impact on performance for the specified duty cycle. The minimum time for the electrolyser to reach operating temperature was 77 minutes, or 1/4 of the total daily run time. This occurred for the most favourable operating conditions for hydrogen generation which is at a high battery SOC (54V bus). In cases with medium SOC (50V bus), the warm-up period lasted over half of the total operating time. At low SOC, the stack temperature never reached the design operating point. During the warm-up period, the electrolyser is unable to draw the rated nominal name-plate power. Models which do not consider thermal effects will over predict the actual daily hydrogen output. A power de-rating factor should be employed in the basic theoretical models to reflect the reduced capacity.

The energy efficiency of the electrolyser is calculated based on the energy content (lower heating value) of the hydrogen produced divided by the electrical energy input. The values obtained range from 52 to 58 percent, i.e., 10 to 20 percent lower then the values reported in the literature [78]. Duty cycles are generally not reported when efficiencies are stated so it is difficult to assess if the lower efficiency is due to the operating mode. However, given the transitional response observed, it is reasonable to expect lower efficiencies for cyclic operation than for steady-state operation.

It is also evident that the electrolyser performance is time dependent. For the experiments conducted with a supply voltage above 49 V, the current draw declined after the electrolyser reached a stable operating temperature. A current decline of 12 to 18 percent was observed for the 49.6 to 54 V cases respectively. The detailed theoretical models presented for electrolyser operation developed by [12, 60] do not have terms that account for time variation in the VI characteristics. Refinement of the theoretical models is required to accurately reflect the observed operating characteristics. The decreasing slope of the decay trend indicates that stable operation may occur but not within the operating window of a solar day.

If standard models are used to predict hydrogen production for an electrolyser subjected to daily cycling, the error estimate should account for the observed variation. Further discussion of the observed performance decline is addressed in Section 5.2.

5.1.2   Bus Coupled Step Function Response

In the experiments described above, the constant voltage condition would only occur when the battery SOC is not changing. A more realistic operating scenario includes bus voltage variation as the batteries respond to the instantaneous current demands required to balance energy flows. During periods where the renewable input exceeds the demand load, both the absolute value and the rate of change in bus voltage are heavily dependent on the battery charging characteristics.

The battery charging profile used in the model presented in Figure 5.1 is not representative of a real system. The net energy required to recharge the batteries is accounted for, but the charge delivery characteristics are not considered. During the period between 7:00 and 9:00 hrs all excess energy is devoted to battery charging. The simulation assumes that the rate at which the batteries can absorb charge is not limited. As the batteries near 100 percent SOC, the power input profile peaks and then abruptly falls to zero. In actual operation, as the batteries approach full charge, their ability to absorb power diminishes. Therefore, the control system must actively proportion the power diverted to battery for recharging and to the other system loads (i.e., the electrolyser). A more accurate electrolyser operating scenario would have a rising input voltage as the battery SOC increases. The electrolyser response would then be a hybrid

combination of the steady-state voltage curves given in Figure 5.2. An upper limit on hydrogen production exists depending on the rate at which the system transitions from the lower to the higher voltage states.

The second experiment conducted to observe the electrolyser transition characteristics involves combined electrolyser operation and battery recharging. The electrolyser input voltage is derived from the bus voltage as the batteries are charged from an initially depleted state. The batteries are charged at the maximum allowable rate of 24 A. Sufficient input current is available to operate the electrolyser at the associated bus voltage, (i.e., the batteries are current limited while the electrolyser is voltage limited). Based on the battery manufacture's voltage-to-SOC correlation, the experiment was conducted with an initial 40 percent battery SOC. Electrolyser voltage, current, temperature and hydrogen production are measured for the six hour operating window. A reference case is assessed where the batteries are fully charged at the start of the experiment. This case was run for an additional 16 hours to obtain an estimation of the steady-state operating performance.

Figure 5.3 illustrates the influence of both thermal and bus voltage transition on the electrolyser's ability to draw power from the system. A reference line is drawn indicating the steady-state performance achieved after approximately 24 hours of operation. The upper curve is the best case scenario where the batteries are fully charged at the start of the experiment. Since the voltage is constant, this curve has a similar shape as those in Figure 5.2. The lower curve of Figure 5.3 represents the case where the batteries are initially depleted and charged at the 24 A limit. The input voltage at the electrolyser rises during the first five hours as the batteries are charged at the maximum rate. After that point, the bus voltage is essentially constant during the float charging portion of the cycle.
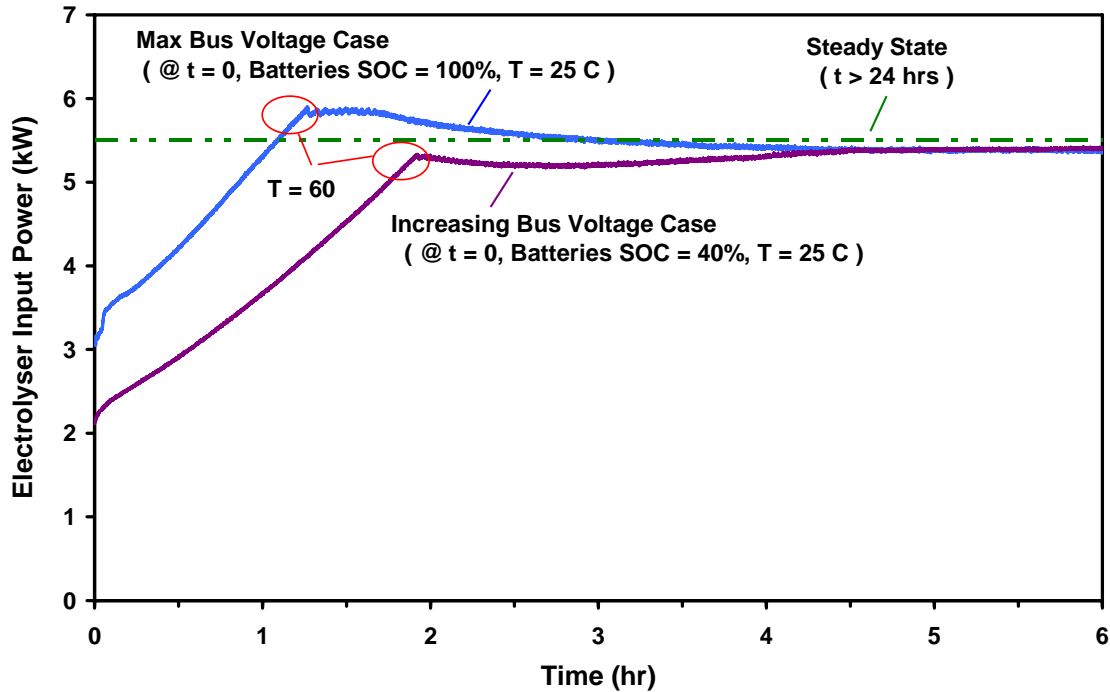
Figure 5.3 Coupled Electrolyser Operation and Battery Charging

Had the electrolyser performed at the steady-state level for the six hour period (i.e., the ideal electrolyser response), it would have generated 6696 L of hydrogen based on the measured conditions after 24 hours of continuous operation. The reference case produced 6206 L during the initial six hours while the case with the 40 percent initial battery SOC generated only 5707 L.

Relative to the steady-state, there is theoretically a 7.3 percent loss in hydrogen production due to the thermal transient for the case were the batteries are fully charged at the start of the experiment (i.e., the best case scenario that exists in real operation). A 14.8 percent loss is observed for the case that started with the depleted batteries. Furthermore, at the start of the low SOC run, the electrolyser is only able to draw 42 percent of the steady-state power. The power draw increases in a roughly linear manner during the first two hours until the nominal stack operating temperature is reached.

From a system design standpoint, the reduced power sinking capability of the electrolyser during the transition period may dictate the need for backup dump loads to provide the equivalent system load.

These experiments indicate that the thermal transients and the bus limiting interactions must be considered when modeling the hydrogen production for a renewable-regenerative system subjected to cyclic operation.

5.2   Electrolyser Response to Transient Events

The electrolyser's primary function in an IRENE-like system is to buffer excess energy from the renewable resource. Since renewable resources are inherently variable, the electrolyser will be subjected to a dynamic input power profile. The common assumption made in modeling of renewable-regenerative systems is that the electrolyser performance is not adversely affected by dynamic operation. A series of experiments were conducted to probe the validity of this assumption.

5.2.1   Variable Duration Events

In a real IRENE system, a sudden reduction in power available for hydrogen production would occur when the system services the transients from higher priority loads or when a temporary interruption in the renewable energy resources input occurs (e.g. clouds or winds in excess of the turbine cut-off speed). In an ideal case, the simple act of switching the electrolyser off for a brief period should not alter the basic operating characteristics.

The dynamic event for the first experiment is restricted to temporary removal of electrolyser input power. Prior to the turn-off event, the electrolyser is operated for a sufficient period to achieve stable operation. Following the reinstatement of power, the conditions are again held constant until stable operation is achieved. The experiment is nominally run at a constant bus voltage of 54 V and stack temperature of 60 °C. A hardware current limit equal to the maximum allowable stack current of 110 A is implemented. Two different duration off-pulses (referred to as 'events') were applied during the experiment. The first shutdown lasted 90 minutes while the second event was only 2 minutes.

The experimental results are illustrated in Figure 5.4, a time series plot of electrolyser current and hydrogen production. The electrolyser current draw immediately following the 90 minute shutdown at 24:00 hrs increases to the upper maximum, a 14 percent gain

over the final conditions prior to the shutdown event at 22:30 hrs. This indicates that the rest period may in fact enhance performance. However, in the long-term, a net reduction in performance is observed as the steady-state current draw at 47:00 hrs is 7 percent below the previous recorded value at 22:30 hrs. The response to the second off-pulse, occurring at 48:00 hrs, is similar to the first event with a short-term improvement in performance followed by a decline to stable operation at yet a lower level.
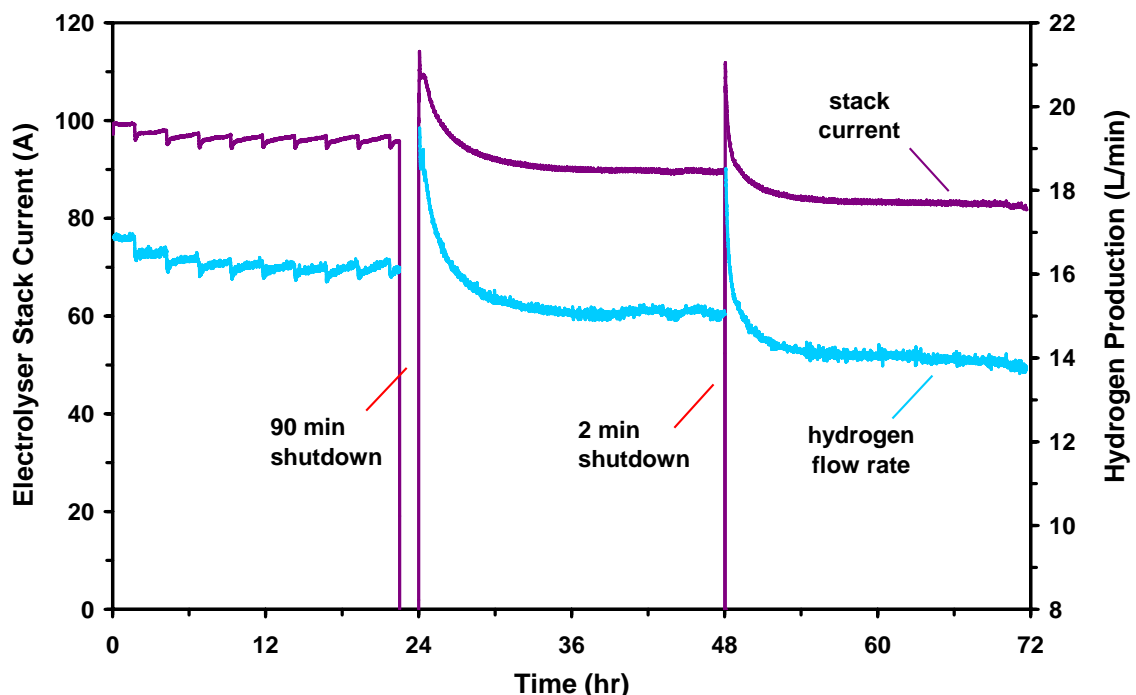
Figure 5.4 First Observation of Dynamic Induced Electrolyser Performance Decline

Ripples observed in the current and hydrogen production prior to the first pulse event are due to variations in electrolyte concentration. During the 90 minute off period, the electrolyser control algorithm was modified to increase the frequency of stack electrolyte adjustment. By adding smaller quantities of make-up water more frequently, less variation in electrolyte concentration occurs. This point is raised to clarify that the change in smoothness of the current and hydrogen production profiles before and after the first off-pulse is not related to the pulse event but rather to the improved process control.

The 2 minute pulse duration was chosen as it corresponds to the minimum time required to reboot the IRENE computer control system, an event that a real system would be

expected to cope with. The progressive decline in current draw raises concerns regarding the viability of operating an electrolyser in the duty cycles anticipated in a real system implementation.

Although the current draw decreases due to the transient event, hydrogen production directly tracks stack current at all stages of the experiment. The ratio of the stack current to the hydrogen produced is 5.94 ± 0.05 A/(L/min). The Faraday efficiency, which is a measure of the hydrogen production to current input, remains essentially constant while the VI characteristic is clearly time dependent.

It is interesting that the characteristic response is similar given the difference in duration of the two off-pulses (2 to 90 minutes). These results indicate that power disturbances have a significant impact on electrolyser performance. Furthermore, the changes in operating point are not predicted by the theoretical electrolyser models.

5.2.2   Fixed Two Minute Off-Pulses

A second experiment was conducted to examine the extent of the performance decline outlined above.

The operating conditions were altered to avoid current limiting during the transition phases. This was accomplished by reducing the electrolyser operating temperature to 30 °C. Preceding the experiment, the electrolyser was inactive for several days. An initial 24 hour operating period is completed at a constant 54 V bus voltage to obtain a stable operating baseline. Following this, six cycles consisting of a 2 minute shutdown event followed by 24 hours of operation were conducted.

A time series plot of electrolyser current is presented in Figure 5.5. The 35 percent shift in baseline current draw with respect to the previous experiment is due to the temperature change. The response to the first two shutdown events is similar to the initial experiment conducted at the standard stack temperature of 60 °C. This indicates that the mechanism driving the performance decline is not fundamentally altered by temperature. With each successive shutdown event, the net change between stable operating point diminishes, but is always negative. A 23 percent decline in current draw is noted from initial stable operating point to final condition after the six interrupt events.
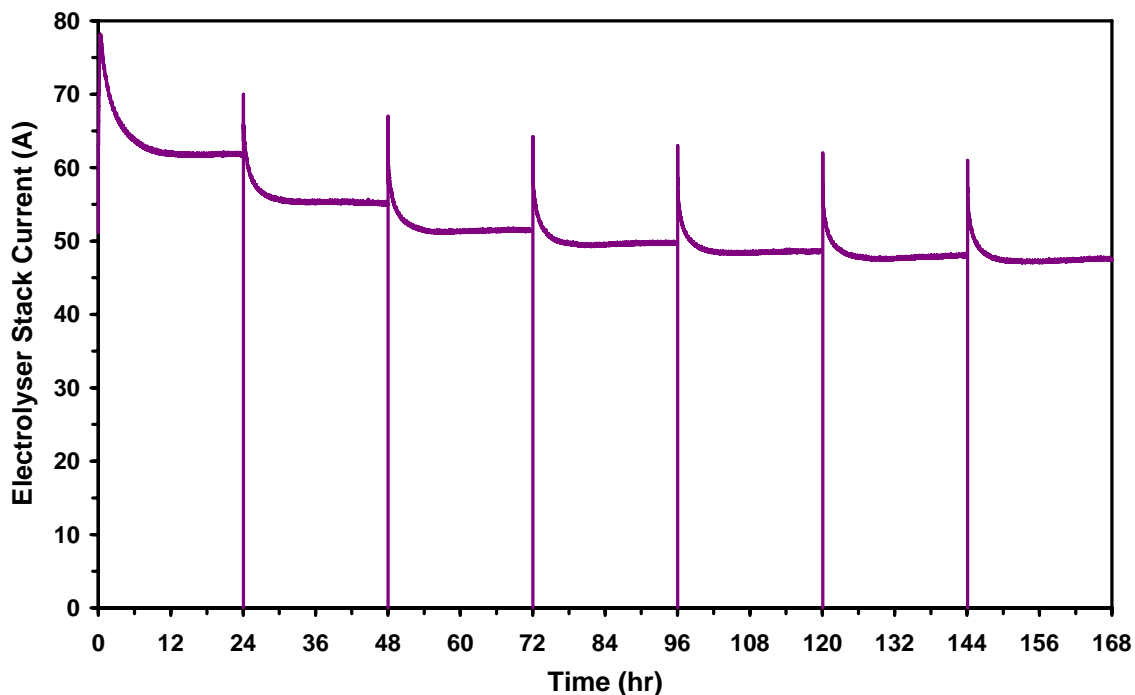
Figure 5.5 Electrolyser Response to Repeated Two Minute Shutdowns

Figure 5.6 is an overlay plot of the seven 24 hour periods. The shape of the current response is similar for events two through six. The current on start-up is typically 25 percent higher then the previous steady-state value but only lasts for approximately 5 minutes. Subsequently, the current decays following an exponential response for the next six hours. As such the current draw exhibits considerable dynamics as it transitions towards a stable value. The response time represents a significant portion of the daily input profile associated with renewable resources such as solar and tidal.

Based on the observed performance, estimates for the daily hydrogen production for a renewable-regenerative system with unsteady input power will be inaccurate if dynamic effects are not taken into consideration.
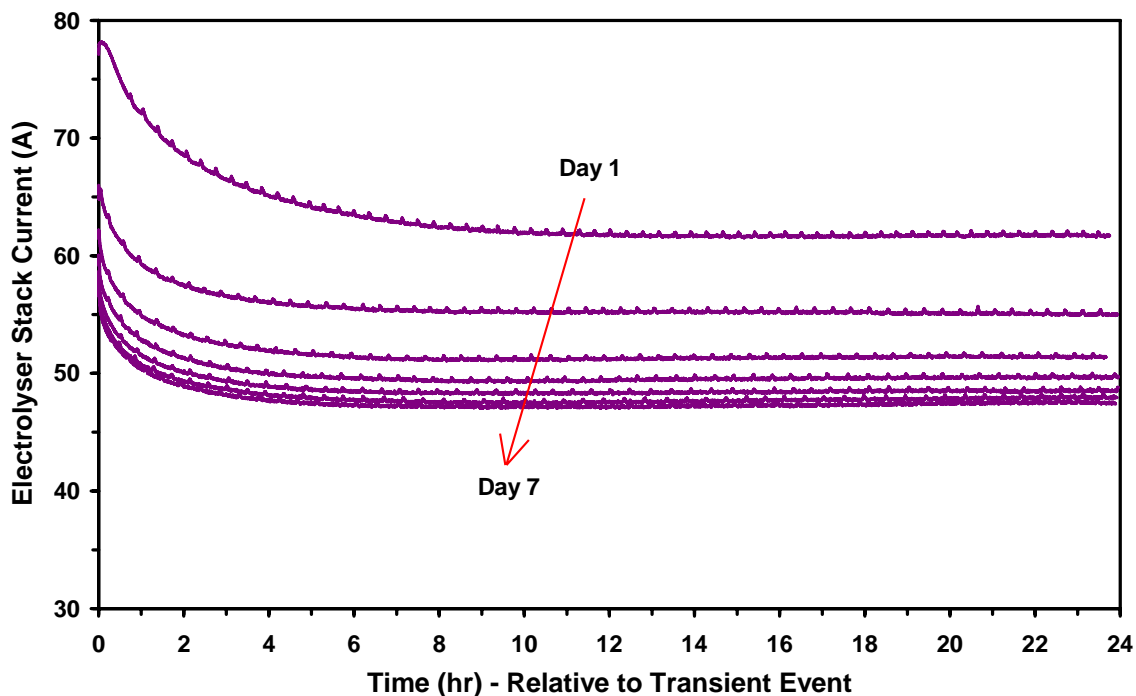
Figure 5.6 Two Minute Shutdown Response: Overlay of Daily Data from Fig. 5.5

5.2.3   Minimum Holding Current

A repeat of the previous experiment was conducted to determine if the short-term shutdown events cause permanent electrolyser performance degradation. The second objective was to determine if the observed decline would be altered by applying a minimum holding current during the transient event as opposed to a complete shutdown.

The same procedure is followed as the last experiment. A 24 hour rest period is observed at the start of the experiment followed by a 24 hour operating period at a constant 54 V bus voltage to obtain stable baseline performance. Two cycles consisting of a 2 minute shutdown (i.e., 0 A) event followed by 24 hours of operation are then conducted. The third cycle employs a 1 A minimum holding current (roughly 1 percent of the nominal maximum stack current) during the 2 minute transient event. The fourth and fifth cycles utilize a 10 A minimum while the final two events are conducted at 5 A.

The results, with appropriately scaled transition currents, are illustrated in Figure 5.7. Current draw during the initial 72 hour period has a similar characteristic shape as in the previous experiment but the absolute values are shifted. The current at 24:00 hrs is approximately 18 percent higher than the value at the end of the previous experiment

indicating that a partial recovery of performance occurred during the rest period. However, in absolute value, the current draw during the first 72 hours of the repeat experiment aligns with the 24:00 to 96:00 hr period of the previous experiment.

The 1 A holding current employed during the event at 72:00 hrs does not dramatically alter the decay characteristics. However, the 10 A current utilized during the events at 120:00 hrs and 144:00 hrs minimizes the current decay following the transient event. The intermediate 5 A current employed during the final two events at 144 hrs and 168 hrs contains aspects of both the 1 and 10 A events.
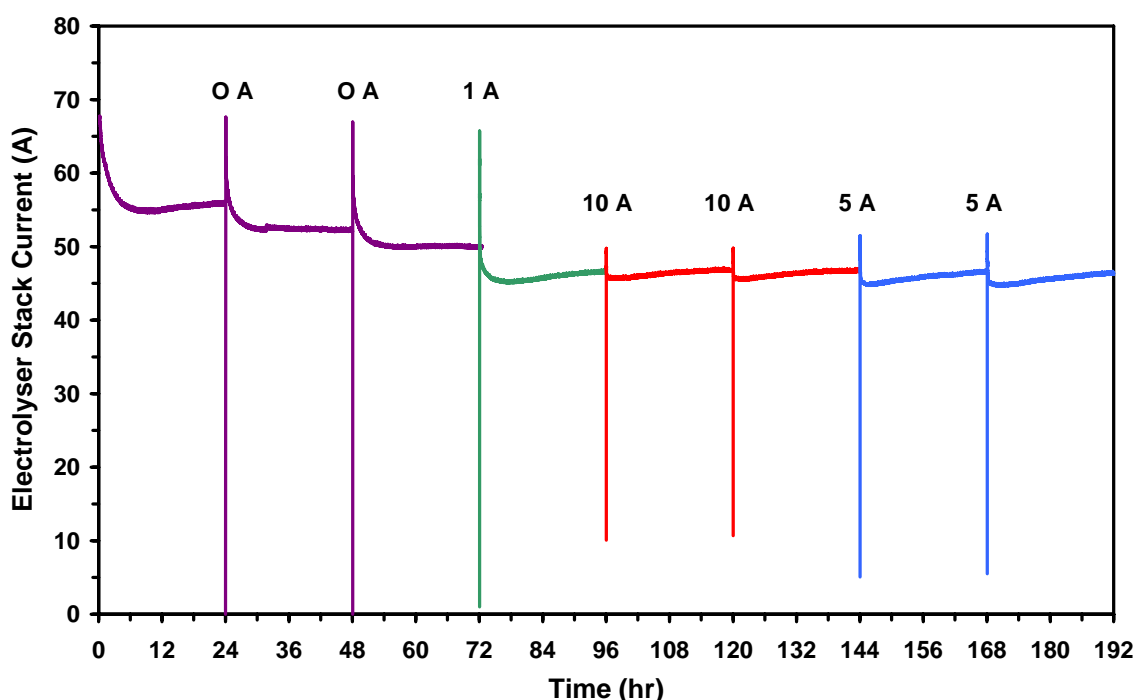
Figure 5.7 Electrolyser Response to Minimum Holding Current

The difference in response characteristics is more pronounced in Figure 5.8, an overlay plot of the eight 24 hour periods. An initial current spike is observed each time the electrolyser is subjected to a step change; however, the spike duration is less then 30 seconds for the events with a minimum holding current. These data points have been omitted from the figure to improve clarity. The upper three curves are the electrolyser current draw during the initial 24 hour period and the two 0 A events. The 1 A event follows a similar decay response; however, the current during the initial three hour window is not larger than the previous steady-state value. A partial recovery in

performance is observed during the period from 6:00 hrs to 24:00 hrs but a net 8 percent shift in operating point occurs due to the event. In comparison, the 10 A holding current reshapes the decay profile to a step change. An immediate 1.5 percent reduction in current is noted, but after 10 minutes a steady recovery trend develops. During the remainder of the 24 hour period, initial losses are fully recovered. Dynamics noted during the initial three hour operating window of the previous cycles are essentially eliminated. The second 10 A event has the identical response indicating that degradation can be minimized if sufficient minimum current is maintained. The response to the intermediate 5 A current displays the aspects of both the 1 A and 10 A events. The initial decay is more dynamic then the 10 A event but retains the recovery and repeatability aspects.
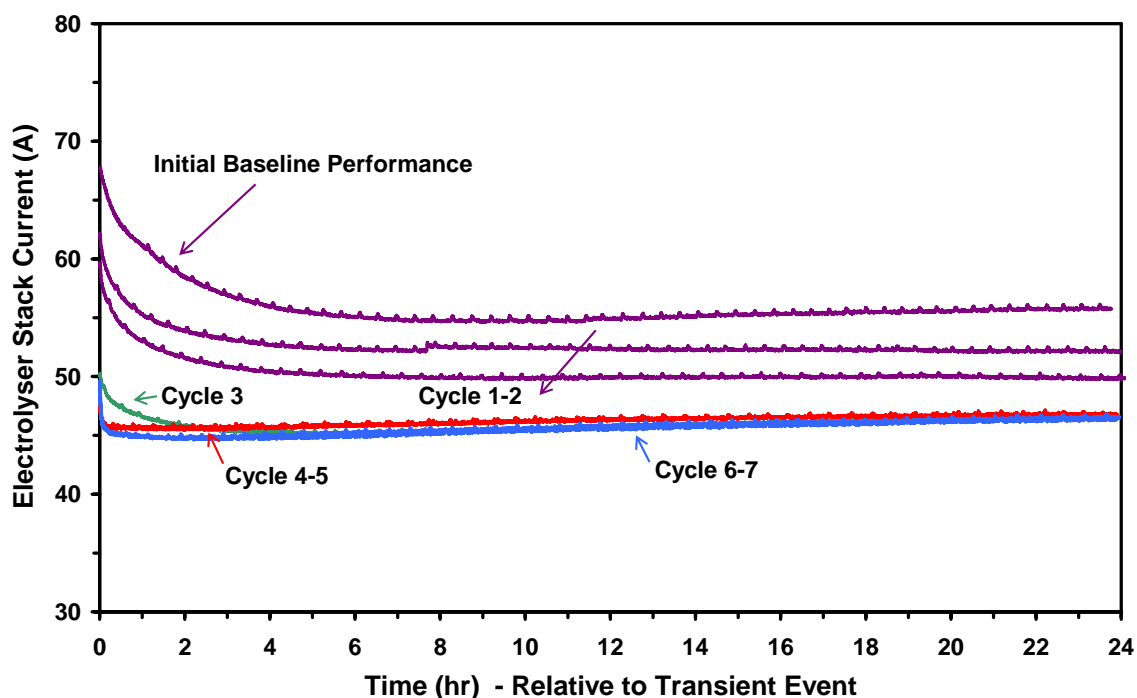
Figure 5.8 Hold Current Response: Overlay of Daily Data from Fig. 5.7

Further insight into the electrolyser response characteristics can be gained by observing the stack voltage during the two minute transient events. Based on the Gibbs function, the thermo-neutral voltage for electrolysis is 1.48 V at 30 °C [60].

The stack voltage during the two minute transient events is illustrated in Figure 5.9. Values are reported in terms of the average cell voltage calculated from a single

measured stack voltage for all 26 electrolyser cells. When the stack is switched off, the voltage drops below the threshold within the first 2 second. In the case where a 1A holding current is maintained throughout the transient event, the average voltage crosses below this threshold within the first 3 seconds of the transient event. The voltage is insufficient to maintain the electrolysis process. The net current supplied to the stack is conducted through parasitic paths that are inherently part of the physical device.

The response to the 5 A holding current differs considerably. The voltage undergoes a step change from 2.1 V to 1.7 V when the current is initial lowered but remains steady throughout the remainder of the two minutes. The voltage is sufficient to maintain the fundamental electrolysis process.
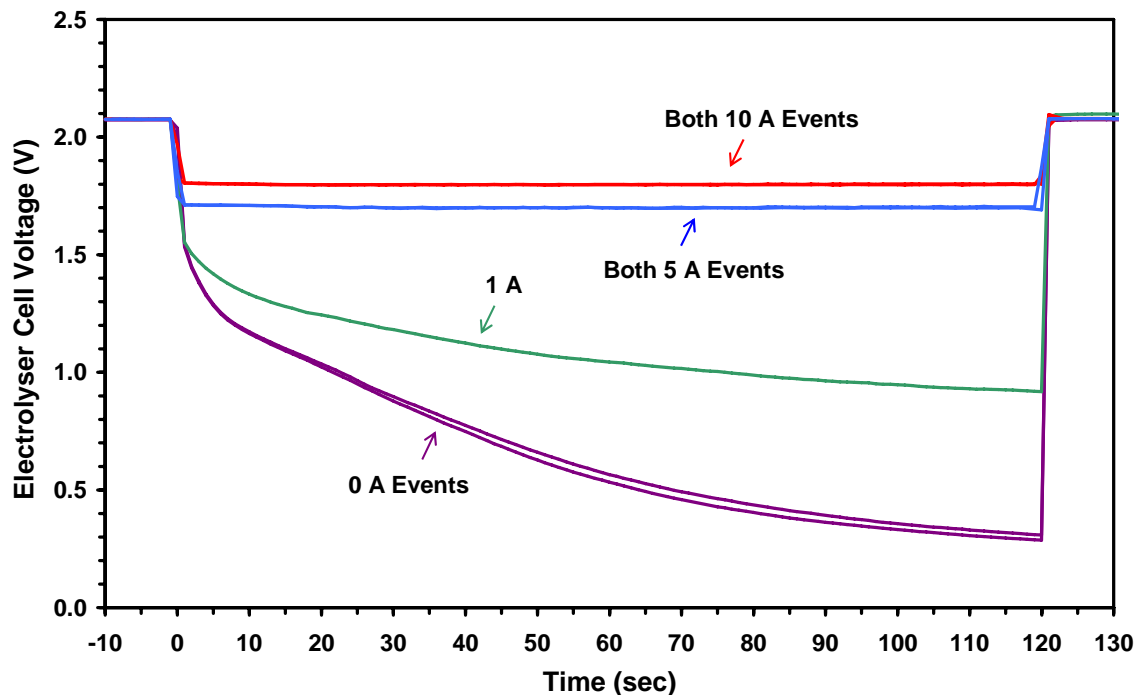
Figure 5.9 Electrolyser Stack Voltage During Two Minute Transition Events

This experiment clearly demonstrates that electrolyser performance is negatively impacted by discontinuities in the input power. Additional data is required in order to make a definitive statement regarding the extent of the long-term degradation introduced by dynamic events. However, the trend observed indicates that dynamic operation induces both short-term and long-term degradation. Partial recovery of the short-term

degradation is possible if a sufficient rest period is employed. The application of a minimum holding current reduces the decay due to dynamic cycling.

From an operational standpoint, it may not be feasible to operate the electrolyser for sustained periods on battery power when the renewable resource is not available. Determining under what conditions to supply standby current and when to impose a minimum length shutdown is a non-trivial control and optimization problem. Further discussion of the implications associated with the observed electrolyser performance is given in Chapter 7.

5.2.4   Rapid Cycling

The operating conditions imposed in the previous experiment were designed to isolate the electrolyser's response to a single dynamic event. This is not representative of the operating profile for an electrolyser employed in a real renewable-regenerative system which would encounter dynamic events on a more frequent basis. An experiment was conducted to examine the electrolyser's response to an input power profile that contains dynamic events on a more realistic time scale.

In this experiment, regular electrolyser operation at constant input voltage is interrupted by 30 second duration dynamic events on 10 minute intervals. The transient events are applied during the first 6 hours of the experiment followed by 18 hours of steady-state operation to assess overall stability. Two dynamic events are considered, a full stack shutdown and operation at 10 A. A third case without transient events is completed as a reference. Similar bus voltage and stack temperature (54 V bus and 30 °C respectively) are applied to allow direct comparison with the previous experiments. Likewise, a 24 hour rest period is introduced between operating cycles.

The electrolyser current draw is plotted against the baseline response for uninterrupted operation, see Figure 5.10. Data points at low stack currents occurring during the 30 second dynamic events have been removed to improve clarity. The cycle utilizing the 10 A minimum holding current does not deviate significantly from the basic electrolyser response to uninterrupted operation. Minor overshoot is noted immediately following the dynamic event but settles to the steady operating curve within the 10 minute interval.

The background performance decay, observed in the previous experiments, is not altered by the dynamic cycling. The performance deviation during the interval from 6:00 hrs to 24:00 hrs is on average less than 1 A.
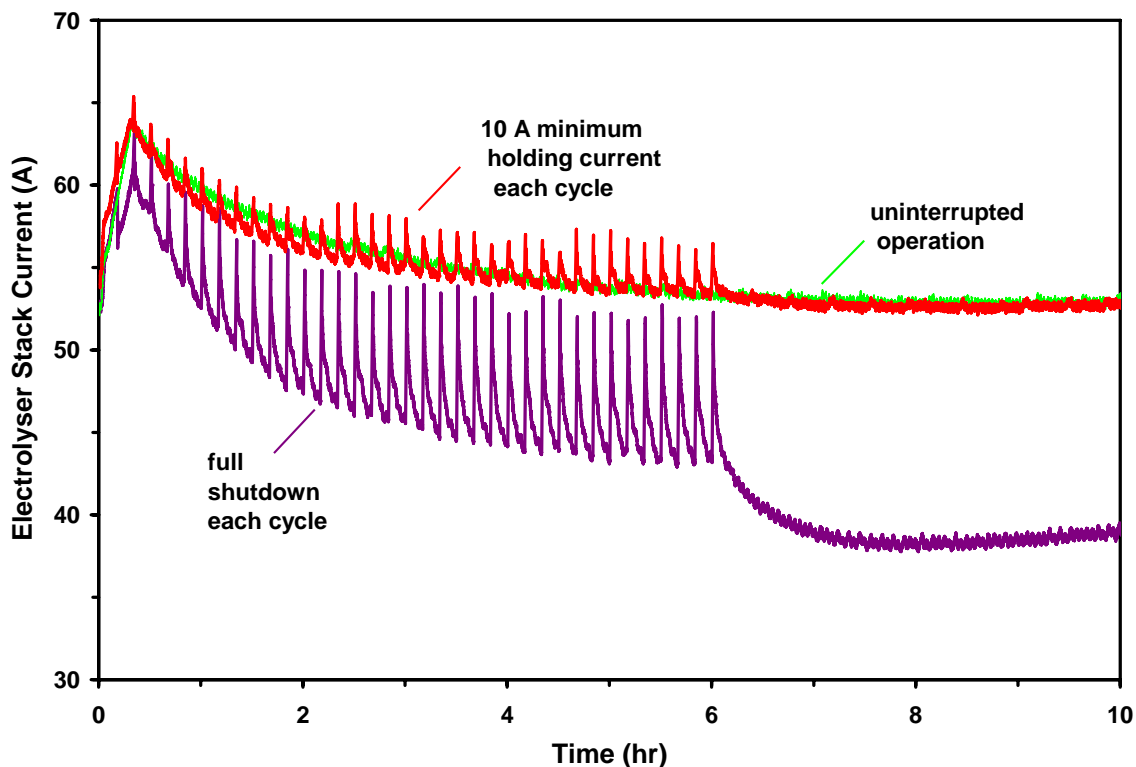
Figure 5.10 Electrolyser Response to Rapid Cycling

The response for the experiment conducted without the minimum holding current shows a significant decline in performance during both the 6 hour cyclic period and subsequent sustained operating period. At 6:00 hrs, the performance has declined by 19 percent relative to the reference case. After the last dynamic event occurs, the performance continues to deteriorate for an additional two hours leading to a 27 percent loss in performance at 8:00 hrs. The 24 hour trend (not illustrated in the figure) shows a steady moderate recovery in performance during the remaining 16 hours but the end value is still 20 percent lower than for the other two cases.

The results from this experiment clearly indicate that electrolyser performance is degraded by repetitive shutdown cycles. Increasing the shutdown frequency accelerates the performance decline. On the other hand, a potential very useful finding is that instating a basic holding current minimizes the impact of dynamic events. If a

renewable-regenerative system employs a similar type of hydrogen generation technology as the one implemented in IRENE, a high priority must be assigned to maintaining the minimum electrolyser current during dynamic operation.

5.3 Electrolyser Response to Long Time Scale Cycling

Experimental results presented thus far indicate that electrolyser's VI characteristic has a time dependent aspect. It is therefore important to determine the electrolyser response to operating cycles on time scales which are relevant to common renewable resource inputs. Experiments described in Section 5.2 indicate that a significant shutdown period (multiple hours) is required to avoid performance degradation. IRENE-like systems that rely on highly transient input sources, like wind, will require enhanced temporary energy buffer capacity (i.e., battery storage) to maintain minimum electrolyser current during periods of high resource variability. However in a solar based system, where electrolyser operation is restricted to daylight hours, sufficient recovery time may exist to forgo with the holding current during the night.

5.3.1 Variable Duty Cycles

The experiments described in this section were conduced to determine the electrolyser's response to operating cycles on time scales that are relevant to a solar resource. A reference case was first conducted to assess the repeatability of the electrolyser. Six cycles consisting of 24 hours of operation at constant input voltage and stack temperature (54 V and 30 °C respectively) followed by a 24 hour rest period were conducted. The duration of each portion of cycle was then reduced to 12 hours to emulate daily operation of a solar system during periods with high resource availability (i.e., summer time operation). This revised cycle was repeated three times. A final cycle employing a 6 hour operation followed by an 18 hour rest period was conducted to assess operation of a solar system during periods with reduced resource input (i.e., operation during winter months).

Figure 5.11 illustrates the time series results for three repetitions of the six cycles conducted with the 24 hour on, 24 hour off operating pattern. The electrolyser current

follows very similar trends all 6 cycles with a maximum 2 A deviation at similar time intervals between any two cycles. The initial current draw is on average 12 percent higher then the steady-state value achieved after 24 hours of operation. The 24 hour period between experiments is sufficiently long that degradation in performance is not observed on the subsequent start-up.
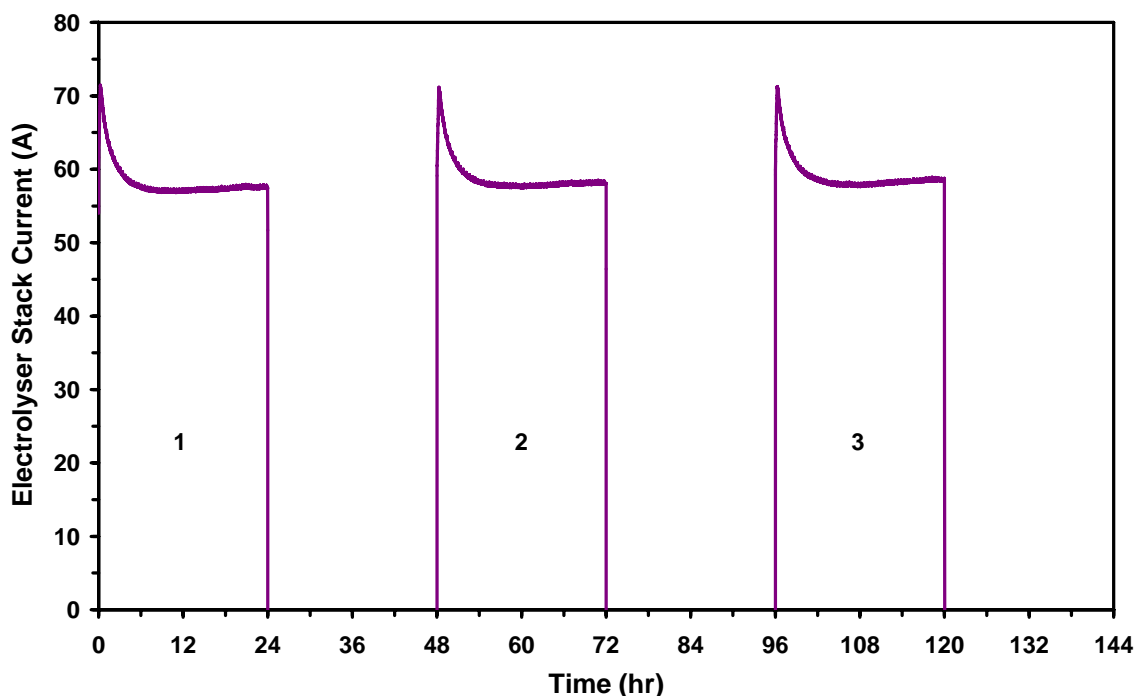
Figure 5.11 Electrolyser Baseline Response to 48 Hour Operating Cycle

Figure 5.12 presents the results for the 24 hour cycle experiments. Operation with the 50 percent duty cycle is illustrated between 0:00 hrs and 72:00 hrs. Current draw is again repeatable. The maximum deviation when compared to the initial 12 hour operating periods of the 48 hour cycle experiment is 2 A. Reducing the rest period to 12 hours does not adversely influence electrolyser operation. On the 12 hour time scale, the electrolyser current draw approaches stable operation near the end of the run. The three cycles employing 6 hour operation are illustrated in period from 70:00 hrs to 144:00 hrs. The current draw does not reach a stable level before operation is terminated. However, the results indicate that this does not lead to significant degradation provided sufficient time recovery time is employed.

Net hydrogen production is another measure that can be used to assess the variability introduced by the duty cycle. Table 5.2 documents the production for the initial 6 hour period of each cycle. Deviation from the average hydrogen production of 3712 L is only ±1 percent.

These results indicate that the typical duty cycle associated with daily operation of the electrolyser in a solar based renewable-regenerative system does not introduce significant performance degradation provided high frequency events are properly dealt with.
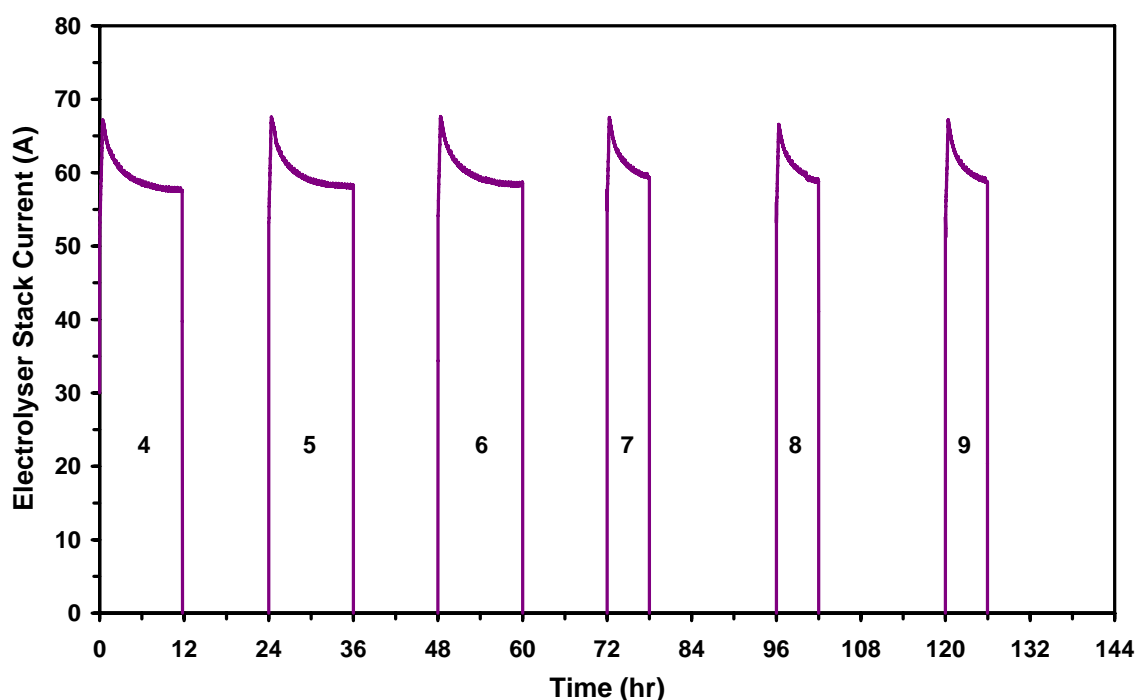
Figure 5.12 Electrolyser Response to 24 Hour Operating Cycles

	Total H$_2$ Produced During Initial 6 Hour Period (L)		
	24 Hour Run	12 Hour Run	6 Hour Run
Cycle 1	3698	3670	3750
Cycle 2	3747	3703	3703
Cycle 3	3750	3697	3692

Table 5.2 Hydrogen Production Comparison

5.3.2 Variable Duration Rest Periods

The experiment described in this section was conduced to determine the electrolyser responses to rest periods of variable duration. In previous experiments it has been noted rapid cycling of electrolyser results in a loss in performance. Performance is generally restored by suspending electrolyser operation for period of 12 to 24 hours. A range of rest periods, from 12 hours down to 1 hour, are examined to determine the minimum pause in operation required to avoid the 'transient event' based performance decline.

The experiment consist of electrolyser operation at constant input voltage and stack temperature (54 V and 30 °C respectively) followed by rest period of variable duration, arranged in a descending pattern: 12, 10, 8, 6, 5, 4, 3, 2, and 1 hours respectively.

The electrolyser current draw associated with this operating pattern is reported in Figure 5.13. Each 6 hour operating period exhibits the initial performance decay characterised in the previous experiments. The total deviation in current draw at the end of the operating period for cycles 1 through 4 is less than 0.2 A. A step change in current of 0.9 A between cycles 4 and 5 is noted. A progressive decline in performance of 0.1 A is noted for cycles 5 through 9. Between cycles 9 and 10, a 0.6A decrease is observed.

Figure 5.13 Electrolyser Response to Variable Duration Rest Periods

The relative change in current draw at the 6 hour operating point between cycles 1 and 10 is only 2.8 percent of the total oper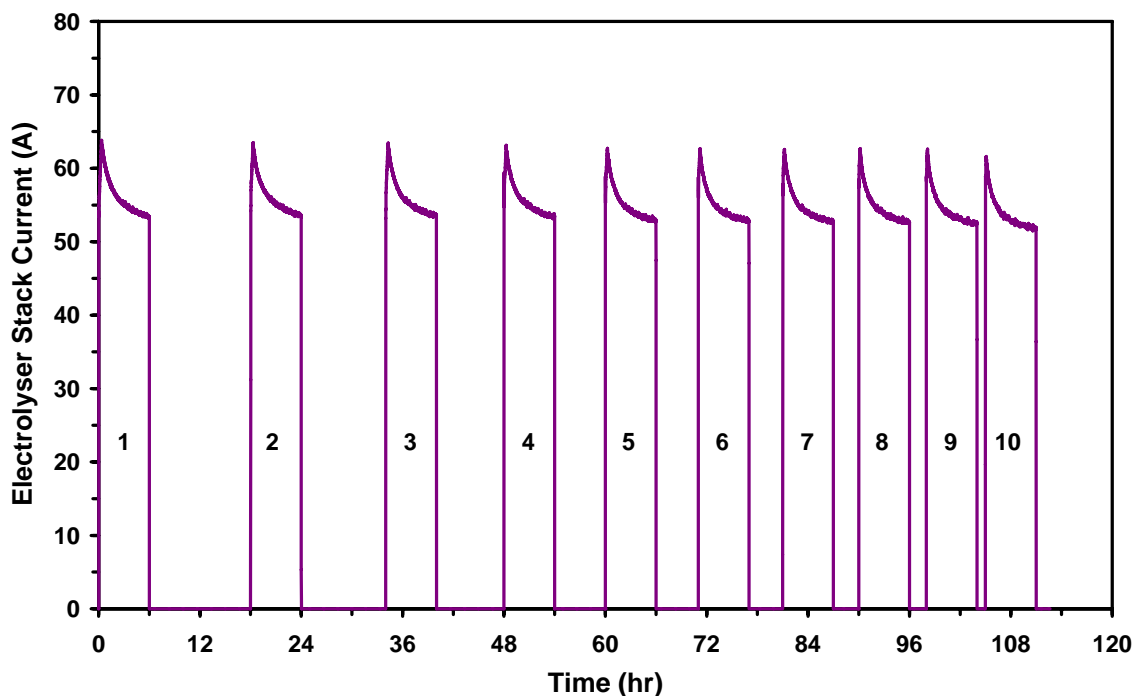ating current. A larger decline was anticipated given the initial observations made for a pause in electrolyser operation presented in Section 5.2.1. The overall trend observed in this experiment suggests that rest periods less then 8 hours in duration are not sufficiently long to avoid performance declines. However, the extent of the performance decline associated with a 1 to 6 hour pause in operation is less then what occurs as a result of a brief 2 minute shutdown.

5.4   Summary

The experiments outlined in this chapter investigate the electrolyser's response to operation under a variety of dynamic conditions. In an IRENE system, the electrolyser plays a critical role in transforming excess renewable input energy into hydrogen. The electrolyser's transition characteristics have a significant impact on performance for time scales that are relevant to renewable resources. During a 6 hour operating window, a 7.3 percent reduction in hydrogen production, relative to steady-state levels, was observed for the most favourable operating conditions. The reduction is due primarily to the thermal transition and time dependent decay in current draw.

The time dependent aspects are currently not addressed in the theoretical models for electrolyser operation. However, the experiments have shown that the time decay phenomena is significant in relation to operating duty cycles associated with periodic renewable resources such as solar power.

Operation of the electrolyser from highly transient input sources has the potential to rapidly degrade performance. Introduction of short duration pauses in operation, a characteristic of system based on a wind resource, results in net decline in performance over stead-state operation. The application of a minimum holding current during the transient can largely remedy the negative impact of the dynamic cycle. Experiments indicate that partial recovery of transient induced performance degradation occurs if a sufficient rest period is introduced between successive operating cycles.

Chapter 6

Renewable-Regenerative System Experiments

A primary motivation for developing the IRENE test-bed was to create a platform for examining the operating characteristics of a renewable-regenerative system in a controlled environment. The goal was to observe the dynamic response and interplay between components as the system responds to the demands of a time varying load and resource input. To this end, an experimental investigation employing and coupling all of the IRENE sub-systems was undertaken. This multi-week "hardware simulation" utilizes an input power profile representative of a solar renewable resource. The load is fashioned after a residential demand with frequency components that a real system would be expected to service. The resource and load patterns are repeated to assess the stability of the system to ongoing operation.

The "simulation" aspect applies only to the generation of the resource and demand profiles (i.e., from data file). Since the hardware responds in real time, a control algorithm is required to guide system operation. In the experiment, all system components are employed and the energy flows between devices are measured to enable accurate assessment of the actual operating efficiencies. Characterizing the operational limitations that arise due to the common bus configuration provides insight into the design of real systems. Control aspects related to bus management for low battery capacity systems are also probed.

The hardware simulation experiment illustrates the potential of the IRENE system to capture the dynamic behaviour of a renewable-regenerative system. As in many experimental endeavours, the answer to the questions raises many new ones. In general, the results indicate that the behaviour of a renewable-regenerative system is more complicated to predict than one would expect.

6.1   Resource and Load Profile Definition

The resource data employed in the renewable-regenerative hardware simulation was obtained from Natural Resources Canada for a solar-based renewable power system [77]. The data was previously used in a simulation study conducted in "RE-H2" a modeling program developed by NRCan to investigate hydrogen and renewable energy applications in residential buildings.   Utilizing this resource input profile provides valuable experimental data for model verification.   The profile was calculated from a numerical model requiring insolation data and PV module performance specifications. Exact details of the array size, orientation, efficiency factors etc., are not available but the data was generated for a residential scale system, in summer time operation near Ottawa, Canada. The daily power production profile reflects the natural variability of the resource.

The seven day renewable input power profile was available as a 5 minute time series, illustrated in Figure 6.1.   The peak magnitude is 7.7 kW, which is within the working range of IRENE renewable input power supply proxy. This magnitude is also reasonable considering the nominal power rating of the load bank and electrolyser (3 kW and 6 kW respectively).   Days one, three, and five have sustained renewable power generation above 5 kW for periods exceeding 6 hours. This corresponds with time intervals used in the electrolyser characterization work outlined in Section 5.3. It is therefore expected that stable electrolyser operation will be achieved within the operating window available with this profile.

The demand load, illustrated in Figure 6.2, is derived from measured load data for 20 British Columbia residences, courtesy of BC Hydro [79]. The data is from non-electric heated, single family dwellings, taken at a similar time of year as the solar resource data. Standard analysis techniques were used to up-sample the hourly average data values to generate a representative 5 minute data set. The maximum load is limited to 3 kW to fit the capacity of the programmable load bank.
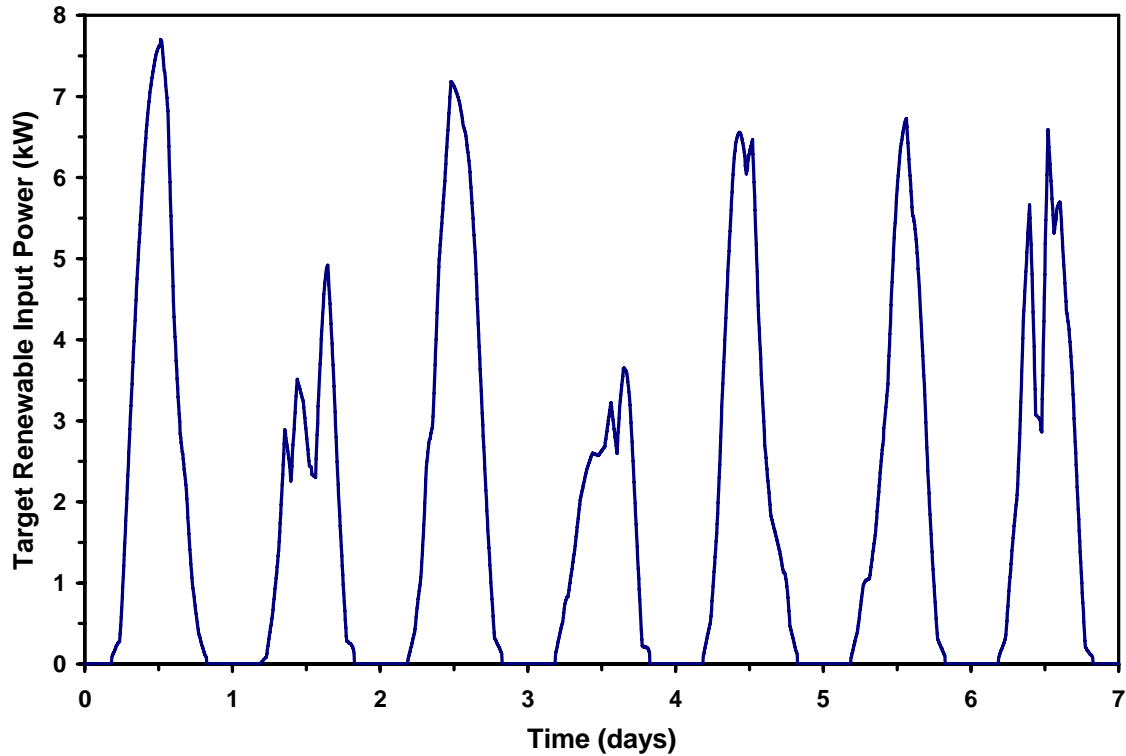
Figure 6.1 Resource Input Power Profile for Renewable-Regenerative Experiment
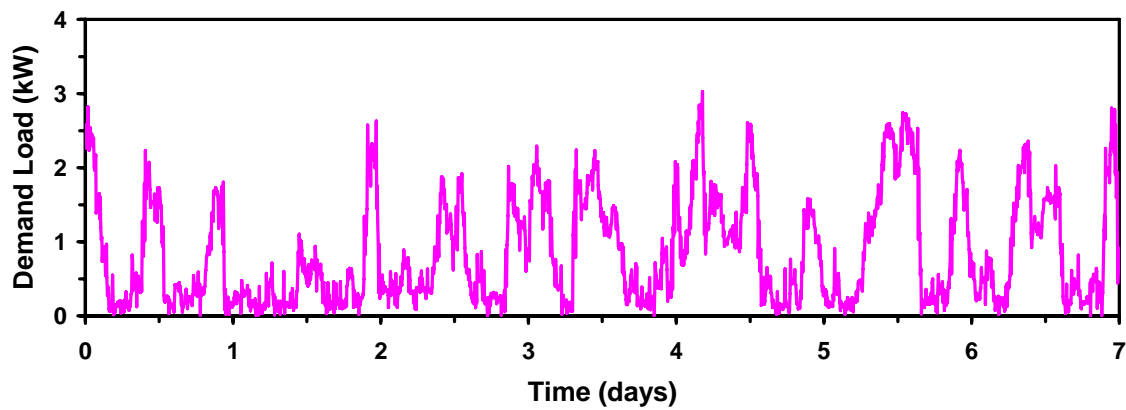
Figure 6.2 Demand Load Profile for Renewable-Regenerative Experiment

During the course of the 21 day experiment, the seven day resource and load pattern was repeated three times. Although more data was available, the choice to repeat the pattern was intentional so that changes in performance are detectable. Resource and load data are arranged in a file format compatible with the IRENE system controller and are updated at the designated time stamp.

6.2   Control Methodology

IRENE is a complex system and requires significant setup to implement a long-term experiment. A detailed description of the LabView program that supervises equipment operation and executes the experiment specific control algorithm is beyond the scope of the current discussion. However, knowledge of the control methodology is required to provide a framework for subsequent discussion of the system response to the specified resource and load inputs. Only control aspects that directly impact operation of the renewable-regenerative experiment are mentioned.

The IRENE system controller is a module implemented within the main data acquisition program. Therefore, it has direct access to all measured system parameters (voltages, currents, flow rates, temperatures etc). The IRENE system controller manipulates the set-points of the main ESS power supply, Nexa fuel cell system, electrolyser stack current control module, and AC load bank to achieve the control objectives discussed below. An overview of each device is given in Section 3.4 and specific details for the integration and operation is provided in Chapter 4. The basic control related input parameters and overall control system hierarchy is illustrated in Figure 6.3. A schematic diagram of the hardware configuration employed in this experiment is illustrated in Figure 6.4.
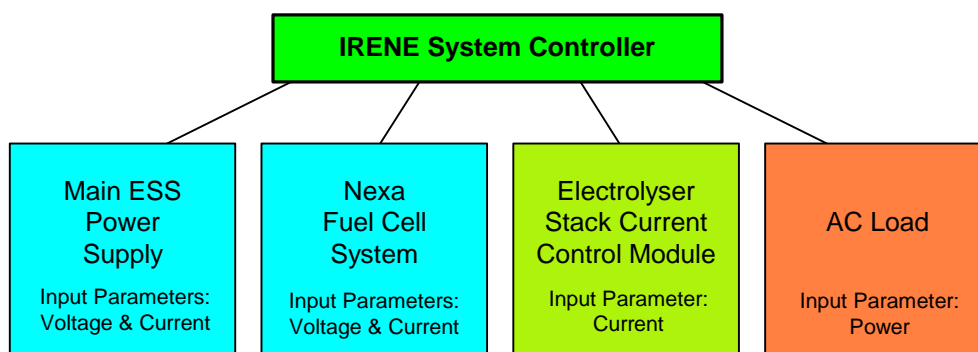
Figure 6.3 Basic Control Hierarchy
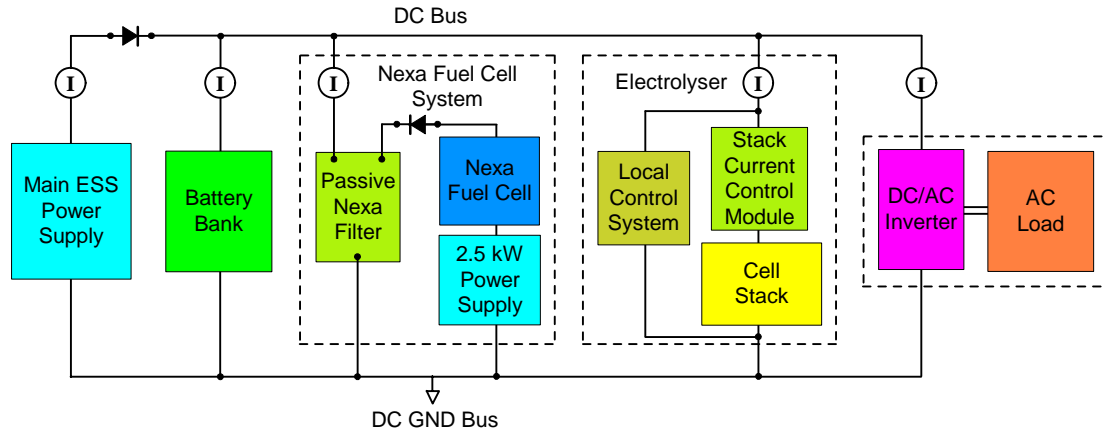
Figure 6.4 IRENE Hardware Configuration Schematic

The control logic employed in the renewable-regenerative coupled system experiment follows seven constraint and objective statements outlined below. These objectives represent the simplest control approach that could be implemented to achieve a functional IRENE system. Considerable latitude exists for future refinement of the system controller; however, the initial design was sufficient to provide stable operation during the three week experiment. The control scheme is derived primarily from bus voltage constraints and allowable current flows between system components.

The order of the control statements reflects their relative importance to system operation. Values assigned for the target bus voltage, battery charge limit, and low voltage shutdown limit are derived from device limitations. The battery discharge limit, minimum electrolyser current, and fuel cell engagement threshold voltage are assigned based on a working knowledge of the system boundaries accumulated through the design, construction, commissioning, and experimental investigations conducted thus far. They reflect conservative bounds for system operation. The system response to the designated input and demand load profiles will be reshaped by manipulating the control parameter values. However, the actual sensitivity to changes in control set-points can only be determined experimentally. Initial experimentation with the coupled IRENE system is limited to the single set of control values defined below.

1) Primary control objectives:

    apply renewable input power as per data file value

    apply AC load demand as per data file value

    maintain $V_{bus} = V_{bus\,target} = 54\,V$ while using all available renewable input power

2) Control action for excess renewable input:

    If $V_{bus} > 54\,V$ then:

        limit renewable input power

3) Battery current constraint:

    $-35 < I_{battery} < 17\,A$ (supplement renewable input power if required)

4) Electrolyser operating condition:

    $I_{bus\,excess} \geq I_{elect\,min\,threshold} = 13\,A$

5) Fuel cell operating condition:

    If $V_{bus} < V_{fuel\,cell\,engage\,threshold} = 48\,V$ then:

        operate fuel cell so $0 < I_{battery} < 5\,A$ up to P_{max} fuel cell

6) Hydrogen buffer operation constraint:

    fuel cell and electrolyser operation is mutually exclusive

7) Low bus voltage condition:

    If $V_{bus} < V_{low\,bus\,shutdown\,threshold} = 46\,V$ then:

        supplement input renewable input power

IRENE System Controller Logic Statements and Constraints

6.2.1   Control Algorithm Implications to System Operation

The primary objective of the system controller is to apply the specified renewable input power profile and demand load while directing power transfer between system components (control statement 1). To accomplish this objective the bus voltage must remain within a range that maximizes the controller's ability to distribute power. Since the electrolyser power consumption is manipulated through passive reduction of the input voltage, as noted in Section 4.3, the broadest range of control options exist at high bus voltages. In addition, the battery capacity is marginal given the instantaneous current demands on the system, so maintaining a high state-of-charge is beneficial for system stability. Thus, the system controller attempts to maintain the bus voltage at 54 V which corresponds to the battery float voltage (voltage at 100 percent SOC) and the maximum

sustained electrolyser input voltage. The maximum allowable bus voltage is 56 V based on battery, Nexa filter module, and electrolyser input voltage constraints. Momentary operation above the target 54 V bus voltage occurs while the controller responds to changes in the load and input power settings. However, prolonged operation at bus voltages exceeding 54 V (control statement 2) will result in permanent battery damage and therefore must be avoided.

Control Actions During Periods With Excess Renewable Input Power

When the renewable input power exceeds the AC load demand, the IRENE system controller assesses the battery state-of-charge to determine if the energy should be directed to temporary storage or hydrogen production. Maintaining a high battery state-of-charge has priority over hydrogen production for the reasons mentioned in the preceding discussion. However, battery charge rate limitations (control statement 3) may dictate that the power be split between the two energy sinks. The electrolyser is operated when the IRENE system controller detects that 'excess' power exists (i.e., available input renewable exceeds the output load and battery recharging demands). The current set-point of the electrolyser stack current control module is adjusted to track the excess power. Given the electrolyser operating characteristics, outlined in Chapter 5, a minimum electrolyser threshold input current has been assigned (control statement 4).

At any instant, the system may not be able to consume all of the available renewable input power due to device limitations and dynamic response rates. The difference between the available renewable input power (i.e., the data file value) and the actual power delivered to the system by the ESS power supply *associated* with the renewable input is defined as the 'unused' renewable input power. (Note: the main ESS power set-point is based on a combination of control inputs. Therefore some book keeping is required to identify the correct proportion of the actual power delivered by the main ESS power supply with the correct 'source'. Further clarification of the sources will be made in the subsequent discussion.) Since the available renewable input power is a construct within the control system (i.e., a number from a data file) the 'unused' designation refers to power was never introduced to the IRENE system. All power delivered to the IRENE

bus by main ESS power supply and Nexa fuel cell system is distributed to the various loads or energy buffers.

Renewable input power may remain unused for four reasons. First, if the excess is insufficient to meet the electrolyser's minimum input requirement, then the surplus is effectively lost. Second, power may remain unused if the absolute maximum rating of the electrolyser is exceeded. This occurs in IRENE-like systems when the peak generation capacity exceeds the system load (i.e., 8 kW of generation versus 5 kW of power sinking capability) and is primarily a system design issue. The third aspect, which is explored in Chapter 5, deals with the electrolyser's transition rate characteristics. In this case, the excess power is within the electrolyser's nominal working range but it simply can not absorb the power. A fourth mechanism that results in unused power is an artifact of the specific operating nature of the electrolyser's stack current control module. Since it is not generally applicable to other renewable-regenerative system, the portion of unused power associated with this mechanism is included within item three discussed above. A description of the electrolyser control issue is outlined next.

The electrolyser's stack current control module receives a current set-point from the IRENE system controller but is limited in operation to discrete states, as discussed in Section 4.3. The stack current control module tracks the net current error and adjusts between states at the appropriate intervals to produce an average current equal to the set-point. However, the switching rate and related electrolyser current profile requires an innovative control strategy to avoid introducing oscillations in the IRENE system controller. A small operating current window, roughly 2 A is needed to implement the control logic within the IRENE system controller. During highly transient bus conditions, the IRENE system controller may issue an electrolyser set-point at the lower end of the current window, resulting in a small loss in power transfer.

If the system is unable to absorb all of the available renewable input power, the IRENE system controller reduces the actual power input to an acceptable level. Determining the appropriate main ESS power supply settings to transfer the reduced input power is a non-trivial task. Since the renewable input is specified in terms of power, the controller actively tracks the bus voltage and adjusts the main ESS power supply voltage and

current set-points accordingly. The main ESS power supply functions primarily as a voltage source. If the current limit set-point is exceeded, the supply switches operating modes and becomes a current source. The transition between voltage limiting and current limiting operation creates scenarios where it is difficult to predict which control parameter will be dominant. The problem is compounded by the fact that the operating mode can only be assessed from the measured ESS output voltage and current, creating a feedback loop issue due to the time delays involved with data communication and application of the set-points within ESS power supply.

An additional problem arises due to the limited battery buffering capacity. Sudden changes in bus voltages are observed when the AC load setting is altered. Thus, implementing a control algorithm to limit the renewable input power given the dynamic nature of the bus is difficult. A time delay factor (2 seconds) between successive control loop iterations has been incorporated into the IRENE system controller to improve stability but results in small deviations from the optimal set-points. However, the operation of the data logging module is independent from control loop so the experimental results, recorded in the output data file, capture actual system response to the 'non-ideal' control input.

The difference between the available renewable input energy (i.e., the integral of the available renewable input power from the data file values over a specified time period) and the actual energy delivered to the system by the ESS power supply associated with the renewable input constitutes the net unused renewable input energy. In post-experiment analysis, the ratio of the unused renewable input energy relative to the available renewable input can be determined. This is an important measure to assess overall system performance.

Control Actions During Periods With Excess Demand Loads

In operating scenarios where the load demand exceeds the renewable input, the power balance must be met by the energy buffer. The battery bank is the primary resource for servicing short-term imbalances. Once the batteries are depleted to an intermediate state-of-charge, the fuel cell is invoked. Since the actual demands on the battery were unknown before conducting the experiment, a maximum battery discharge current

(control statement 3) has been established as a safeguard. The 35 A discharge limit was chosen based on previous observations of the bus voltage fluctuations associated with battery discharge events. If the discharge current limit is exceeded, the IRENE system controller temporarily increases the main ESS power supply power setting to lower the battery discharge current to the specified limit value.

Bus voltage is used as an indicator of battery SOC. Advanced integration schemes exist to monitor SOC but require in-depth battery characterisation and are sensitive to minor changes in long-term battery performance [80]. Although voltage does not predict battery SOC with great precision, it is sufficient for this application. In the IRENE system the batteries are considered fully charged when $V_{battery}= V_{battery\ float} = 54$ V under no load conditions. The battery voltage at a minimum recommended SOC is $V_{battery} = 46$ V. Since the batteries are directly connected to the bus, the working voltage range of the bus is thus defined.

The fuel cell power contribution is moderated to provide a net positive battery current that is proportional to the error between the fuel cell engagement threshold voltage and bus voltage (restricted to cases where $V_{bus} < V_{fuel\ cell\ engage\ threshold}$). The fuel cell threshold voltage is set at $V_{fuel\ cell\ engage\ threshold} = 48$ V (control statement 5) to ensure that a minimum residual battery capacity is available to buffer the fuel cell output. This control method is employed because the fuel cell is viewed as an assistive device where operation is restricted to servicing the imbalance between the renewable input power and the demand load. Thus, the fuel cell is not used to recharge the batteries except in cases where the battery voltage has dropped below the fuel cell engagement threshold voltage. This occurs when the fuel cell is unable to supply sufficient power to cover the shortfall between the renewable input power and the demand load. When the net imbalance is reduced to a level within the fuel cell power output range, the batteries are gradually recharged until the bus reaches the fuel cell engagement threshold voltage. In this instance, the battery charge rate is restricted to a value less then the battery's maximum charge rate (control statement 3) so that 'excess' current is not detected by the IRENE system controller which may initiate electrolyser operation. If operated at the fuel cell engagement threshold voltage, the electrolyser would draw approximately 20 A of current from the bus, a load that the fuel cell system could potentially support. But

clearly electrolyser operation based on fuel cell derived power is pointless and counter productive from an energy standpoint due to the losses involved (i.e., it is irrational to use a given amount of hydrogen to make less hydrogen). Therefore, operation of the fuel cell and electrolyser is mutually exclusive (control statement 5).

An additional feature has been incorporated to prevent battery discharge beyond the recommended minimum state-of-charge. If the bus voltage drops below the low bus shutdown threshold voltage (control statement 7), the main ESS power supply is adjusted to provide a net zero battery current. By intervening in this manner, premature termination of the experiment due to low voltage shutdown of the inverters (a hardware safety feature) is avoided. Application of the low bus voltage safety system constitutes a 'failed' experiment from an energy balance perspective. However, it allows a measure of freedom to explore load profiles that push the system to the limit. The power artificially added due to battery current limiting and the low bus safety system is recorded for post-experiment analysis.

As with the ratio of the unused renewable input energy to the available renewable input energy, the ratio of the energy added to maintain the control objectives (i.e., due to battery discharge limiting and low bus conditions integrated over a specified period of time) to the actual input energy provides another metric for assessing system performance. Both ratios indicate the degree to which the system meets the energy buffering objective but point to different parameters that would need to be addressed to achieve a functional, real-world system given the desired operating scenario.

6.2.2 Experiment-Specific Control Features

In addition to the basic control logic presented thus far, two additional measures are taken in the implementation of the renewable-regenerative coupled system experiment. The first measure addresses the findings reported in Chapter 5 which clearly illustrate that electrolyser performance is degraded due to repeated on/off cycling. The control objectives outlined in the preceding section are based strictly on instantaneous power values. Therefore, the IRENE system controller may cycle the electrolyser during periods were excess renewable input power oscillates about the electrolyser minimum engagement threshold. To avoid this scenario, the electrolyser operates continuously

throughout the experiment but the power draw and hydrogen production are only associated with the renewable-regenerative experiment during periods when the minimum electrolyser operating conditions are met. The implementation is complex and requires the IRENE system controller to maintain a *virtual electrolyser operating state* so that post-experiment analysis can be completed.

During periods when the electrolyser is 'off', the main ESS power supply output is augmented by the measured power required to run the electrolyser in 'standby' mode. A standby current equal to the minimum electrolyser current is employed to ensure a smooth transition between the standby and run modes. The current added to offset standby operation and the virtual electrolyser state is recorded for similar time intervals as the basic experimental data. Once the experiment is compete, the measured main ESS power supply current is adjusted to reflect when the electrolyser was 'on' and 'off' and is subsequently used to report the actual power transferred to the IRENE system (i.e., electrolyser operation in standby mode does not introduce a parasitic bus load). Likewise, measured hydrogen production is limited to times when the electrolyser was 'on'.

The added benefit associated with the above electrolyser operational method is that the exact point at which the system has sufficient 'excess' power to run the electrolyser can be observed directly. Determining the transition point through other means is difficult due to the dynamic nature of the electrolyser's V-I-temp-time characteristics, as discussed in Chapter 5.1. For instance, the electrolyser requires a higher input power to meet the minimum electrolyser current when it is at room temperature than when it is at 60 °C, the operating set-point temperature; however, both of these values depend on the previous operating history. Since electrolyser operation is maintained throughout the experiment the exact power draw at the minimum electrolyser current is known.

The second feature added to the IRENE system controller is a *virtual fuel cell* to augment the Nexa fuel cell system. The virtual fuel cell is an artificial device implemented within the IRENE system controller that manipulates the main ESS power supply settings to deliver an additional power to the bus with similar characteristics as the fuel cell system. The virtual fuel cell uses the same control logic as the Nexa fuel cell system presented in

the preceding discussion. The power added and virtual fuel cell operating state is recorded in the data log. The benefit of the fuel cell simulator is that long duration experiments can be completed without subjecting the Nexa to unnecessary runtime hours. The Nexa fuel cell system is fully functional and the operator can select between the real fuel cell or the simulated version (or a combination of the two) at any point in the experiment. This flexibility enables verification of the virtual fuel cell against the real device and allows for experimental assessment of the system response to a larger effective fuel cell system.

6.3   Experiment Energy Balance

Simulation results for renewable-regenerative system models are often reported in terms of the net energy balance, as discussed in Section 2.1. A similar approach is taken here to provide an overview of the results from the renewable-regenerative coupled system experiment conducted with IRENE test-bed.

The experiment was conducted based on the resource and load profiles specified in Section 6.1 and the control methodology outlined in Section 6.2. Throughout the experiment, currents, voltages, temperatures, flow rates etc., were sampled on a continuous basis at roughly 10 kHz. See Section 4.6 for instrumentation specification. Average values for all parameters were logged on 6 second interval resulting in some 4 million recorded data points for the two week period under investigation. From this data the energy flows were calculated. According to the measurements taken, the total energy input to the system from the renewable input proxy, batteries, and fuel cell system during the 14 day experiment is 726.7 kWhr. Likewise, the total energy consumed by all energy sinks is 728.0 kWhr. The difference, 1.3 kWhr or 0.2 percent, represents the net error associated with the measurement devices, calibration constants, and losses in precision due to truncation of data in the recording process. The error is negligible and indicates that data can be reported with a high degree of confidence. The fact that the output is slightly higher than the input does not imply that IRENE is capable of generating energy, it simply points to a very small net calibration error in the energy sinks.

6.3.1 Overall Energy Balance

Daily energy balances are calculated by integrating the power flows recorded for the various inputs, outputs, and internal sub-systems over a 24 hour period. Data points for each day are plotted in Figure 6.5. Smooth connector lines included to improve visualization of the seven day trends. Reported values do not include the energy required to operate the electrolyser in standby mode. Standby mode was implemented to avoid the electrolyser performance decline associated with repeated on/off cycling.   This requirement may be eliminated by implementing a more advanced system controller. Therefore, energy demands to support standby operation are not considered a system load for the purposes of the renewable-regenerative experiment.

Three weeks of data were collected for the experiment as illustrated in Figure 6.5. A shift in the electrolyser operating characteristic occurred on day 15 of the experiment which altered the system performance during the remainder of the experiment. For example, a comparison of day 8 to day 15 and day 10 to day 17 reveals that the actual input energy to the system declined by 5.6 kWhr and 4.1 kWhr respectively. A similar change in electrolyser input energy values is noted (declines of 16 and 11 percent respectively). The observed phenomenon is not yet fully understood. It is unclear if change in performance is related to the specific long-term operational behaviour of the electrolyser employed in the IRENE system, or is more systemic in nature and would be observed in other IRENE-like system. Since explanations of this performance change are at this stage purely speculative, the last week of data has been omitted from the analysis. The data collected during the first 14 days of the experiment does not exhibit a marked decline in electrolyser performance and forms the basis of the subsequent analysis.
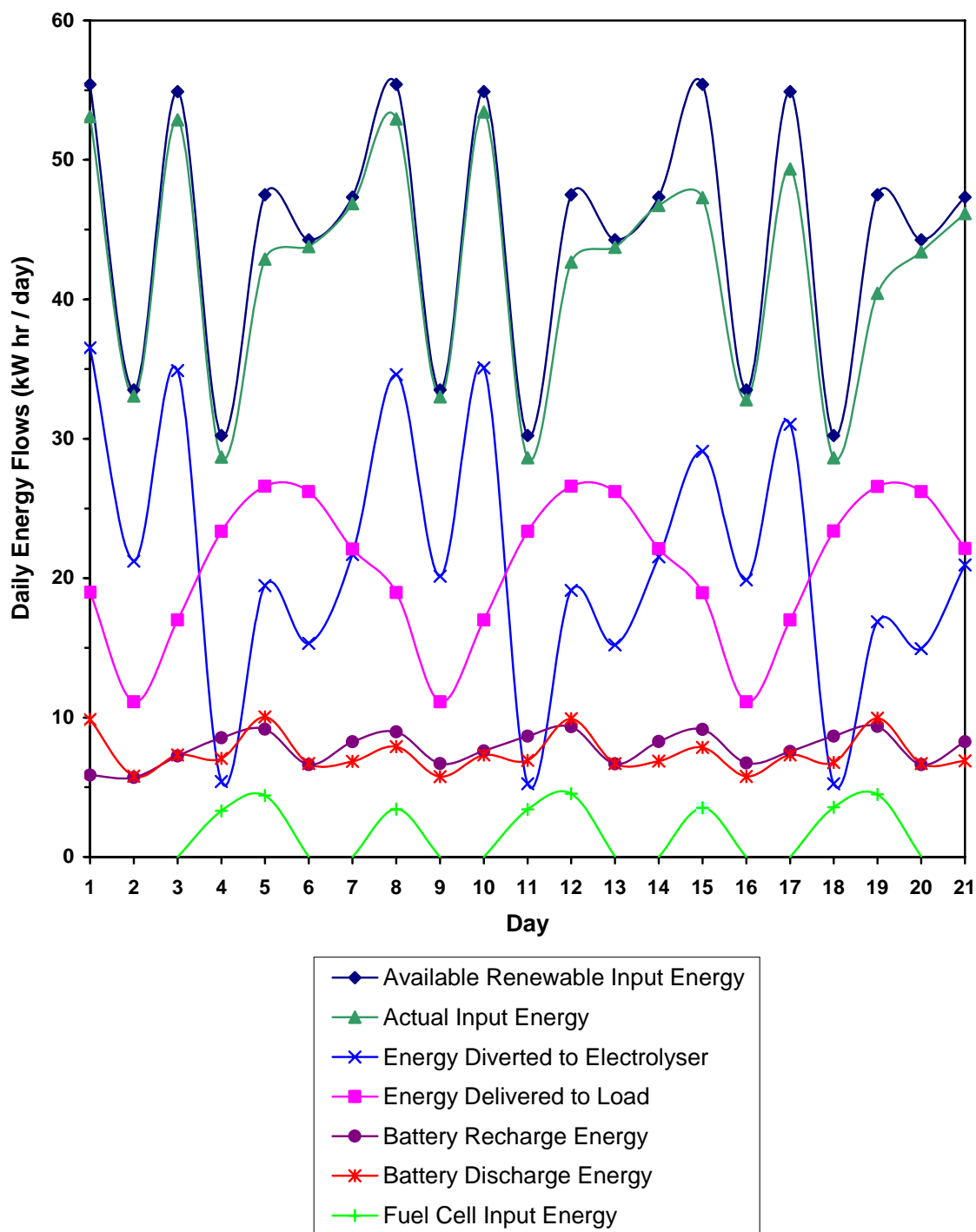
Figure 6.5 Daily Energy Balance for Three Week IRENE System Experiment

During the three weeks of data reported, the input and load profiles are repeated three times. This pattern is clearly evident in the daily energy flows. The following assessment

of the overall experiment is made from the daily energy flows for the first two weeks. A summary of the key values is reported in Table 6.1.

	Day 1-14 (kW hr)
Available Renewable Input Energy (A)	626.3
Actual Input Energy from Main ESS Power Supply	602.4
portion Artificially Added by Control System	10.1
portion Associated with Renewable Resource (B)	592.3
Energy Supplied by Fuel Cell	19.2
Hydrogen Consumed	14.7 (m^3)
Energy Supplied by Batteries	105.1
Energy Source Sub-total	726.7
Energy Absorbed to Recharge Batteries	107.6
Inverter Input Energy	314.9
Energy Delivered to AC Load	290.7
Energy Diverted to Electrolyser	305.5
Energy Input to Electrolyser Stack	283.6
Hydrogen Produced (m^3)	51.9 (m^3)
Energy Sink Sub-total	728.0
Total Unused Renewable Input (A-B)	34.0
portion due to Minimum Electrolyser Input Threshold	14.0
portion due to Absolute Maximum Electrolyser Rating	9.4
portion due to Electrolyser Transition Rate Limitations	10.6

Table 6.1 Energy Balance Results for Two Week Renewable Energy Experiment

The total available renewable input energy for the two week period is 626.3 kWhr. The actual input energy supplied to the system from the main ESS power supply is 602.4 kWhr. Of this, 10.1 kWhr is artificially added to the control objectives during periods with excessive battery discharge. Thus, the energy input to the system derived from the renewable source is 592.3 kWhr.

The energy added is only 1.5 percent of the actual input energy. This indicates that energy buffering capacity is generally sufficient to meet the load demands during periods with low renewable input given the specific load and resource profiles. It is feasible that the energy supplement could be reduced to zero by increasing the battery discharge current limit as it was set at a rather conservative level, only 35 A.

The total unused renewable input energy (as defined in Section 6.2.1) is 34.0 kWhr or 5.4 percent of the available renewable input. Substantial variation in the daily unused renewable energy occurs, with daily variations ranging from a low of 2.7 percent to a high of 10.7 percent, indicating that system performance is dependent on correlation between the input and load profiles. Further discussion of the unused renewable energy is reported following the presentation of the high level system energy balance.

Throughout the experiment, the bus voltage remained above the critical low level threshold so the low level safety system was not required. Therefore, the entire 290.7 kWhr AC demand load is serviced by the renewable input and energy buffer sub-systems. The input energy to the DC/AC inverter is 314.9 kWhr leading to an average conversion efficiency between the DC bus and the AC load of 92.3 percent.

At the start of the experiment, the batteries were fully charged. During the experiment, the batteries contributed a total of 105.1 kWhr to the bus. Conversely, they absorb 107.6 kWhr for recharging. Batteries require more energy to recharge than what is released during discharge due to the internal losses involved [80]. The estimated final battery SOC is 30 percent. However, the operating conditions on the first and last day of the experiment must be considered when evaluating the final battery state of charge. During the first day, the bus voltage was on average higher than day 8, so a larger proportion of the renewable input was directed to hydrogen production while the batteries supplied the AC output load. During the final 5 hours of day 14, the batteries were supplying energy to the load and were thus being depleted. Therefore the battery SOC at the end of the experiment should be lower than at the start given the additional discharge involved. The pattern of battery energy supply/draw over the 14 day period is more important than the specific final SOC value. After the first two days, a consistent pattern of energy flow to and from the battery buffer is established indicating that the experiment is not depleting

the battery's temporary energy store to supply a net system energy imbalance. An initial ramp in period (two days in this case) is required for the battery state to normalize. If the five 14 day periods between day 3 to day 17 and day 7 to day 21 are investigated, the batteries contributed on average a total of 102.8 ± 0.2 kWhr to the bus and absorbed 111.9 ± 0.3 kWhr for recharging giving a nominal 91.9 percent round-trip efficiency. During these 14 day intervals, the batteries supply 32.7 percent of the energy delivered to the inverter to service the output load.

During the experiment, the IRENE system controller diverted 305.5 kWhr to the electrolyser, which operated for 114.5 hours. Therefore, 51.6 percent of the input energy from the renewable resource is transferred to the hydrogen buffer. The electrolyser stack consumed 283.6 kWhr for a net electrolyser input utilization ratio of 92.5 percent. The electrolyser's local control system and ancillary devices consumed 4.1 kWhr of the input energy and the balance was dissipated by the stack current control module. Hydrogen compression was not performed given the limitations of the electrolyser unit, as outlined in Section 4.2. Compression is an energy intensive process and would add a considerable parasitic load to the electrolyser system (approximately 1/5 of the total input energy). The net hydrogen output from the electrolyser is 51.9 m^3 at STP. Based on the higher heating value (141,780 kJ/kg [76]), the energy content of the hydrogen is 183.8 kWhr resulting in an electrolyser energy efficiency of 60.2 percent. Daily efficiencies vary by ± 5 percent over the first 11 days. The daily efficiency declines during the final three day due to a drop in hydrogen production as discussed below.

The fuel cell operated for 21 hours and contributed 19.2 kWhr to the bus. This represents 6.1 percent of the energy delivered to the inverter to service the output load. The fuel cell consumed 14.7 m^3 of hydrogen at STP, which is equivalent to 28.3 percent of the hydrogen generated by electrolysis of the excess renewable input. Based on the higher heating value of the hydrogen consumed, the average fuel cell energy efficiency is 36.7 percent.

By the end of the experiment, 37.2 m^3 of surplus hydrogen was produced. The daily hydrogen production and consumption are illustrated in Figure 6.6. Both follow predictable trends given the seven day input and load pattern; however, a small reduction

in hydrogen production is noted from day 12 onwards. As mentioned at the start of this section, a significant shift in electrolyser response was noted on day 15. The observed decline in hydrogen production near the end of the two week period foreshadows the pending change.

Based on the fuel cell's hydrogen consumption to net energy output, a projection of the fuel cell output for the full 51.9 m^3 of hydrogen generated is 67.8 kWhr. In this case, a hydrogen energy buffer efficiency of 22.2 percent would be realized.
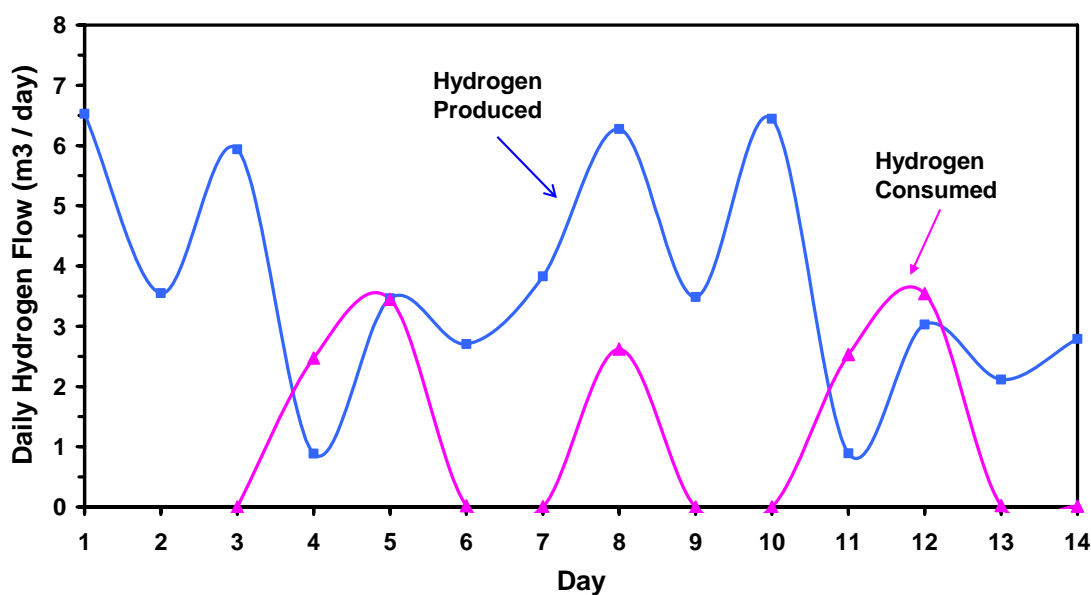
Figure 6.6 Daily Hydrogen Production and Consumption

6.3.2 Unused Renewable Input

In the IRENE system, any excess energy should, in principle, be converted into hydrogen by the electrolyser. In reality, the electrolyser is unable to utilize all of the available excess renewable input energy, as illustrated in Figure 6.7. The energy added to limit battery discharge is also graphed to illustrate the relative magnitudes of the energy flows. On all days, sufficient unused renewable input energy is available to offset the energy added by the IRENE system controller to meet the specific control constraints. Apart from the first two days, the daily energy added to limit the battery discharge rate follows a repeatable seven day pattern. The unused renewable input energy is higher on day 1 than day 8 as a result of the transition to a stable operating cycle. A small deviation also

occurs on day 10, but in general, the unused renewable input energy follows a seven day pattern.

Figure 6.7 Daily Energy Supplement and Losses

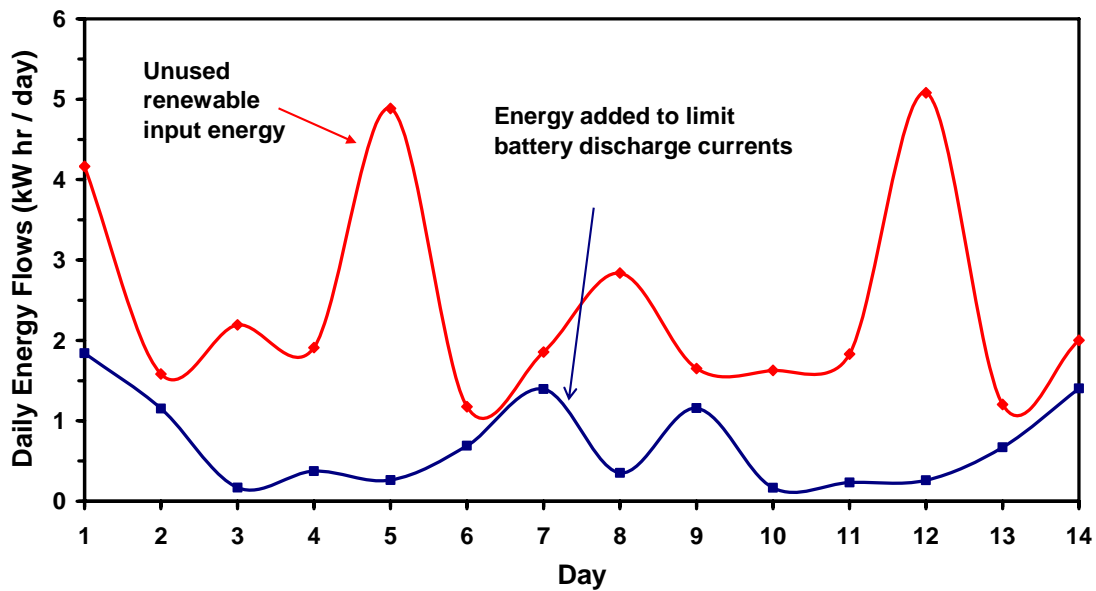The electrolyser is unable to utilize all of the input energy for the three reasons discussed in Section 6.2.1. In summary, at any given instant, the excess power may be insufficient to meet the electrolyser's minimum operating requirement. Second, the excess power may exceed the absolute maximum rating of the electrolyser. And third, the electrolyser power draw may be limited by the transition rate characteristics explored in Chapter 5. In this final case, the input power is within the electrolyser's nominal working range but it simply can not absorb the power.

Over the two week duration, the proportion of unused renewable input energy attributed to the three causes is as follows: 14.0 kWhr or 41.2 percent is due to the minimum electrolyser input requirement; 9.4 kWhr or 27.6 percent is due to the maximum capacity issue; and 10.6 kWhr or 31.2 percent is due to the transition limiting operating phase. A detailed 14 day breakdown of the unused renewable input energy is present in Section 6.4.

The maximum capacity issue has been addressed in the detailed theoretical models of renewable-regenerative energy system discussed in Section 2.1. However, the unused energy due to the minimum electrolyser operating conditions and the electrolyser

transition rates are not generally included in the models. Figure 6.8 illustrates the daily loss of renewable input energy due to the electrolyser minimum requirement and transition related affects. A basic seven day trend is evident but there is some variability in the proportions of energy loss due in part to the active nature of the IRENE system controller and the limited operating states of the electrolyser current control module.

On day 1 the electrolyser transition losses are higher than day 8 because the electrolyser operates for a larger portion of the day in thermal limiting mode due to the higher bus voltage associated with the initial battery SOC. The most noticeable difference in the unused energy trends occurs between day 5 and day 12. The net unused energy associated with the minimum electrolyser operating condition and the electrolyser transition rates is similar for these two days at 4.5 and 4.7 kWhr respectively. However, on day 5 losses due to the minimum electrolyser operating condition exceed the losses due to electrolyser transition rates. This pattern is reversed on day 12. On both days, the excess power available for hydrogen production during the morning hours oscillates about the minimum electrolyser operating point. Under these conditions, a combination of the logic conditions within the IRENE system controller defining run and standby modes coupled with the limited thermal transition rate at low electrolyser input current results in the differences observed. On day 12 the electrolyser ran for 18 minutes longer (a 4 percent increase) but absorbed 0.34 kWhr less input energy (a 2 percent decrease) than on day 5. An alternate representation of the unused energy is presented in the next section.
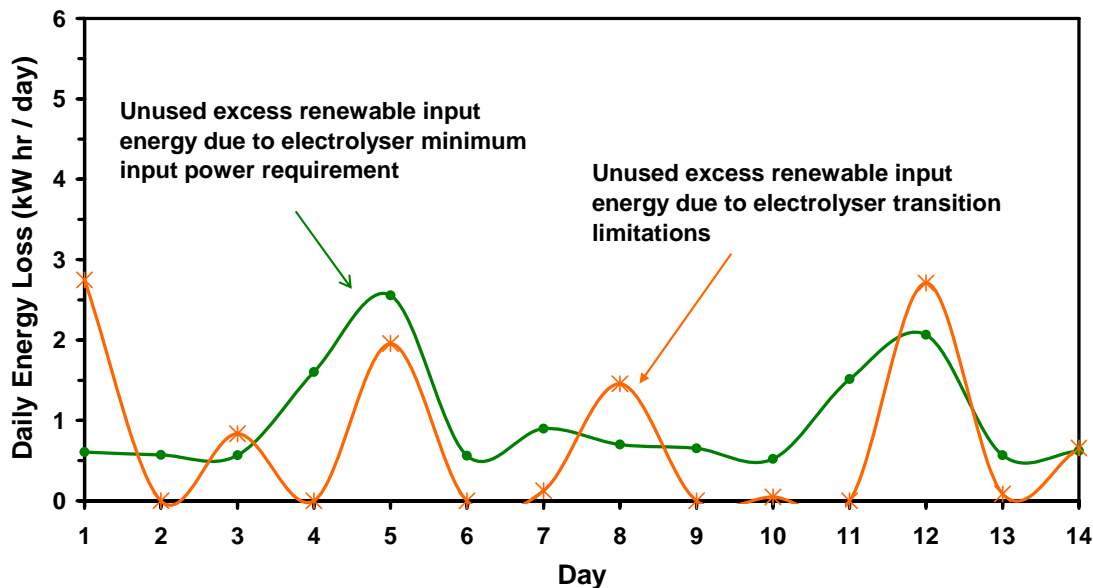
Figure 6.8 Daily Breakdown of Electrolyser Energy Losses

6.3.3 Energy Analysis Summary

On an energy basis, the IRENE system was able to directly service the load given the input energy available from the renewable resource. The batteries play an important role in maintaining the daily energy flows buffering approximately 1/3 of the output demand. But over the long term, the system does not deplete the battery's energy store to make up for net deficiencies in the renewable input (i.e., the system is operating in a sustainable manner). Roughly 1/2 of the renewable input energy is directed to hydrogen production and converted with 60 percent energy efficiency. The fuel cell consumes approximately 1/4 of the hydrogen produced to offset 6 percent of the demand load during periods with low renewable input, resulting in a net surplus of hydrogen at the end of the two week period. From an overall energy stand point, the experiment is a success. However, the projected round-trip efficiency of the hydrogen energy buffer (based on total fuel usage) is only 22 percent versus 92 percent for the battery buffer.

6.4　Observation of System Dynamics During Long-Term Operation

The analysis presented in the previous section focused on the 'big picture' energy balance. One of the broader goals of the IRENE project was to investigate the dynamic operating nature of a renewable-regenerative system. The data presented in this section is included to fulfill this objective. The intent is to illustrate the dynamic interactions that occur between components as the system responds to the input and demand loads. Analysis is limited to a discussion of the general trends observed. Data is grouped into one week segments and arranged to allow comparisons between similar days in the operating cycle. The renewable input power profile is included as a reference (plot A in the figures) to illustrate when power is available to the system.

Bus voltage is an important operating parameter since it influences the power transfer that can occur between system components. A plot of the bus voltage over the two week experiment is given in Figure 6.9. The high degree of similarity between week one (plot B) and week 2 (plot C) indicates that the system is responding in a consistent manner. The net difference in bus voltage for similar time periods is compared in plot D. After day 2, the voltage difference is, on average, less the 0.2 V. The largest difference occurs between days 1 and 8, but even this is less then 2 V.
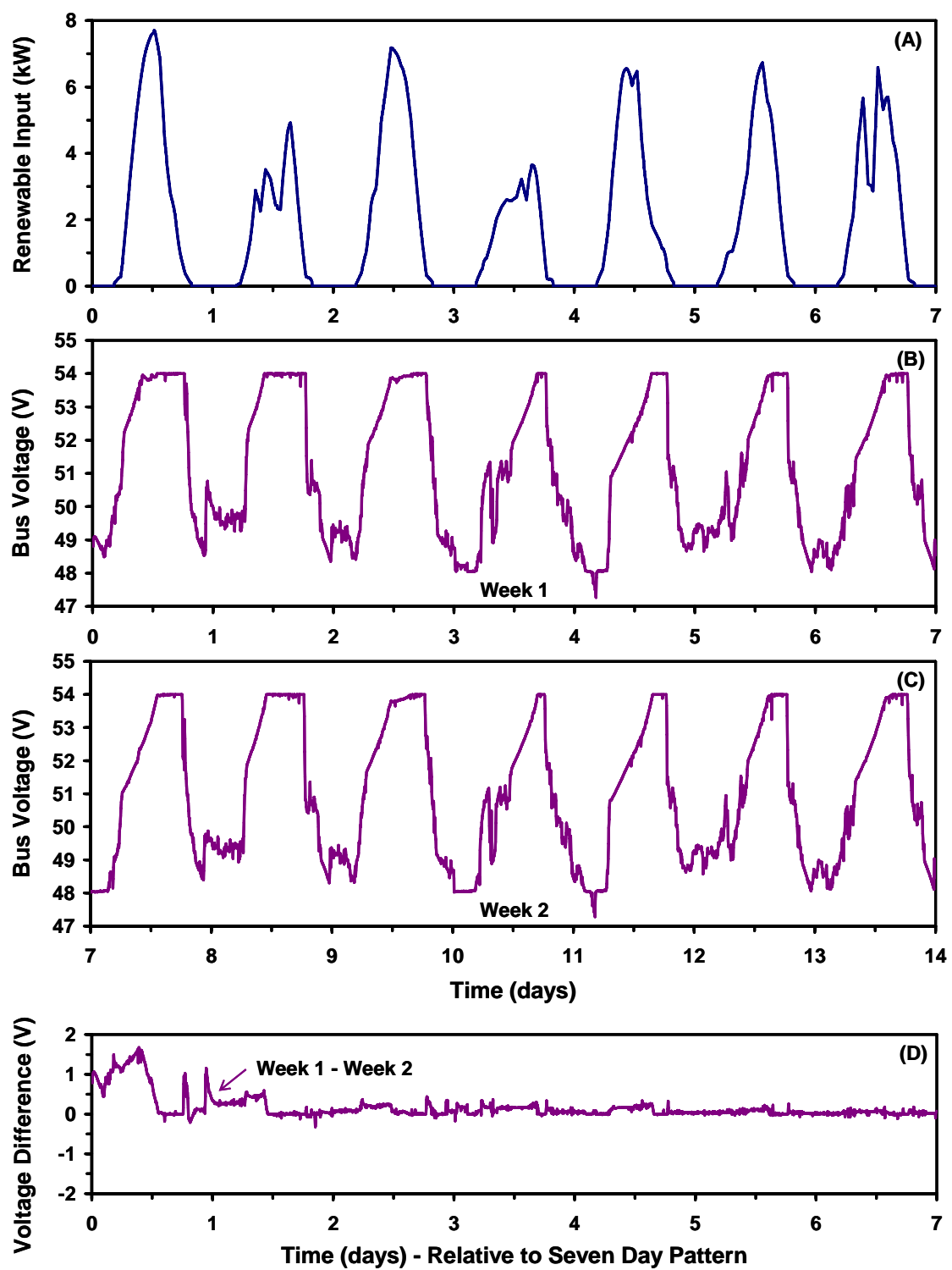
Figure 6.9 Bus Voltage Dynamics

The experiment begins with a period of zero renewable input power and high load demand, as illustrated in Figure 6.1 and Figure 6.2 respectively. The batteries and/or fuel cell must support the load during this initial period. Although the batteries are fully charged at the start of day 1 (i.e., $V_{bus} = 54$, $I_{battery} = 1A$ to maintain the float voltage), the high initial battery discharge immediately lowers the effective bus voltage to 49 V. This illustrates the dynamic range in bus voltage that occurs due to the limited battery buffering capacity. Daily bus voltage swings ranging from 5 to 6 V are noted. Day 4 and day 11 illustrate that rapid shifts in bus voltage occur under real operating conditions.

The bus voltage achieves the target operating voltage of 54 V for a minimum of three hours each day. This does not imply that the batteries are fully charged, but rather that battery charge limiting is not in effect during those intervals. Results from other experiments have shown that the batteries require approximately 24 hours at 54 V to reach a full state of charge. The need for active limiting of the bus voltage at the target voltage is evident given the duration of each day that is spent at the upper bound. Serious battery damage would occur due to an over voltage condition if the bus voltage was left unconstrained.

Periods where the bus voltage is held constant at 48 V indicate times where the fuel cell's output capacity is sufficient to meet the load, as discussed in Section 6.2.1. The actual fuel cell power contribution to the bus is illustrated in Figure 6.10. Day 4 in the cycle imposes the largest demands on the energy buffer since it has the highest net load to renewable energy input ratio at 0.81. Day 3 ends with a period of high load that depletes the batteries. The load continues at the start of Day 4 and requires the fuel cell input power for 4 hours until the renewable source is available. Day 4 has the lowest net renewable input energy of the seven day pattern and battery recharging is limited by the brief period that the bus is maintained at 54 V, less then 3 hours. The evening load is approximately 5 times less then in the morning which is beneficial given the limited battery recharging. However, by the early part of day 5, the battery buffer is depleted and the fuel cell is required for 4.3 hours to service the load. During this period the bus voltage drops below the 48 volt fuel cell threshold voltage indicating that the fuel cell is unable to supply sufficient power to meet the demand. The overload condition lasts approximately 20 minutes and within an hour the bus voltage has been resorted. The

control methodology developed for the fuel cell system handles the situation in a reasonable manner.
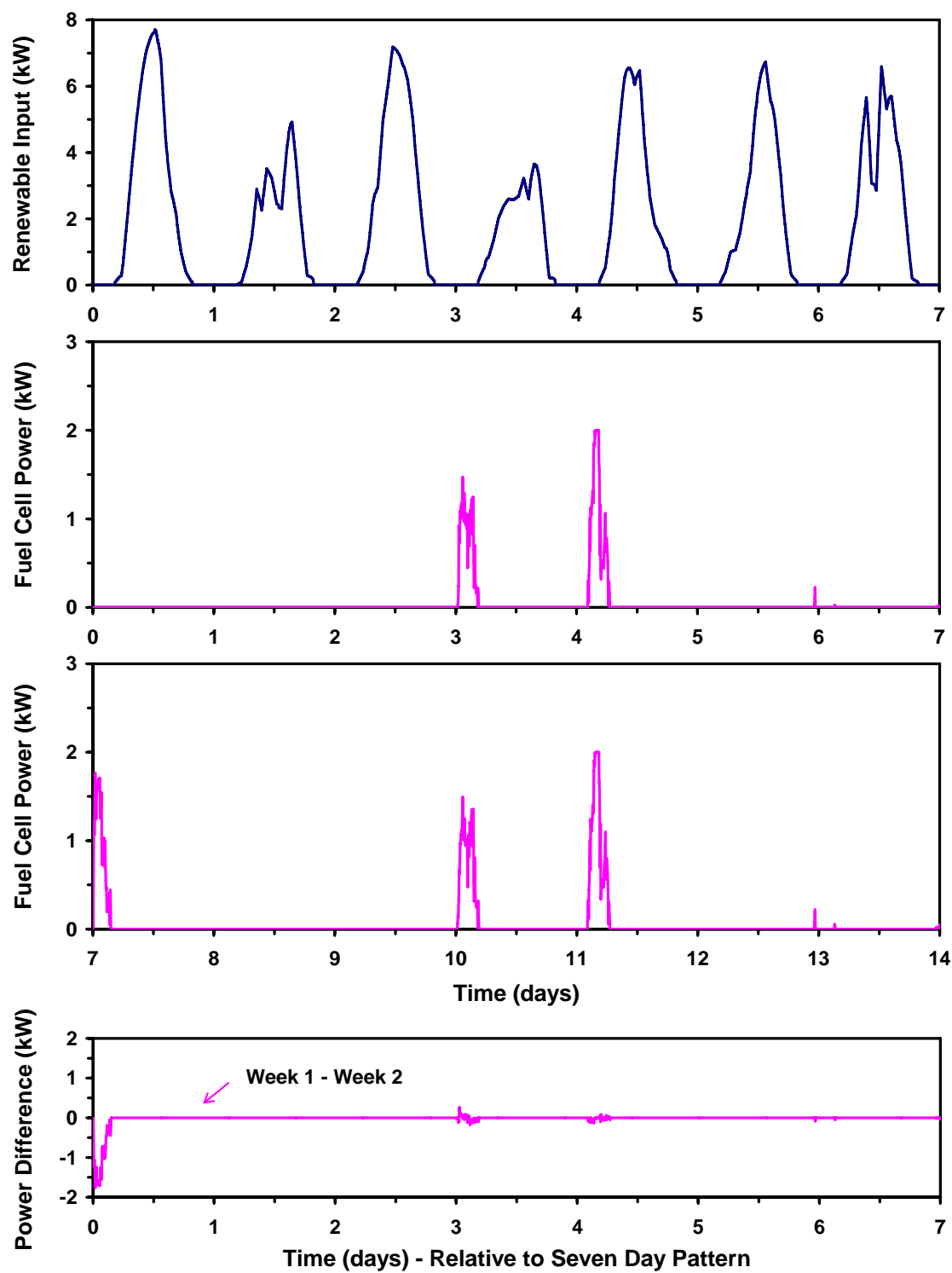

Figure 6.10 Fuel Cell Power Contribution

The power delivered to the system bus by the batteries is illustrated in Figure 6.11. Positive values indicated power delivered to the bus by the batteries while negative values denote power supplied by the bus for battery recharging.

As discussed previously, a steady charge/discharge pattern is established by day 2 as indicated by the plot of the net power difference between weeks one and two. In the IRENE system, the batteries are required to buffer currents at the Hz level (predominately 120 Hz) due to the demands of the AC inverters. The data presented here suggests that they also play an integral buffering role at the minute to hourly level given the 'high frequency' signal content when plotted on the daily time scale.

A clearly defined recharging pattern is evident consisting of a period of relatively constant power draw at approximately -1 kW (i.e., recharging at the limiting current value) followed by a gradual decay in power absorbed during constant voltage recharging (i.e., once the bus reaches 54 V). The relative smoothness of the recharging profile compared with the discharge portion indicates that the IRENE system controller is able to maintain the specified battery charge limiting conditions. Conversely, it implies that during the battery recharge period, the electrolyser is absorbing the difference between the renewable input and the load demands.

The electrolyser input power profile is plotted in Figure 6.12. The week-to-week comparison indicates that, apart from day 1, the deviation in input power is on average less then 0.2 kW during the standard operating periods. As alluded to above, the power input power profile varies considerably in magnitude throughout the daily operating periods. Days 2 and 7 of the one week pattern clearly illustrate the unsteady nature of the input profile that an electrolyser is subjected to under real system operating conditions. The profile has little in common with the steady-state test conditions typically employed in electrolyser characterization work, discussed in Chapter 2. Based on the power profiles observed, a comprehensive understanding of the electrolyser's dynamic response is required for accurate modeling of a renewable-regenerative system.
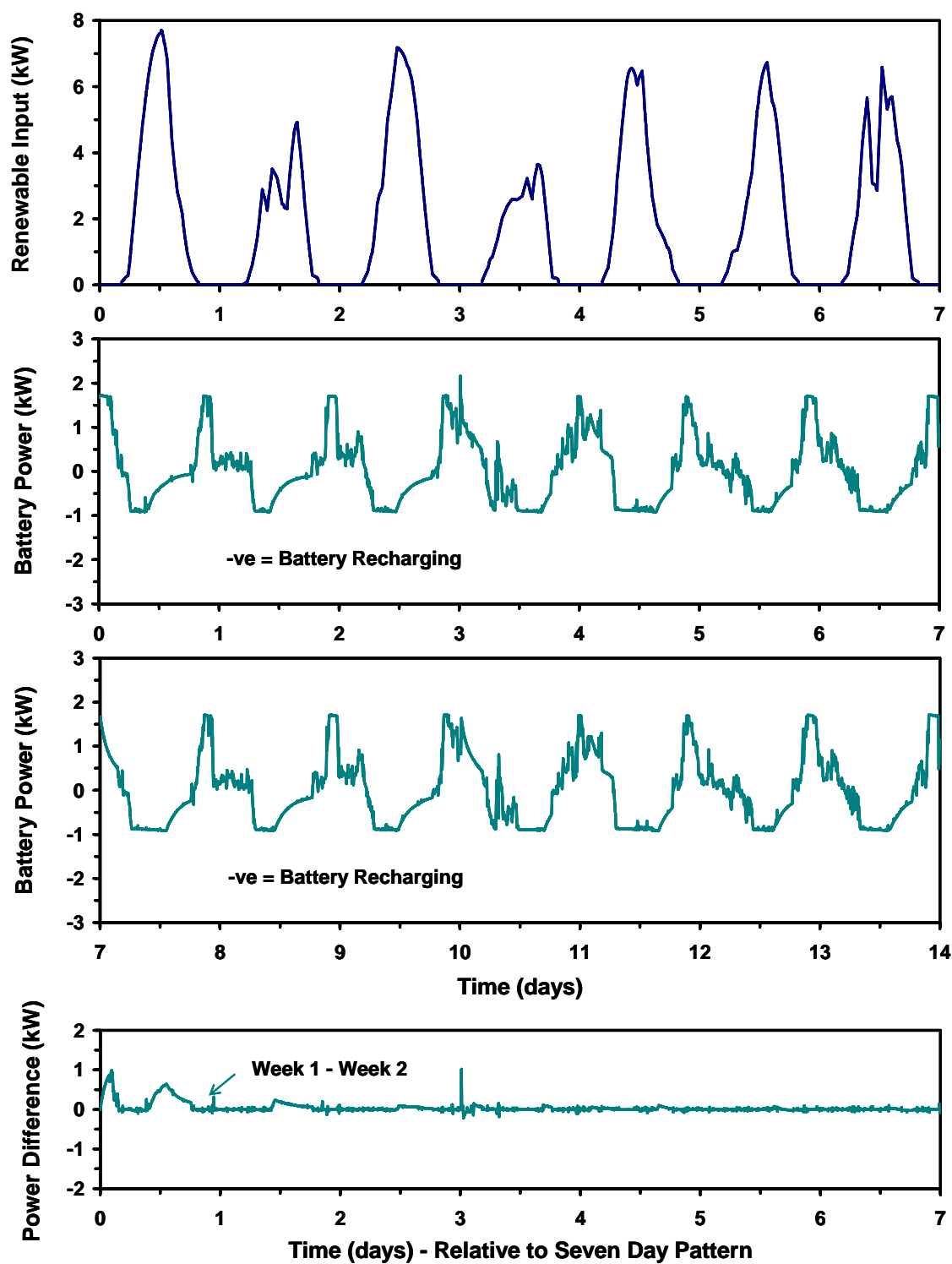
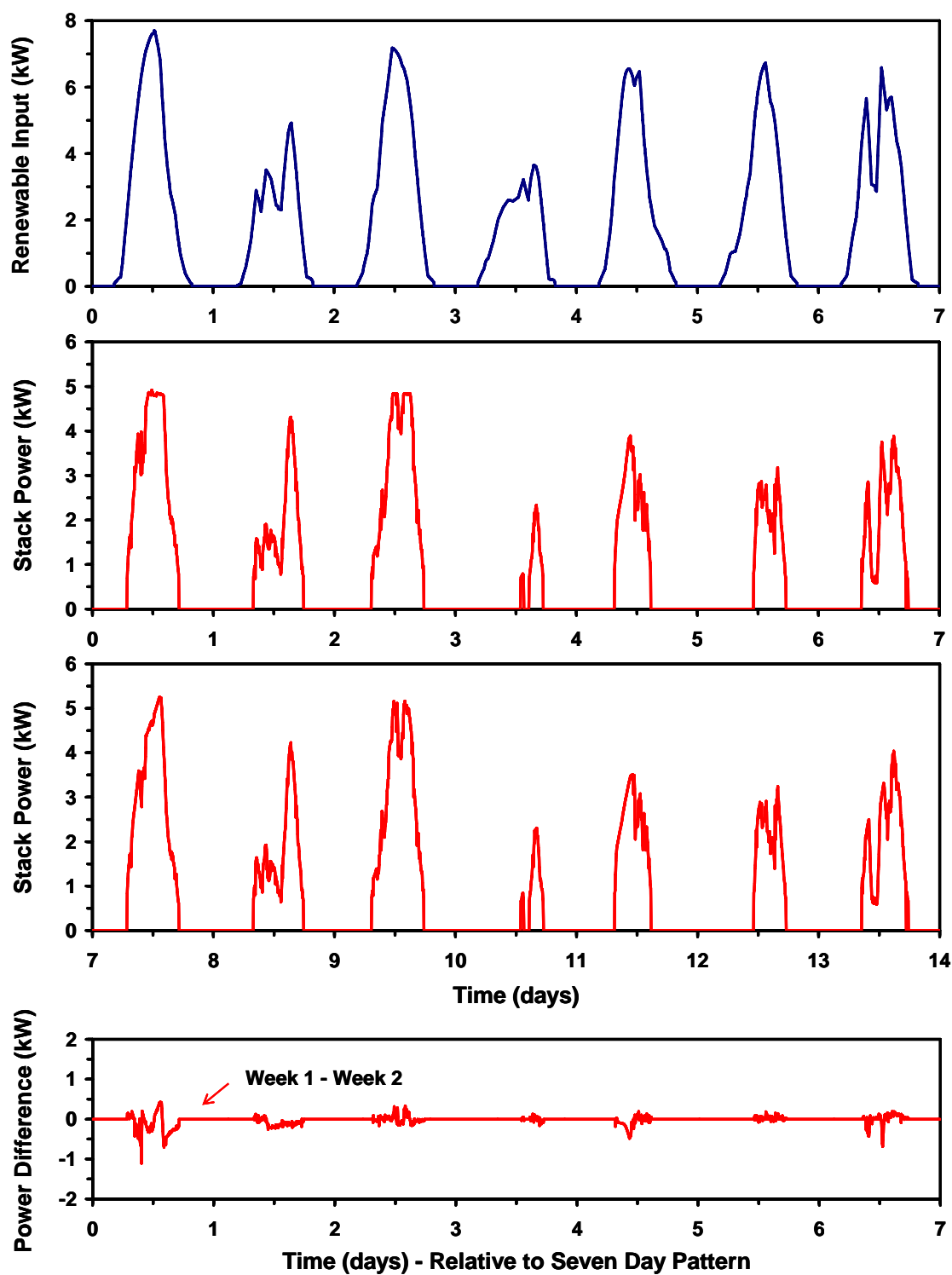**Figure 6.11 Battery Power Delivered to IRENE System**

Figure 6.12 Electrolyser Input Power Profile

Figure 6.13 is a plot of the unused renewable input energy (defined in Section 6.2.1 discussed in Section 6.3.2) associated with the minimum electrolyser input (denoted A) and electrolyser transition rate dependence (denoted B). The conditions under which these two types of unused input power arise were discussed in Section 6.3.2. The intent with the plots presented herein is to illustrate the relative timing and magnitudes of the two classification of unused power.

Losses due to the electrolyser minimum threshold input occur each time the electrolyser changes operating states. The quantity of power lost due to the minimum threshold is influenced by a combination of factors including the renewable input power profile, load demands, and battery recharge requirements. Two general classes of days are observed.

On days with a strong renewable input and moderate loads, day 3 for instance, only a small portion of the excess power is lost due to the minimum electrolyser requirement. In comparison, on a day where the renewable input is barely sufficient to meet the load demand, for example days 4 and 5, significant power is lost since the excess fails to meet the electrolyser minimum during a large portion of the day. The energy lost due to the minimum electrolyser input on day 5 is over 4 times that of day 3.

Losses due to the electrolyser's inability to absorb power during the thermal transition phase (discussed in Section 5.2) is most pronounced on days where surplus power is available but substantial battery recharging required, for instance day 5. In that case, the bus voltage and hence the electrolyser input voltage is limited by the battery recharge rate. The electrolyser consumes a portion of the excess renewable input power available but the constraint on input voltage reduces the rate at which the electrolyser reaches operating temperature. In this particular case, a boost converter between the bus and the electrolyser would be beneficial to raise the electrolyser input voltage. This would increase the net power absorbed by the electrolyser but may not result in complete utilization of the available excess power due to the limits on the thermal transient response of the electrolyser. Condition exists where the maximum input voltage is applied but the power absorbed is less then the rated nominal value, as outlined by the experiments conducted in Section 5.1.2.

On a per event basis, the unused energy associated with the electrolyser transition limit is typically larger than for the minimum electrolyser threshold but occurs less frequently. In the Section 6.3.2, values for the average unused energy were presented for the two week experiment which indicate that the net effect of the minimum threshold requirement represents a larger overall loss in energy at 14.0 kWhr than for transition limiting at 10.6 kWhr.

The data presented in this section illustrates that the response of renewable-regenerative system under actual operating conditions is highly variable. The interaction between system components is complex and limitations imposed by individual devices constrain the system operation in ways that are not always obvious.
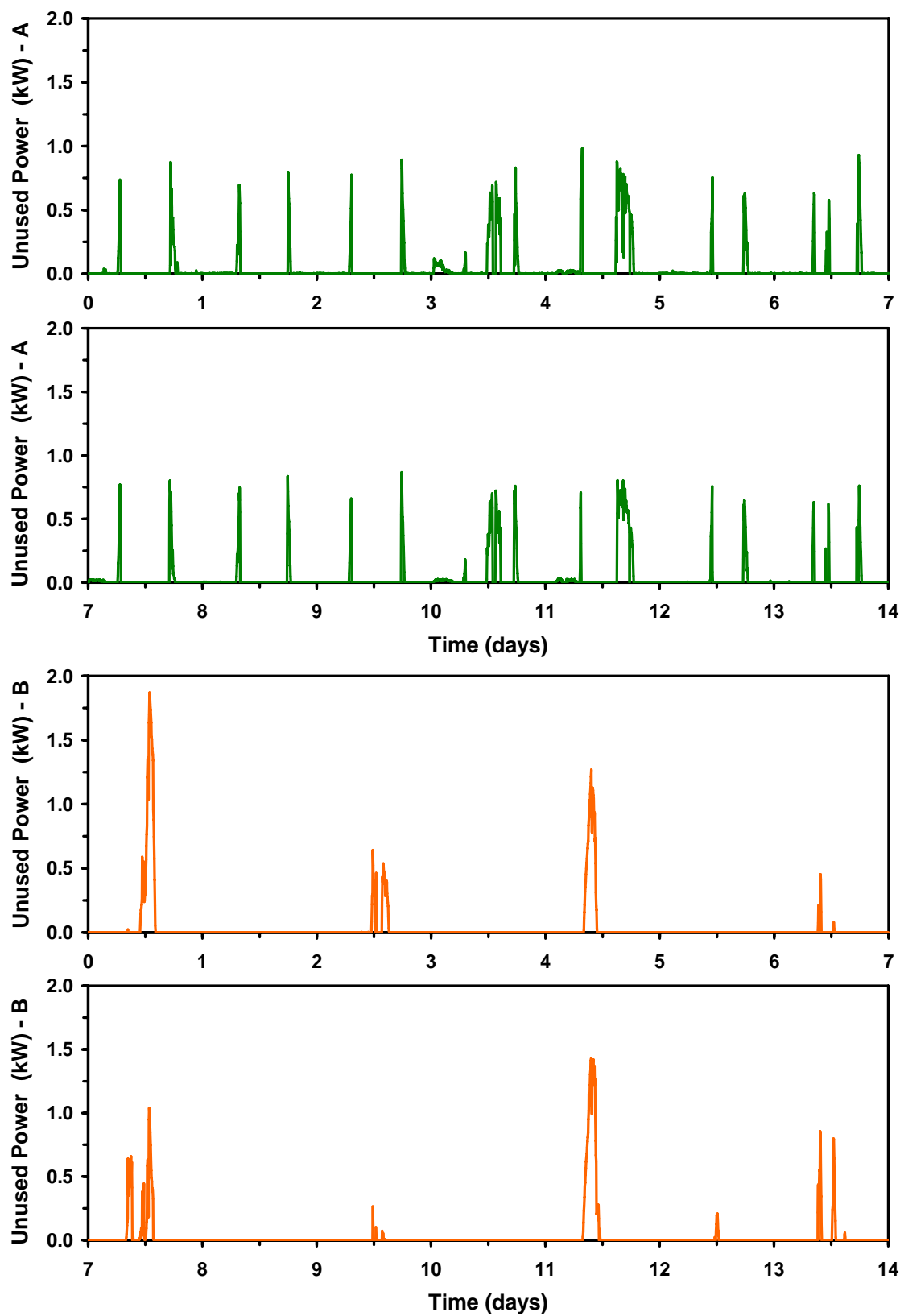
Figure 6.13 Unused Renewable Input: A) Electrolyser Threshold, B) Transition Rate

6.5   Summary

The experiment presented in this Section involves the operation of the entire IRENE system under conditions that are representative of the real demands that would be placed on a solar based, residential scale, renewable-regenerative system.   The control methodology required to implement the experiment is presented and implications of the various constraints and control objectives discussed.

A multi-week renewable-regenerative coupled system experiment was conducted with a repetitive renewable input and load profile to assess the stability of control system and experimental apparatus. Results for a two week period are presented which show that accurate measurement of the energy flows within the IRENE system is obtained.

Reporting of the overall system energy balance indicates that the energy input from the renewable source was sufficient to meet the demand load.   Furthermore, the energy buffer system was able to capture a significant portion of the daily excess energy and store it as hydrogen. More hydrogen was generated then consumed by the fuel cell. The energy efficiency of the hydrogen buffer subsystem is estimated at 22.2 percent given the load and demand profiles assumed.

The actual response of key parameters over the two week experiment was presented. The data illustrates that the system response is highly dynamic but repeatable.   The similarities in parameter values between weeks one and two is remarkably consistent. The system achieved repeatable operation after the second day. The large variations in bus voltage over the course of each day illustrates that components of a low battery capacity system must be robust to handle the extremes in voltage swing. In addition, the breakdown in unused renewable input energy indicates that the electrolyser minimum operating conditions and the transition rate are important factors to consider if accurate modeling of the coupled system response is required.

Chapter 7

Conclusions and Recommendations

The first objective of the thesis was to identify integration issues that pose barriers to the development of renewable-regenerative systems. The integration issues encountered while developing IRENE are outlined in Chapter 3. The solutions devised to address specific issues are described in Chapter 4. A summary of the integration work is presented in Section 7.1.1.

The second objective was to investigate the dynamic interactions which occur between system components. The dynamic response of the electrolyser under operating conditions relevant to renewable resource inputs are reported in Chapter 5. Further experimentation with the entire IRENE system was conducted to expose the operational characteristics of the coupled system, as reported in Chapter 6. A summary of the experimental work is presented in Section 7.1.2.

7.1   Summary

7.1.1   System Integration

Developing an IRENE-like system with currently available commercial products is a challenging integration task. All of the major components were originally designed for other applications and required modifications for use in IRENE. The components are far from "plug and play". Integration issues encountered during development fall into three general categories: power conditioning, control/communication compatibility, and component reliability. The requirement for accurate, high speed data acquisition introduced a range of development issues but these are related to the specific requirements of the research project and would not impede the implementation of renewable-regenerative systems in general.

Power Conditioning

IRENE is fundamentally a large power conditioning circuit interconnected via a floating DC bus. Problems arise when two or more components compete for control of the bus. System devices must tolerate both the floating nature of the bus and instantaneous ripple noise imposed on the bus. The ripple is due to the fact that the input sources and output demands on the system are not inherently smooth.

The DC/AC inversion process imposes a time varying current draw on the bus to generate the AC output wave form. The AC load characteristics are reflected back to the DC side, but the current demand is amplified by (at minimum) the ratio of the AC to DC working voltages (i.e., to maintain net power transfer, higher currents are imposed on the lower voltage side). A purely resistive AC load reflects a relatively smooth sinusoid at 120 Hz. However, real loads (particularly those with switching elements) impose high-frequency, large-amplitude current demands on the DC bus. If the system is to provide an uninterrupted output, energy storage elements with sufficient capacity must be included on the DC side to service the anticipated transients.

In traditional stand-alone renewable energy systems, the battery bank is sized to fulfill transient source/sink requirements. IRENE was however intentionally constructed with a small battery bank since the basic premise of the project is to utilize hydrogen as the energy buffer media, not batteries. As a result, the DC bus can be readily pushed around by the sources and sinks.

One method for improving bus regulation is through active control of a secondary energy sink, which in this case is the electrolyser. While the electrolyser cannot source current to service a transient demand of the inverters, the power diverted to the electrolyser can momentarily be reduced to lessen the total load on the bus if required. Likewise, power diverted to the electrolyser can be ramped up during periods of high resource input and low demand output from the inverters. Custom power conditioning electronics were developed to attain active control over the electrolyser power flow. The electrolyser is capable of creating a large draw on the DC bus and rapidly discharges the batteries in cases with low to moderate levels of renewable input power. As a result, the system

controller must actively monitor the bus state or large fluctuations in the DC level of the bus will occur.

The power conditioning of the fuel cell output presents an additional integration challenge. The fuel cell is unable to service a current ripple greater then 25 percent of the DC output current. This is insufficient to directly support the ripple generated by the output inverters. A second issue stems from the substantial voltage drop that occurs with increasing current output from the fuel cell. The solution developed to interface the fuel cell to the bus is to float the Nexa on an external current limiting power supply. A large passive LC filter isolates the fuel cell from bus voltage transients.

Control and Communication Compatibility

Numerous integration issues have stemmed from the variations in communication and control protocols used by the individual components. The floating nature of the system introduced the need for extensive use of isolation devices to make physical connections between components. A more difficult challenge arose in developing a unified control program. Each of the major devices functioned only with the OEM proprietary software. Reverse engineering of the communication data stream was required to develop the LabView based system controller. The standard RS232 communications protocol used by a number of the devices imposes a limitation on the data transfer rates and hence the response rate of the devices. In general, the lack of standards on the type of information shared between devices makes the integration of a complex system like IRENE a challenging endeavour.

Component Reliability

The reliability of components used in the individual sub-systems has been disappointing. Each of the major pieces of equipment acquired for this project required repair or custom upgrades before they could be implemented in IRENE. This is perhaps not surprising given the prototype nature of many of the components. For commercial success of an IRENE-like system to occur, the quality of the individual sub-systems would need to be substantially improved (especially in light of the costs).

Data Acquisition

Operation of the dedicated IRENE system controller along with data capture for post experiment analysis relies on the data acquisition system to accurately measure system parameter values. Current, voltages, flow rates temperatures etc., are measured at various points throughout the system. However, operation of many of the individual components creates significant electromagnetic noise which has the potential to interfere with measurement electronics. A wide range of custom signal conditioning and interface devices were required to deal with noise issues in order to create a measurement system that accurately captures the dynamic response of the renewable-regenerative system.

7.1.2   System Operation

The experimental program focused on two distinct aspects of renewable-regenerative system operation. The first series of experiments dealt with the hydrogen buffer response to dynamic operation. The second series investigated the coupled response of the IRENE system to a representative renewable input and user demand load.

Electrolyser Operation

Experiments were conducted to investigate the electrolyser's response to variety of dynamic operating conditions. In a renewable-regenerative system the electrolyser performs the critical function of converting excess renewable input energy into hydrogen. The electrolyser's transient characteristics have a significant impact on the efficiency with which the conversion process occurs. Electrolyser operation on times scales and duty cycles that are relevant to common renewable resources (wind and solar) were probed.

One key finding was the observation that there is a 7.3 percent reduction in electrolyser hydrogen production, relative to steady-state levels, observed for the most favourable dynamic electrolyser operating conditions. The reduction is due primarily to the thermal transient and time dependent decay in current draw. Experiments were conducted that indicate that the time decay phenomenon is significant in relation to operating duty cycles

associated with periodic renewable resources such as solar power. These time dependent aspects are currently not addressed in the theoretical models for electrolyser operation.

Experiments were conducted to probe the electrolyser's response to dynamic operation. Results indicate that short time scale events (i.e., dynamic events on the order of minutes) have the potential to rapidly degrade electrolyser performance. Introduction of short duration pauses in operation, a characteristic of a system based on a wind resource, results in net decline in performance over steady-state operation. However, the application of a minimum holding current during the transient can largely remedy the negative impact of the dynamic cycle.

Experiments indicate that partial recovery of transient induced performance degradation occurs if a sufficient rest period is introduced between successive operating cycles. The minimum recovery time is linked to the previous operating history. For operating duty cycles that do not contain significant high frequency events, a recovery time on the order of several hours is sufficient to restore performance. If the previous operating history includes dynamic operation, a minimum rest period on the order of days is required.

Coupled System Response

Experiments were conducted to determine the response of the entire IRENE system to operating conditions that are representative of the real demands that would be placed on a solar based renewable-regenerative system. To achieve this, a control algorithm was developed to guide system operation. Bus voltage constraints and device current limitations were the primary parameters employed in the IRENE system controller.

A multi-week renewable-regenerative coupled system trial was conducted with a repeated seven day renewable energy input and demand load profile. Results for a two week period indicate that accurate measurements of the energy flows within the IRENE system were obtained. The overall system energy balance reveals that the energy input from the renewable source was sufficient to meet the demand load. However, on average, 5.4 percent of the available renewable input energy remains unused due to system limitations. Energy lost due to the electrolyser minimum operating conditions accounts for 41 percent of the unused renewable input energy while electrolyser transition

limitations account for 29 percent. The balance is due to the overall capacity mismatch between the renewable input generation capacity and the combined system loads. Although there were losses involved, the energy buffer system was able to capture a significant portion of the daily excess energy and store it as hydrogen. For the specified resource and demand loads, more hydrogen was generated than consumed by the system.

Two week trends for key system parameters are reported. They illustrate that the system response is highly dynamic but generally repeatable. Large variations in bus voltage occur over the course of each day as a result of the low overall battery capacity. The battery power profile indicates that the IRENE system controller was able to divert power to the electrolyser in a suitable manner in response to changes in input and load conditions while maintain bus limiting criteria (i.e., actively proportioning power to the load, batteries and electrolyser). A breakdown of the unused renewable input energy is documented to provide data for future model verification purposes.

7.2 Conclusions

A residential scale renewable-regenerative system with hydrogen energy buffering was constructed from commercially available components and system operation under dynamic conditions was demonstrated. The facility is designed to be readily re-configurable to enable testing of new system components as they become available. The test-bed is fully instrumented to log not only the average system parameters (i.e., energy flows, hydrogen production rates, etc., per second), but also to capture the high speed transient interactions which occur between system components.

The integration challenges that arose during construction of this facility, which are generally applicable to the development other of renewable energy systems, have been identified. Innovative solutions were developed to overcome many of the integration issues encountered. Ideally, system components should be chosen so that they are directly compatible in power requirements and operating voltages. The large variation between IRENE components only exacerbated the difficulty of system integration.

Operational experience gathered with the IRENE system indicates that the short term energy buffer, the battery bank in this case, plays an important role in maintaining system stability. The actual current flows on the 'DC' bus more closely resemble that of an AC system due to the output inversion demands. Therefore, buffering for medium time scales (minutes and hours), short time scales (120 Hz fundamental) and high frequency (kHz range) events needs to be considered in the overall system design. This fact was not evident at the onset of the project but was emphasized during actual system operation.

Experiments conducted with the electrolyser indicated that a simple VI relationship is insufficient to characterise the operational behaviour. In applications like IRENE, the electrolyser's transition and dynamic characteristics affect a significant portion of the typical daily operating period (1-6 hours). The electrolyser's ability to absorb power from the bus is significantly reduced during the transition period while the unit is warming up. Likewise the performance decay, observed in repeated experiments, indicates that a minimum 6 hour run period is required to reach the onset of stable operation. These factors must be considered when designing a renewable-regenerative

system (from the viewpoint of the electrolyser's effective power rating) or if an accurate model based prediction of the hydrogen production is to be made.

Experiments conducted with short duration (2 minute) transient events indicate that maintaining a minimum electrolyser current is critical to avoid dynamic event induced performance decline. The requirement for a minimum operating current (and therefore minimum power input) places some constraints on the common operating methodology for renewable-regenerative systems where the electrolyser is viewed as the first load shed when a deficiency in input power exists. While the electrolyser can tolerate a wide variation in input power, the system must have sufficient short term energy buffering capacity to maintain the minimum demand of the electrolyser as well as the other system loads. If the system is unable to support the combined load, experiments have shown that instituting a minimum rest period between electrolyser operating cycles can restore degraded performance induced by rapid electrolyser cycling.

Several conclusions arise from the overall operation of the IRENE system. Unlike the previous experimental systems outlined in Chapter 2, the weak link in the hydrogen energy buffer chain is not the fuel cell, but rather the electrolyser. Both components still have significant room for improvement, but the focus on fuel cell development over the past decade has remedied many of the fuel cell related problems discussed in the literature for previous systems. That said, implementing a hydrogen energy buffer with the components that are currently available remains a challenging task. The systems are inherently complex, expensive, and at this stage are not robust enough for commercial deployment. Considerable advances in component reliability, power conditioning aspects, control, and communication compatibility are needed before the technology will gain market acceptance.

A more fundamental question that underlies the development efforts is 'does it make sense to use hydrogen as an energy buffer for the scale of applications targeted by IRENE?' Experimental results generated in the coupled system experiments of Chapter 6 indicated that the actual operating efficiency of the hydrogen buffer loop was only 22 percent. Considering that hydrogen compression was not included, this represents a 'best case' operating scenario for the IRENE system. The energy penalty associated with the

technology can not be overlooked when evaluating the potential of hydrogen against other energy buffering techniques. In certain applications, such as remote locations were alternate energy services are not available, the losses associated with the energy buffer may be acceptable. However, when other energy sources exist, it may be more effective and expedient to directly utilize the renewable source when it is available, and employ an alternate form when it is not. In either case, the operation of the IRENE system illustrates that if the ratio between the renewable input and demand load falls within the prescribed bounds it is technically possible to service user demand load by employing hydrogen energy buffering. The actual viability of such systems would ultimately be determined by economic and environmental considerations outside the scope of this work.

7.3.   Recommendations

A number of avenues of research with the IRENE system exist that could be embarked upon in the future. Perhaps the most immediate is to repeat the three week experiment presented in Chapter 6 with a view to identifying the mechanism that caused the shift in electrolyser response that was observed during week three. If the observed changes are related to a fundamental change in electrolyser performance that occurs due to the operational duty cycle, the phenomena deserves further investigation. Given the history of electrolyser operational issues encountered during the IRENE project thus far, it is equally as likely that a component within the cell stack failed or reached the service limit. In either case, determining the root cause would provide insight into the changes observed.

Assuming that the immediate electrolyser issues are resolved, implementing an advanced IRENE system controller that would shut down the electrolyser during periods when the renewable resource was unavailable (as opposed to continuous 'standby' operation) would create experimental conditions that are closer to the actual operating conditions found in a real system. The main difficulty in achieving the desired control action is determining under which conditions to impose a minimum electrolyser rest period to avoid transient induced performance decline, and when to accept the penalty associated

with immediate return to service when excess power becomes available. This is a non-trivial control and optimization problem but may lead to the development of valuable new control methodologies for renewable-regenerative systems.

Further work on the IRENE system is required implement permanent solutions to replace the temporary measures taken to make the system operational. In particular, a DC/DC converter that is specifically designed for small PEM fuel cells, like the Nexa, may now be, or will soon become commercially available. Incorporating an appropriate conversion device would make the fuel cell system self contained as opposed to the current configuration which requires the external power supply. Retrofitting the electrolyser with a new low pressure compression system (15 bar) and the input power conditioning module would improve the functionality of the unit. Conversely, replacing the alkaline electrolyser (or augmenting the system) with a PEM electrolyser unit may be a better overall alternative.

Detailed theoretical modeling of the IRENE system is another avenue of work that should be pursued. The operational characteristics observed in the experimental work conducted thus far, in particular the time related response aspects, are not included in the basic models for renewable-regenerative system. A significant contribution could be made in this area of research.

The final suggestion for future work is to employ IRENE as a platform for exploring alternative energy buffering technologies such as vanadium redox flow batteries. Although the focus has been on hydrogen technologies, exploring alternate methods for energy buffering in renewable-regenerative may lead to hybrid designs with enhanced overall performance. The IRENE system provides an excellent foundation for future investigations.

References

1. Boyle, G. Editor, *Renewable Energy: Power for a Sustainable Future*. 1996, Oxford University Press: Oxford.

2. Leonhard, W. Editor, *Distributed Generation and its Effects on the Future Supply Grid*. in *EPE Proceedings - Round Table Discussion*. 2001. Graz, Austria.

3. Milborrow, D., *Wind Power on the Grid*, in *Renewable Electricity and the Grid: The Challenge of Variability*, G. Boyle, Editor. 2007, Earthscan: London. p. 31-45.

4. Palomino, G. and J. Wiles, *Performance of a Grid Connected Residential Photo-voltaic System with Energy Storage*. in *26th IEEE Photo-voltaic Conference Proceedings*. 1997. Anaheim, California.

5. IEA, *Key Stats Report*. 2007, International Energy Agency http://www.iea.org/textbase/nppdf/free/2007/key_stats_2007.pdf

6. Haines, A., K.R. Smith, D. Anderson, P.R. Epstein, A.J. McMichael, I. Roberts, P. Wilkinson, J. Woodcock, and J. Woods, *Policies for accelerating access to clean energy, improving health, advancing development, and mitigating climate change.* The Lancet, 2007. 370(9594): p. 1264-1281.

7. Lund, H. and B. Mathiesen, *Energy System Analysis of 100 Percent Renewabele Energy Ststems: The Case of Denmark Year 2030 and 2050.* in *HyFC Summer School*. 2007. Svendborg, Denmark.

8. National Energy Council, *Advanced Energy Initiative*. 2006, The White House http://www.whitehouse.gov/stateoftheunion/2006/energy/energy_booklet.pdf

9. Peters, R., *The Basics on Base Load: Meeting Ontario's Base Load Electric Demand With Renewable Power supply*. 2007, Pembina Institute http://www.pembina.org/pub/1530

10. Anderson, D. and M. Leach, *Harvesting and redistributing renewable energy: on the role of gas and electricity grids to overcome intermittency through the generation and storage of hydrogen.* Energy Policy, 2004. 32(14): p. 1603-1614.

11. Ghosh, P.C., B. Emonts, and D. Stolten, *Comparison of hydrogen storage with diesel-generator system in a PV-WEC hybrid system.* Solar Energy, 2003. 75(3): p. 187-198.

12. Ulleberg, O., *Modeling of advanced alkaline electrolyzers: a system simulation approach.* International Journal of Hydrogen Energy, 2003. 28(1): p. 21-33.

13. Larminie, J. and A. Dicks, *Fuel Cell Systems Explained*. 2nd ed. 2003, England: John Wiley and Sons Ltd.

14. Dienhart, H. and A. Siegel, *Hydrogen storage in isolated electrical energy systems with photovoltaic and wind energy.* International Journal of Hydrogen Energy, 1994. 19(1): p. 61-66.

15. Mills, A. and S. Al-Hallaj, *Simulation of hydrogen-based hybrid systems using Hybrid2.* International Journal of Hydrogen Energy, 2004. 29(10): p. 991-999.

16. Kolhe, M., K. Agbossou, J. Hamelin, and T.K. Bose, *Analytical model for predicting the performance of photovoltaic array coupled with a wind turbine in a stand-alone renewable energy system based on hydrogen.* Renewable Energy, 2003. 28(5): p. 727-742.

17. Santarelli, M. and S. Macagno, *A thermoeconomic analysis of a PV-hydrogen system feeding the energy requests of a residential building in an isolated valley of the Alps.* Energy Conversion and Management, 2004. 45(3): p. 427-451.

18. Onda, K., T. Kyakuno, K. Hattori, and K. Ito, *Prediction of production power for high-pressure hydrogen by high-pressure water electrolysis.* Journal of Power Sources, 2004. 132(1-2): p. 64-70.

19. Da Silva, E.P., A.J. Marin Neto, P.F.P. Ferreira, J.C. Camargo, F.R. Apolinario, and C.S. Pinto, *Analysis of hydrogen production from combined photovoltaics, wind energy and secondary hydroelectricity supply in Brazil.* Solar Energy, 2005. 78(5): p. 670-677.

20. Ghosh, P.C., B. Emonts, H. Jan[ss]en, J. Mergel, and D. Stolten, *Ten years of operational experience with a hydrogen-based renewable energy supply system.* Solar Energy, 2003. 75(6): p. 469-478.

21. Zoulias, E.I., R. Glockner, N. Lymberopoulos, T. Tsoutsos, I. Vosseler, O. Gavalda, H.J. Mydske, and P. Taylor, *Integration of hydrogen energy technologies in stand-alone power systems analysis of the current potential for applications.* Renewable and Sustainable Energy Reviews, 2006. 10(5): p. 432-462.

22. Vosen, S.R. and J.O. Keller, *Hybrid energy storage systems for stand-alone electric power systems: optimization of system performance and cost through control strategies.* International Journal of Hydrogen Energy, 1999. 24(12): p. 1139-1156.

23. El-Shatter, T.F., M.N. Eskandar, and M.T. El-Hagry, *Hybrid PV/fuel cell system design and simulation.* Renewable Energy, 2002. 27(3): p. 479-485.

24. Sorensen, B., A. Hauge Petersen, C. Juhl, H. Ravn, C. Sondergren, P. Simonsen, K. Jorgensen, L. Henrik Nielsen, H. V. Larsen, P. Erik Morthorst, L. Schleisner, F. Sorensen, and T. Engberg Pedersen, *Hydrogen as an energy carrier: scenarios for future use of hydrogen in the Danish energy system.* International Journal of Hydrogen Energy, 2004. 29(1): p. 23-32.

25. Santarelli, M., M. Cali, and S. Macagno, *Design and analysis of stand-alone hydrogen energy systems with different renewable sources.* International Journal of Hydrogen Energy, 2004. 29(15): p. 1571-1586.

26.   Hollmuller, P., J.-M. Joubert, B. Lachal, and K. Yvon, *Evaluation of a 5 kWp photovoltaic hydrogen production and storage installation for a residential home in Switzerland.* International Journal of Hydrogen Energy, 2000. 25(2): p. 97-109.

27.   Lehman, P.A., C.E. Chamberlin, G. Pauletto, and M.A. Rocheleau, *Operating experience with a photovoltaic-hydrogen energy system.* International Journal of Hydrogen Energy, 1997. 22(5): p. 465-470.

28.   Szyszka, A., *Ten years of solar hydrogen demonstration project at Neunburg vorm Wald, Germany.* International Journal of Hydrogen Energy, 1998. 23(10): p. 849-860.

29.   Agbossou, K., R. Chahine, J. Hamelin, F. Laurencelle, A. Anouar, J.-M. St-Arnaud, and T.K. Bose, *Renewable energy systems based on hydrogen for remote applications.* Journal of Power Sources, 2001. 96(1): p. 168-172.

30.   Galli, S. and M. Stefanoni, *Development of a solar-hydrogen cycle in Italy.* International Journal of Hydrogen Energy, 1997. 22(5): p. 453-458.

31.   Rambach, G. *Integrated, Renewable Hydrogen Utility Systems*. in *Proceedings of the 1999 U.S. DOE Hydrogen Program Review, NREL*. 1999.

32.   Valand, T., W. Bartholdsen, M. Ottestad, and M. Vage, *Grimstad Renewable Energy Park*. 2004 http://www.ieahia.org/pdfs/grimstad.pdf

33.   Szyszka, A., *Demonstration plant, Neunburg vorm Wald, Germany, to investigate and test solar-hydrogen technology.* International Journal of Hydrogen Energy, 1992. 17(7): p. 485-498.

34.   Kauranen, P.S., P.D. Lund, and J.P. Vanhanen, *Development of a self-sufficient solar-hydrogen energy system.* International Journal of Hydrogen Energy, 1994. 19(1): p. 99-106.

35.   Schucan, T., *Final Report of Subtask A: Case Studies of Integrated Hydrogen Energy Systems*. 2000, Paul Scherrer Institute: Switzerland.

36.   Snyder, J., *An Integrated Renewable Hydrogen Energy System*. 2000, University of Nevada: Reno.

37.   Jacobson, R., R. Purcell, and D. Wermers. *Renewable Hydrogen Systems Integration and Performance modeling*. in *Proceedings of the 2001 U.S. DOE Hydrogen Program Review, NREL*. 2001.

38.   Bernier, E., J. Hamelin, K. Agbossou, and T.K. Bose, *Electric round-trip efficiency of hydrogen and oxygen-based energy storage.* International Journal of Hydrogen Energy, 2005. 30(2): p. 105-111.

39.   Agbossou, K., M.L. Kolhe, J. Hamelin, E. Bernier, and T.K. Bose, *Electrolytic hydrogen based renewable energy system with oxygen recovery and re-utilization.* Renewable Energy, 2004. 29(8): p. 1305-1318.

40.   Schenk, N.J., H.C. Moll, J. Potting, and R.M.J. Benders, *Wind energy, electricity, and hydrogen in the Netherlands.* Energy, 2007. 32(10): p. 1960-1971.

41. Conte, M., A. Iacobazzi, M. Ronchetti, and R. Vellone, *Hydrogen economy for a sustainable development: state-of-the-art and technological perspectives.* Journal of Power Sources, 2001. 100(1-2): p. 171-187.

42. Rand, D.A.J. and R.M. Dell, *The hydrogen economy: a threat or an opportunity for lead-acid batteries?* Journal of Power Sources, 2005. 144(2): p. 568-578.

43. Dell, R.M. and D.A.J. Rand, *Energy storage -- a key technology for global energy sustainability.* Journal of Power Sources, 2001. 100(1-2): p. 2-17.

44. Troncoso, E. and M. Newborough, *Implementation and control of electrolysers to achieve high penetrations of renewable power.* International Journal of Hydrogen Energy, 2007. 32(13): p. 2253-2268.

45. Young, D.C., G.A. Mill, and R. Wall, *Feasibility of renewable energy storage using hydrogen in remote communities in Bhutan.* International Journal of Hydrogen Energy, 2007. 32(8): p. 997-1009.

46. Shakya, B.D., L. Aye, and P. Musgrave, *Technical feasibility and financial analysis of hybrid wind-photovoltaic system with hydrogen storage for Cooma.* International Journal of Hydrogen Energy, 2005. 30(1): p. 9-20.

47. Ntziachristos, L., C. Kouridis, Z. Samaras, and K. Pattas, *A wind-power fuel-cell hybrid system study on the non-interconnected Aegean islands grid.* Renewable Energy, 2005. 30(10): p. 1471-1487.

48. Isherwood, W., J.R. Smith, S.M. Aceves, G. Berry, W. Clark, R. Johnson, D. Das, D. Goering, and R. Seifert, *Remote power systems with advanced storage technologies for Alaskan villages.* Energy, 2000. 25(10): p. 1005-1020.

49. Kasseris, E., Z. Samaras, and D. Zafeiris, *Optimization of a wind-power fuel-cell hybrid system in an autonomous electrical network environment.* Renewable Energy, 2007. 32(1): p. 57-79.

50. Chen, F., N. Duic, L. Manuel Alves, and M. da Graca Carvalho, *Renewislands-- Renewable energy solutions for islands.* Renewable and Sustainable Energy Reviews, 2007. 11(8): p. 1888-1902.

51. Zoulias, E.I. and N. Lymberopoulos, *Techno-economic analysis of the integration of hydrogen energy technologies in renewable energy-based stand-alone power systems.* Renewable Energy, 2007. 32(4): p. 680-696.

52. Santarelli, M. and S. Macagno, *Hydrogen as an energy carrier in stand-alone applications based on PV and PV-micro-hydro systems.* Energy, 2004. 29(8): p. 1159-1182.

53. Maclay, J.D., J. Brouwer, and G. Scott Samuelsen, *Dynamic analyses of regenerative fuel cell power for potential use in renewable residential applications.* International Journal of Hydrogen Energy, 2006. 31(8): p. 994-1009.

54. Onar, O.C., M. Uzunoglu, and M.S. Alam, *Dynamic modeling, design and simulation of a wind/fuel cell/ultra-capacitor-based hybrid power generation system.* Journal of Power Sources, 2006. 161(1): p. 707-722.

55. Deshmukh, S.S. and R.F. Boehm, *Review of modeling details related to renewably powered hydrogen systems.* Renewable and Sustainable Energy Reviews. In Press, Corrected Proof: p. 1624.

56. Dufo-Lopez, R., J.L. Bernal-Agustin, and J. Contreras, *Optimization of control strategies for stand-alone renewable energy systems with hydrogen storage.* Renewable Energy, 2007. 32(7): p. 1102-1126.

57. Bilodeau, A. and K. Agbossou, *Control analysis of renewable energy system with hydrogen storage for residential applications.* Journal of Power Sources, 2006. 162(2): p. 757-764.

58. Sherif, S.A., F. Barbir, and T.N. Veziroglu, *Wind energy and the hydrogen economy--review of the technology.* Solar Energy, 2005. 78(5): p. 647-660.

59. De Battista, H., R.J. Mantz, and F. Garelli, *Power conditioning for a wind-hydrogen energy system.* Journal of Power Sources, 2006. 155(2): p. 478-486.

60. Roy, A., S. Watson, and D. Infield, *Comparison of electrical energy efficiency of atmospheric and high-pressure electrolysers.* International Journal of Hydrogen Energy, 2006. 31(14): p. 1964-1979.

61. Vanhanen, J.P., P.S. Kauranen, and P.D. Lund, *Operation experiences of a phosphoric acid fuel cell in a solar hydrogen energy system.* International Journal of Hydrogen Energy, 1997. 22(7): p. 707-713.

62. Vanhanen, J.P., P.D. Lund, and J.S. Tolonen, *Electrolyser-metal hydride-fuel cell system for seasonal energy storage.* International Journal of Hydrogen Energy, 1998. 23(4): p. 267-271.

63. Goetzberger, A., G. Bopp, W. Griesshaber, and W. Stahl, *The PV/hydrogen/oxygen-system of the self-sufficient solar house Freiburg.* in *Proceedings of 23rd IEEE Photovoltaic Specialists Conference, 10-14 May 1993.* 1993. Louisville, KY, USA: IEEE.

64. Hollenberg, J.W., E.N. Chen, K. Lakeram, and D. Modroukas, *Development of a photovoltaic energy conversion system with hydrogen energy storage.* International Journal of Hydrogen Energy, 1995. 20(3): p. 239-243.

65. Dutton, A.G., J.A.M. Bleijs, H. Dienhart, M. Falchetta, W. Hug, D. Prischich, and A.J. Ruddell, *Experience in the design, sizing, economics, and implementation of autonomous wind-powered hydrogen production systems.* International Journal of Hydrogen Energy, 2000. 25(8): p. 705-722.

66. Busquet, S., J. Labbe, P. Leroux, R. Metkemeijer, and D. Mayer, *Stand Alone Power System Coupling a PV Field and a Fuel Cell: First Experimental Results.* 2002 http://www.pvfcsys.cma.fr/publications/index.html

67. Little, M., M. Thomson, and D. Infield, *Electrical integration of renewable energy into stand-alone power supplies incorporating hydrogen storage.* International Journal of Hydrogen Energy, 2007. 32(10-11): p. 1582-1588.

68. Gazey, R., S.K. Salman, and D.D. Aklil-D'Halluin, *A field application experience of integrating hydrogen technology with wind power in a remote island location.* Journal of Power Sources, 2006. 157(2): p. 841-847.

69. Nakken, T., L. Strand, E. Frantzen, R. Rohden, and P. Eide, *The Utsira Wind-Hydrogen System - Operational Experience*. in *European Wind Energy Conference*. 2006. Athens.

70. Bindner, H., *Operational Status of SYSLAB at Riso DTU - Personal Comminucation*. 2007: Copenhagen.

71. Ugursal, I.V. and A.S. Fung, *Impact of appliance efficiency and fuel substitution on residential end-use energy consumption in Canada.* Energy and Buildings, 1996. 24(2): p. 137-146.

72. MacDonald, B.D. and A.M. Rowe, *Experimental and numerical analysis of dynamic metal hydride hydrogen storage systems.* Journal of Power Sources, 2007. 174(1): p. 282-293.

73. Gautam, D., *Soft-Switched DC-toDC Converters for Power Conditioning of Electrolyser in a Renewable Energy System*, in *Electrical and Computer Engineering*. 2006, M.A.Sc Thesis, University of Victoria: Victoria.

74. Proznick, R., *Design and Construction of a High-Pressure Hydrogen Compressor Controller*. 2006, Term Report, University of Victoria: Victoria.

75. Xiao, K., L. Zhao, T. Asada, W. Odendaal, and J. Wyk, *An Overview of Intergratable Current Sensor Technologies*. in *IEEE 38th IAS Annual Meeting Industry Applications*. 2003.

76. Moran, M. and H. Shapiro, *Fundamentals of Engineering Thermodynamics - 4th ed*. 1999, New York: John Wiley and Sons.

77. Mottillo, M., *RE-H2 Model Data - Personal Communication*. 2007: Ottawa.

78. Rosen, M.A., *Energy and exergy analyses of electrolytic hydrogen production.* International Journal of Hydrogen Energy, 1995. 20(7): p. 547-553.

79. Hydro, B.C., *Residential Power Consumption - Personal Communication*. 2007.

80. Schiffer, J., D.U. Sauer, H. Bindner, T. Cronin, P. Lundsager, and R. Kaiser, *Model prediction for ranking lead-acid batteries according to expected lifetime in renewable energy systems and autonomous power-supply systems.* Journal of Power Sources, 2007. 168(1): p. 66-78.